Schweizerische Eidgenossenschaft
Confédération suisse
Confederazione Svizzera
Confederaziun svizra

Federal Department of the Environment, Transport, Energy and Communications DETEC

Swiss Federal Office of Energy SFOE
Energy Research and Cleantech Division

Final report dated 10.10.2024

OPTIM-EASE

OPTImization of building energy systems and Management with **E**nvironmental **A**ssessment and **SE**ctor coupling

---

Source: © petovarga – stock.adobe.com

Date: 31.01.2024

Location: Yverdon-les-Bains and Rapperswil

Publisher:
Swiss Federal Office of Energy SFOE
Energy Research and Cleantech
CH-3003 Bern
www.bfe.admin.ch

Co-financing:

Genossenschaft VSG Grütlistrasse 44 CH-8027 Zürich www.gazenergie.ch	Romande Energie SA Rue de Lausanne 53 CH-1110 Morges www.romande-energie.ch	Energie360° AG Aargauerstr. 182 PF 805 CH-8010 Zürich www.energie360.ch	SGSW Vadianstrasse 8 CH-9001 St. Gallen www.sgsw.ch

Subsidy recipients:
HEIG-VD
Institut de génie thermique
Route de Cheseaux 1, CH-1401 Yverdon-les-Bains
www.heig-vd.ch

SPF Institut für Solartechnik, OST – Ostschweizer Fachhochschule
Oberseestrasse 10, CH-8640 Rapperswil Jona
www.spf.ch
www.ost.ch

Authors:
Xavier, Jobard, HEIG-VD | IGT-LESBAT, xavier.jobard@heig-vd.ch
Marten Fesefeldt HEIG-VD | IESE, marten.fesefeldt@heig-vd.ch
Massimiliano Capezzali HEIG-VD | IESE massimiliano.capazzali@heig-vd.ch
Neha, Dimri, SPF | OST, neha.dimri@ost.ch
Daniel, Carbonell, SPF | OST, dani.carbonell@ost.ch

Acknowledgement to: Agnès François, Vincent Jacquot, Arthur du Vignau.

SFOE project coordinators:
Andreas Eckmanns, andreas.eckmanns@bfe.admin.ch
Nadège Vetterli, nadège.vetterli@anex.ch

SFOE contract number: SI/502189-01

Disclaimer: As an additional research question, the FOGA (Research, Development and Promotion Fund of the Swiss Gas Industry) analysed the impact of using renewable gas. According to the SFOE's heating strategy, the use of renewable gas for heating purposes should be avoided.

Zusammenfassung

Das optimale Energiekonzept einer Gruppe von Gebäuden sollte sich von der Summe der optimalen Lösungen der einzeln betrachteten Gebäude unterscheiden. In Bezug auf diese Aussage versucht das Projekt OPTIM-EASE, Antworten auf folgende Forschungsfragen zu geben: 1) Welche Methoden und Mittel sind am besten geeignet, um dezentrale Energiesysteme für einzelne Gebäude und Gebäudegruppen zu identifizieren und zu entwerfen, um die Kosten und die Umweltauswirkungen zu minimieren ? 2) Wie können unterschiedliche und manchmal gegensätzliche Kosten- und Umweltziele gemeinsam angegangen werden ? 3) Inwiefern kann die Gruppierung von Gebäuden die Kosten und Umweltauswirkungen ihres Energieverbrauchs durch die Nutzung ihrer Synergien im Vergleich zu Einzelbetrachtungen verringern ?

Um diese Aufgabe zu bewältigen, wurde im Rahmen des OPTIM-EASE-Projekts ein auf Python basierender Multi-Objektiv-Rahmen, "optihood", entwickelt und auf vier Fallstudien angewendet, die eine Vielzahl von Konfigurationen und Ergebnissen zeigen. Dieses Framework stellt ein Instrument zur Verfügung, mit dem die Auswahl der Technologien, ihre Kapazitäten und ihr stündlicher Betrieb im Jahresverlauf auf der Grundlage der jährlichen Äquivalenzkosten und/oder der Treibhausgasemissionen optimiert werden können.

In allen Fallstudien erwies sich der Zusammenschluss von Gebäuden zu einer Energiegemeinschaft im Vergleich zur Summe der Einzellösungen als vorteilhaft in Bezug auf die Kosten und die Verringerung der Umweltauswirkungen. Wenn nur der Strom zwischen den Gebäuden innerhalb eines Mikronetzes geteilt wird, erwiesen sich die Strompreise als die wichtigsten Faktoren für potenzielle Kosten und Umweltvorteile. Die Ergebnisse zeigen eine Senkung der Kosten und der Treibhausgasemissionen um 16 % bzw. 9 %. Die niedrigen Stromkosten ermöglichen eine höhere Deckung des Wärmebedarfs durch den Einsatz von Wärmepumpen. Wenn zweitens die Wärmeströme innerhalb eines Wärmenetzes zwischen den Gebäuden aufgeteilt werden können, sind höhere Gewinne zu erwarten, wenn die Infrastruktur des Wärmenetzes weniger als 7 % bis 40 % der jährlichen Äquivalenzkosten des Systems kostet. Mit den KBOB-Faktoren für Treibhausgasemissionen sind Luftwärmepumpen die dominante Technologie, wenn die Treibhausgasemissionen optimiert werden. Allerdings wurden die CO_2-Emissionen von Erdwärmesonden in der KBOB im Jahr 2023 auf die Hälfte des vorherigen Wertes aktualisiert, was die Wettbewerbsfähigkeit von Erdwärmepumpen in den untersuchten Studien verbessern könnte, wenn die Treibhausgasemissionen optimiert werden. Wärmegeführte KWK für Fernwärme mit Verbrennungsmotor kann unter bestimmten Bedingungen des Wärme- und Strombedarfs ebenfalls optimal sein (Beispiel: 7 MFH-Cluster). Photovoltaik wird gegenüber thermischen Solarkollektoren zur Dachbedeckung bevorzugt, wenn es um die Optimierung von Kosten und Treibhausgasemissionen geht. Diese Arbeit deckt bei weitem nicht den großen Bereich der Heizung und Kühlung im Gebäudesektor ab. Weitere Forschungen sind notwendig, um den Bedarf an Klimaanlagen, saisonalen Speichern sowie anderen Technologien wie Photovoltaikfassaden, Brennstoffzellen usw. besser zu berücksichtigen.

Résumé

Le concept énergétique optimal d'un groupe de bâtiments devrait être différent de la somme des solutions optimales des bâtiments considérés séparément. En relation avec cette affirmation, le projet OPTIM-EASE tente de fournir des réponses aux questions de recherche suivantes : 1) Quels sont les méthodes et les moyens les plus appropriés pour identifier et concevoir des systèmes énergétiques décentralisés pour des bâtiments individuels et des groupes de bâtiments afin de minimiser les coûts et les impacts environnementaux ? 2) Comment des objectifs différents et parfois opposés en matière de coûts et d'environnement peuvent-ils être traités ensemble ? 3) Dans quelle mesure le regroupement de bâtiments peut-il réduire les coûts et les impacts environnementaux de leur consommation d'énergie en exploitant leurs synergies par rapport à des considérations individuelles ?

Pour mener à bien cette tâche, dans le cadre du projet OPTIM-EASE, un cadre multi-objectif basé sur python, "optihood", a été développé et appliqué à 4 études de cas montrant une variété de configurations et de résultats. Ce cadre fournit un outil qui permet d'optimiser, en fonction du coût annuel équivalent et/ou des émissions de gaz à effet de serre, le choix des technologies, leurs capacités et leur fonctionnement horaire au cours de l'année.

Dans toutes les études de cas, le regroupement de bâtiments au sein d'une communauté énergétique s'est avéré bénéfique en termes de coûts et de réduction des impacts environnementaux par rapport à la somme des solutions individuelles. Si seule l'électricité est partagée entre les bâtiments au sein d'un micro-réseau, les prix de l'électricité se sont avérés être les principaux facteurs de coûts potentiels et d'avantages environnementaux. Les résultats montrent une diminution des coûts et des émissions de gaz à effet de serre de 16 % et 9 % respectivement. Le faible coût de l'électricité permet d’obtenir une couverture des besoins en chaleur plus importante par le biais de pompes à chaleur. Ensuite, si les flux de chaleur peuvent être partagés entre les bâtiments au sein d’un réseaux de chaleur, on peut s'attendre à des gains plus importants si l'infrastructure du réseau thermique coûte moins de 7 % à 40 % du coût annuel équivalent du système. Avec les facteurs d'émissions de gaz à effet de serre de la KBOB, les pompes à chaleur à air sont la technologie dominante lorsque les émissions de gaz à effet de serre sont optimisées. Cependant, les émissions de CO_2 des sondes géothermiques ont été mises à jour dans la KBOB en 2023 à la moitié de la valeur précédente, ce qui pourrait améliorer la compétitivité des pompes à chaleur géothermiques dans les études étudiées lorsque les émissions de gaz à effet de serre sont optimisées. La cogénération pour le chauffage urbain avec moteur à combustion interne peut également être optimale dans certaines conditions de demande de chaleur et d'électricité (ex : 7 bâtiments multifamiliaux). Le photovoltaïque est préféré aux capteurs solaires thermiques pour couvrir les toits lorsqu'il s'agit d'optimiser les coûts et les émissions de gaz à effet de serre. Ce travail est loin de couvrir le vaste domaine du chauffage et de la climatisation du secteur du bâtiment, d'autres recherches sont nécessaires pour mieux prendre en compte les besoins de climatisation, les stockages saisonniers ainsi que d'autres technologies telles que les façades photovoltaïques, les piles à combustible...

Summary

The optimal energy concept of a group of buildings is foreseen to be different from the sum of the optimal solutions of the buildings considered separately. In relation to this statement, the OPTIM-EASE project, tries to provide answers to the following research questions: 1) What are the most appropriates methods and means to identify and design distributed multi-energy systems(DMES) for individual buildings and groups of buildings in order to minimize the cost and environmental impacts? 2) How are different and sometimes opposite cost and environmental objectives handled together? 3) To which extent can grouping buildings reduce the cost and environmental impacts of their energy consumption by exploiting their synergies compared to individual considerations?

To carry out the task, a python-based multi-objective framework “optihood” was developed and applied to 4 case studies showing a variety of configurations and results. This framework provides a tool that can optimize according to the equivalent annual cost and/or greenhouse gases emissions the choice of technology, their capacities and their hourly operation over the year.

Across all the case studies, grouping buildings within an energy community is proven to be beneficial in terms of cost as well as to mitigate environmental impacts compared to the sum of individual solutions. If only electricity is shared between the buildings within a microgrid, electricity prices were shown to be the main drivers of potential cost and environmental benefits. Results show decrease in cost and GHG emissions of respectively 16% and 9%. A lower electricity cost allows a larger share of heat to be delivered through heat pumps. Then if heat flows are allowed to be shared between buildings, more gains can be expected if the infrastructure for the thermal grid costs less than 7% to 40% of the equivalent annual cost of the system. With the considered greenhouse gas (GHG) emissions factors from the KBOB, air source heat pumps are the dominant technology when GHG emissions are optimized. However, CO_2 emissions of the borehole heat exchanger were updated in the KBOB in 2023 to half the previous value, thereby increasing the competitiveness of ground-source heat pumps in the investigated studies. Heat-driven cogeneration systems for district heating with internal combustion engine can also be optimal in certain conditions of heat and electricity demand (ex:7 MFH cluster) photovoltaic is preferred over solar thermal collector to cover the roofs when optimizing cost and GHG emissions. The installed photovoltaic capacity was found to increase with the grid electricity and feed-in tariffs as the decreased grid electricity consumption and the increased revenue from feeding in excess photovoltaic electricity offsets higher investment costs. This work is far from covering the vast domain of heating and cooling of the building sector, more investigation is needed to better account for cooling needs, seasonal storages as well as other technologies such as photovoltaic facades, fuel cells, etc.

Main findings

- Grouping buildings into an energy community offers advantages in terms of both cost reduction and environmental impact mitigation. When local electricity production is exchanged within a microgrid, the price of electricity becomes the primary factor influencing potential benefits, enabling a larger share of heat to be delivered through heat pumps. Additionally, if heat exchange between buildings is permitted, further gains can be anticipated if the cost of the thermal grid infrastructure is less than 7% to 40% of the system's equivalent annual cost.
- Based on the cost and greenhouse gases emissions assumption, photovoltaic is the preferred technology to be installed on roofs. However, for small buildings, installation of photovoltaic array is not suggested at the cost optimum. For larger buildings and for energy communities, photovoltaic panels are almost always installed. The installed photovoltaic capacity increases at higher grid electricity and feed-in tariffs owing to the offset of higher investment costs with the decreased grid electricity consumption costs and the increased feed in revenues.
- Neighborhoods with significant heating and electricity demands, including buildings like hotels or at least 7 MFH are more suited to be powered with cogeneration district heating systems (heat-led). Heterogeneity in energy demands is also a key feature to benefit from grouping the buildings together while designing the energy systems instead of providing individual solutions.
- Consideration of dynamic GHG emissions of the electricity has been found to be interesting to reduce emissions during the operation phase with intelligent controls. However, high level of emissions during wintertime did hinder the use and size of the heat pump and PV systems.

Contents

Abbreviations

ASHP: Air source heat pump

BHE: Borehole heat exchanger

CAPEX: Capital expenditures

CHP: Combine heat and power

COP: Coefficient of performance

DHW: Domestic hot water

DHWS: Domestic hot water storage

DMES: Decentralized multi-energy systems

DSM: Demand side management

ESCO: Energy service company

GHG: Greenhouse gases

GSHP: Ground source heat pump

GWP: Global warming potential

HP: Heat pump

HWS: Hot water storage

ICE: Internal combustion engine

KPI: Key performance indicator

LCA: Life cycle assessment

LCC: Life cycle costing

MFH: Multi-family house

MOO: Multi objective optimization

OPEX: Operational expenditures

PV: Photovoltaic

SGSW: Sankt-Galler Stadtwerke

ST: Solar Thermal

STC: Solar Thermal Collector

WP: Work package

Extended Summary

Context & Project description

The energy demand profiles (thermal and electrical) of buildings vary over the year and many factors influence the demand such as the building typologies, user behavior, heating, cooling and domestic hot water consumptions, etc. In addition, the success of heat pumps for space heating increases electricity demand in winter. Conversely, on the supply side, decentralized intermittent electricity production systems (mainly photovoltaics) are used increasingly in order to meet the Swiss objectives for the energy sector and the Paris Agreement's goals. Consequently, there is an increasing mismatch between the building electricity demand and the decentralized electricity supply. Increased interest in innovative solutions such as micrograids and sector coupling concepts paves the way to find better solutions by looking at more than one building and by synergistic planning of heating, cooling, and electricity supply systems. These solutions for energy control, conversion and storage strategies are called "decentralized multi-energy systems" (DMES). They are emerging in Switzerland, offer a large potential for deployment and bring new business opportunities for energy service companies (ESCOs) while reducing energy consumption, costs and environmental impact of the buildings.

In this context, the following questions need to be answered:

- What are the most appropriates methods and means to identify and design DMES for individual buildings and groups of buildings in order to minimize the cost and environmental impacts?
- How are different and sometimes opposite cost and environmental objectives handled together?
- To which extent can grouping buildings reduce the cost and environmental impacts of their energy consumption by exploiting their synergies compared to individual considerations?

These challenges are dealt with by multi-objective optimization methods (MOO) combined with energy simulation tools. However, while MOO procedures at the building level can lead to specific optimal solution for decentralized multi-energy systems, results may change substantially when groups of buildings or whole neighborhoods are looked at together (for example within a microgrid). Considering a group of buildings together enables the valorization of the synergies between their demands (heating, cooling, DHW, electricity) and decentralized electricity production. In addition, the consideration of the synergies between electricity and heat demand can improve the efficient and rational use of energy. Furthermore, for a larger overall demand, technologies such as CHP may become economically feasible and optimal, while not being attractive for single buildings. Thereby, the optimal solution at the neighborhood level is not necessarily equal to the sum of the optimal solutions for each single building such as schematized in the Figure 1:

Figure 2 OPTIM-EASE project hypothesis: the optimum energy management for a group of buildings is not equal to the sum of the "optimal" solutions of each building looked at individually.

Considering and exploiting the synergies between buildings can lead to benefits regarding cost and environmental impacts of the energy system and its management concept. It is thus necessary to assess the influence of aggregating buildings within a neighborhood to define optimal choice of components and control strategies.

In order to provide a realistic cost and dynamic environmental assessment, the OPTIM-EASE project aims to focus on three goals:

- To enhance and optimize the synergies between energy needs (thermal & electrical), decentralized energy production, eventually within a microgrid, and the electricity grid to mitigate the cost and environmental impacts.
- To study the influence of dynamic and multi-criteria environmental impact considerations on the optimal energy concepts definition for buildings and group of buildings.
- To assess the influence of grouping buildings compared to individual solutions from cost and environmental KPIs.

Based on the context and project goals, three research questions have been identified and will be tackled during the project:

1. What is the influence of the synergies of the energy demand, local production and choice and management of components, when grouping buildings instead of considering them separately?
2. How will the cost and environmental optimal solution of interconnected buildings evolve according to their size and group's composition?
3. Compared to traditionally used cost and energy KPIs, what is the influence of including dynamic Life Cycle based environmental impacts on the optimal solutions at the building and building group levels?
4. Which technologies that are not competitive at the single building level can become of interest when considering groups of buildings?

Procedures and methodology

To tackle the issue at hand, a MOO framework called Optihood was developed based on the oemof tool due to its alignment with most of the required criteria. This framework integrates MILP optimization techniques with dynamic energy and life cycle assessment (LCA) simulations. Drawing from a predefined set of technologies including among other specific case study technology : heat pumps (both air source: ASHP and ground source: GSHP with borehole heat exchangers), photovoltaic (PV) panels, solar thermal (ST) collectors, for HP and energy storage options (both electrical and thermal), Optihood optimizes the selection, sizing, and operation of the energy system, guided by two objective functions assessing respectively costs (mean annual cost) and environmental impact (mean annual GHG emissions). Additionally, the tool facilitates the optimization of building energy systems under two scenarios: 1) Individual buildings with their respective energy systems, where surplus electricity is sold to the local energy provider. 2) Buildings organized into an energy community via an electrical microgrid and eventually a thermal grid, enabling shared local electricity and heat production among them; electricity purchases are pooled to benefit from favorable pricing.

For specific case studies, gas technologies (Boilers and heat-led CHP) using either natural, synthetic, or renewable gas were included when they were already present (Romande Energy case study) or when relevant to answer stakeholders' questions (SGSW case study, and renewable gas assessment). However, according to the SFOE's heat strategy 2050, fossil gas is banned from the energy sector and synthetic and renewable gases are used to cover heat requirements at high temperatures for industrial processes and not for buildings. Due to low relevance for the future energy landscape in Switzerland, the detailed results on these technologies are kept to their specific sections in the report (3.2, 3.3, 3.4)

Romande Energie case study

This case study carries out a retrospective optimization of the energy framework applied to a novel real estate development in the Lausanne region of Switzerland. The development comprises six Minergie A buildings, each equipped with photovoltaic (PV) panels and utilizing ground source heat pumps (GSHP) for space heating (SH). Building 4 also provides heat to buildings 5 and 6 and generates domestic hot water (DHW) using a GSHP, while buildings 1, 2, and 3 use solar thermal (ST) panels and a backup gas boiler for DHW production. To simplify the optimization, buildings 4, 5, and 6 are considered as a single entity.

Table 1 presents detailed information on the number of dwellings, dwelling and shop areas, roof area, installed energy systems, and storage capacities for each building. Additionally, the cooling and refrigeration equipment for the supermarket is owned and operated by the retail company, with electricity consumption accounted for in building 4. It is noteworthy that the condenser heat from the cooling and refrigeration equipment contributes to balancing the heat source for the GSHPs through the borehole heat exchanger (BHE). Table 2 presents the energy cost hypothesis and energy demand for all the investigated scenarios.

Buildings	Nb of dwellings	Dwellings area (m²)	Shops area (m²)	Available roof area (m²)	GSHP (kW)	Gas boiler (kW)	PV (kWc)	Solar thermal (m²)	DHW storage (L)	SH storage (L)
1	76	7 751	1 003	1100	188	320	~50	88	3 500	3 000
2	72	6 883	932	1100	170	300	~47	73	3 500	3 000
3	44	3 940	516	630	92	200	~30	37	2 500	1 000
4 (5&6)	92	8 237	810	1650	220	-	107	-	6 000	2 000
TOTAL	284	26 811	3 261	4 480	670	820	234	198	15 500	9 000

Table 1: Buildings areas and actual installed energy system in the Romande Energy case study

Investigated scenarios		Energy cost hypothesis			Energy demand
		Gas	Electricity	Electricity feed-in	
group vs individual	Group Optimization	8.7 c./kWh	19 – 12 c./kWh	7.2 c./kWh	From 2021 monitoring
	Individual Optimization with Peak/Off-peak prices	8.7 c./kWh	22 - 12 c./kWh	9.5 c./kWh	From 2021 monitoring
	Individual Optimization with constant prices	8.7 c./kWh	22 c./kWh	9.5 c./kWh	From 2021 monitoring
Price sensitivity study	gas/electricity price ratio of 2/1	22 c./kWh	44 c./kWh	18.3 c./kWh	From 2021 monitoring
	gas/electricity price ratio of 3/1	14.7 c./kWh	44 c./kWh	18.3 c./kWh	From 2021 monitoring
	gas/electricity price ratio of 4/1	11 c./kWh	44 c./kWh	18.3 c./kWh	From 2021 monitoring
Heat pump operation optimization		8.7 c./kWh	19 – 12 c./kWh	7.2 c./kWh	From 2021 monitoring
EV influence (gas/electricity of 3/1)		14.7 c./kWh	44 c./kWh	18.3 c./kWh	From 2021 + 250 EV (525 MWh)

Table 2: Summary of the scenarios investigated in the Romande Energy case study.

1. Group vs individual.

The study investigates the energy tariffication boundaries in the context of a real estate development in the Lausanne region, Switzerland. Large consumers benefit from lower energy prices due to scale effects, leading to variations between energy community and individual solutions. Three optimization scenarios are examined: one for the energy community and two for individual buildings with different electricity pricing schemes. The energy community, considered a large consumer, owns an electrical microgrid connecting buildings and a transfer station. Gas prices are consistent across all scenarios at 9.7 c./kWh, while electricity prices vary based on peak/off-peak schemes (19/12 c./kWh for energy communities and 22/12 c./kWh) and constant schemes (22 c./kWh).

The results highlight the cost and GHG emissions advantages of the grouped optimization over individual optimizations. In terms of magnitude, decrease in cost and GHG emissions range respectively by 16% and 9%.

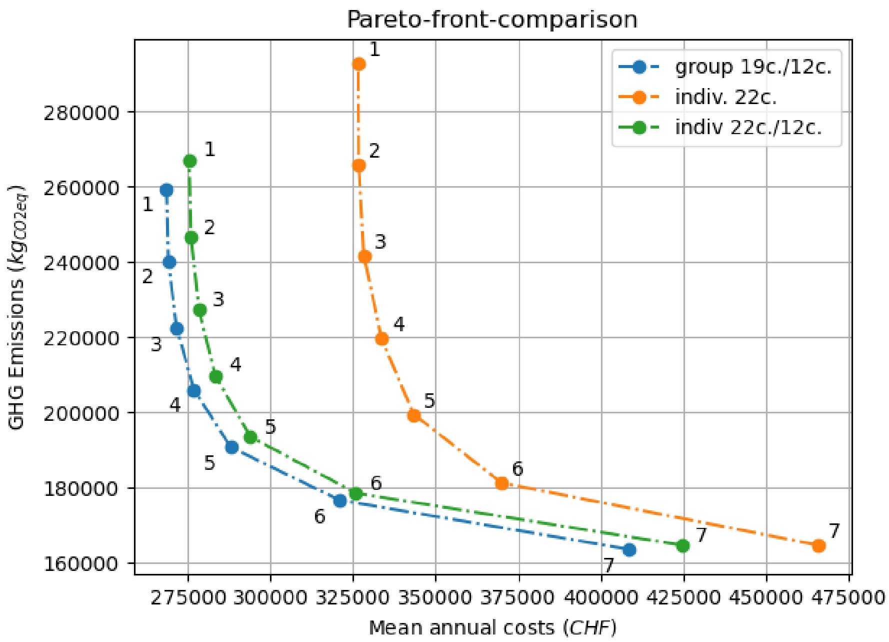

Figure 1 : Pareto front representation of the 3 scenarios investigated in the Romande Energie case study: orange line: individual optimization of the building with constant electricity prices of 22c./kWh, green-line: individual optimization of the buildings with peak/off-peak prices, blue-line: grouped optimization with peak/off-peak prices. See section 3.1 for detailed results on points 1 to 7.

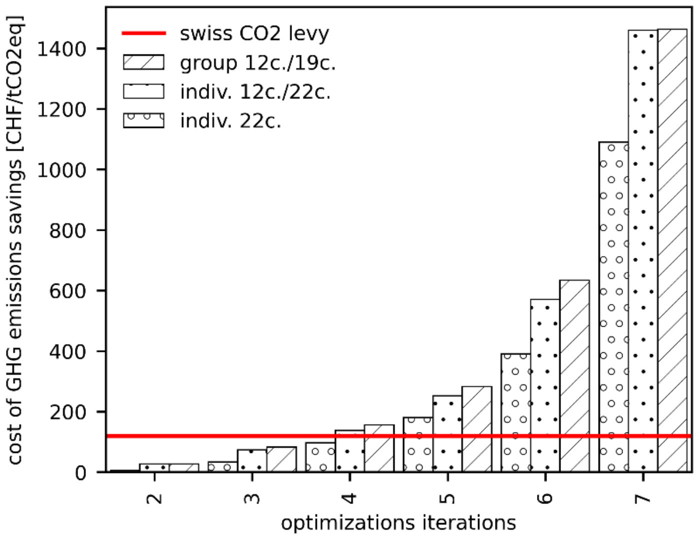

Figure 2 : Cost of CO2 savings between the pareto front point of for the three scenarios comparing group and individual solutions, (group 12c./19c, individual 12c./22c and 22c.) in relation to the actual CO_2 levy in Switzerland (120 CHF/tCO2eq).

Figure 2 shows for all scenarios the cost differences per GHG emissions savings in tCO_2eq saved between the cost optimum and the other optimization iterations on the Pareto front and reveals the competitiveness of the decarbonisation measures in relation to the CO_2 tax applied on fossil fuels in Switzerland set at 120 CHF/tCO_2eq (red line). From the 5th iteration, all scenarios present savings higher than the tax. Obviously, the scenario with the highest electricity cost shows the best potential of cost effective decarbonation.

2. Operation optimization

This scenario centers on optimizing the operation of the energy system in regards of heat and electricity use and production and dynamic prices and GHG emissions of the grid electricity. The system configuration remains constant, corresponding to the actual installed equipment of this test case. Consequently, there is no optimization carried out regarding the selection of technologies or their capacities. The energy pricing structure aligns with the group price scheme employed in scenario “group vs individual".

No obvious benefits in operation optimization were found for the space heating production in contrast with the DHW production where heat can be stored, and use shifted more efficiently. Figure 3 depict the DHW generation by groundwater heat pumps (GWHP) in comparison to the effective electricity price[1] over a five-day period for cost optimized control strategies. GWHP production occurs when possible and at full power during low-cost periods, while during high-cost period the GWHP load is rationally scaled to cover the demand.

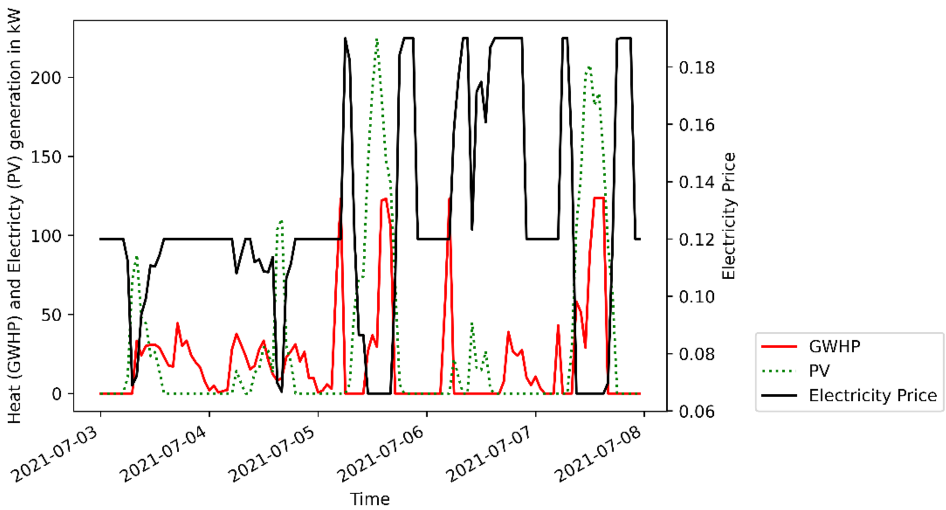

Figure 3 Domestic hot water generation by the GWHP in comparison to the real electricity price over a five-day period for the cost optimized control strategy.

In a similar manner GWHP operation optimization can be carried out considering dynamic GHG emissions calculated according to Ecodynelec tool [1] for the grid electricity and the locally produced electricity with PV. Same days as previously are shown in Figure 4. By considering the GHG emissions, the previous shifts noted in Figure 3 are now occurring when the GHG emissions are low. The GWHP tries to operate as much as possible on periods with low GHG emissions for electricity. The similar

[1] The price signal is calculated considering the price of the electricity bought from the grid and from the PV installation.

pattern in both optimization iteration suggests that both electricity price and GHG emissions have some common dependences (e.g., the PV production have low levelized costs and low GHG emissions).

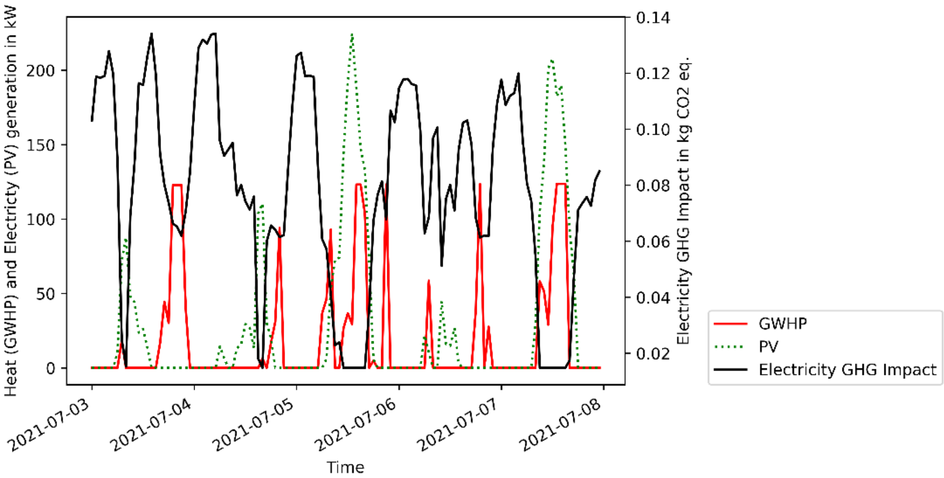

Figure 4 Domestic hot water generation by the GWHP in comparison to the electricity GHG emission impact over a five-day period for the GHG emission optimized control strategy.

3. Integration of electric mobility

This scenario investigates the impact of incorporating electric vehicles (EVs) into the energy system of the group scenario with the price boundary favorizing important local energy production, price scenario 3/1. 250 EVs (525 MWh) were considered representing 38% of the actual electricity demand. The hourly profile was derived from monitoring data and scaled to the assumed number of vehicles.

Higher electricity demand from EVs necessitates a greater reliance on the electricity grid. Without EVs, the self-sufficiency rate (local electricity consumption over total electricity consumption) reaches 45% at the economic optimum. With EVs, the self-sufficiency rate drops to 25% at the economic optimum. Despite the increased electricity demand, the CHP capacity utilization remains relatively unchanged since the CHP is sized to meet the heat demand.

Energie360 case study

The Energie360 case study is composed of 4 newly constructed residential buildings, with 77 dwellings (10'300 m^2), built as per MINERGIE-ECO® and SIA-Effizienzpfad Energie standards. The key interest in this case study lies in highlighting the benefits of linking the energy systems together to supply the demands of the buildings. The buildings were thermally and electrically connected, also the same grid electricity pricing was considered in both individual and grouped optimizations.

The considered technologies in this case study include heat pumps (air-source and ground-source), PV, thermal energy storages and electric rods for covering the heating peaks. Optimizing the buildings together with the target of cost minimization led to 7 % cost savings and 3 % environmental impact reduction as opposed to the buildings being optimized separately. The cost optimum collective solution for buildings was to implement a central PV, central ASHP and central storages for DHW and space heating. While decentral installations of ASHP and thermal energy storages (without any PV installation) were selected when buildings were optimized individually. The cost of district heating and electricity links were neglected in this evaluation and therefore, the economic and environmental benefits of collective optimization would arise only if they do not cost more than the respective reductions gained. These reductions would be even higher if lower grid purchase costs were assumed in collective optimization than in case of the buildings optimized individually. Between air-source and ground-source heat pumps as the alternative heating technologies, we found that an air-source heat pump (ASHP) was chosen in the cost optimization. This is true with an assumption where a ground-source heat pump (GSHP) costs 2.6 times higher than an ASHP per kW of installed heating capacity (including boreholes). A GSHP, however, would be more economical if it costs 1.5 times (or less) higher than an ASHP, which may not be unrealistic. Moreover, the currently installed PV capacity and heat pump capacity could be reduced by 60 % and to less than half, respectively, as a result of collective cost optimization of the buildings, by employing 37 % larger thermal energy storage capacity. The currently installed heating system was designed based on the typical design values by the building codes, and the PV capacity was selected to maximize the utilization of the available roof area. While interpreting these reductions in the installed capacities, it should be noted that the measurement data used in the optimization was not from a typically cold period. Additionally, the reduction in capacities relies as well on the optimum operation of the systems (and optimum use of synergies in power-to-heat conversion), which could be achieved in practice by using a smart controller.

Furthermore, about 7-40 % reductions in total annualized cost were observed when buildings were optimized together as a group in multi-objective optimization with costs and emissions as the two competing targets (compared to buildings optimized individually). Again, it is important to note here that the costs/emissions associated with district heating and electricity links were not included and an equal grid-purchase tariff has been assumed for individual and grouped optimizations. An intriguing observation was noted in the environmental optimum, where again an ASHP installation was selected instead of a GSHP when minimizing the emissions. This choice, however, could be linked to the higher LCA impact of GSHP (about 2.7 times more) and a higher-than-expected SPF of ASHP (about 3.7 compared to 4.1 from GSHP).

In addition, the cost optimum central installation of PV and GSHP along with central thermal energy storages achieved 10 % lower total annualized cost when compared to the corresponding cost optimum decentral installation without any PV. The GHG emissions in the former case were found to be 12 % lower than the optimum decentral installations without PV. This is clearly because of the use of emission-free PV electricity in case of central PV and GSHP installation. If decentral PV installations are included as well along with decentral GSHP and decentral storages, the cost of the corresponding central installation was found to be 14 % lower at a negligibly (< 1 %) higher environmental impact. Further, an operation optimization of the currently installed system design (on site) resulted in both higher costs and emissions (1.7 times and 1.2 times, respectively) than the cost optimized central design with PV, GSHP and thermal energy storages. The higher costs and emissions are predominantly due to the higher installed capacities in the current installation, which is based on the design values from the planning process and not the actual measured data during system operation. Also, the actual on-site installation consists of two GSHPs, one mainly for DHW and the other for providing space heat, instead of a single GSHP providing both DHW and space heat in the cost optimized central design (PV, GSHP and thermal energy storages). In terms of the self-sufficiency factor, the operation optimization of the currently installed system capacities achieved a 9 % higher value compared to the cost optimum central design of PV, GSHP and thermal energy storages. But the generated PV electricity was mainly fed into the grid in the former case and thus, the self-consumption factor was about 38 % lower.

Finally, we found that both the choice and the sizing of technologies in the optimum design solutions are rather sensitive to the cost/price assumptions. As mentioned earlier, the cost optimum solution for buildings optimized individually was to implement decentral installations of ASHP and thermal energy storages (without any PV). If the installation cost of PV was reduced by 5 %, then installing decentral PV resulted in lower total annualized cost compared to not installing them (using only the grid). If we assume the environmental benefits from electricity fed into the grid to be equal to the environmental impact of grid electricity, then the annualized environmental impact as well is lower in the former case. Moreover, when the buildings were optimized collectively, the cost optimum installed PV capacity increased from no PV installation in case of low grid-purchase cost (8.49 c/kWh) to central PV installations for both medium (27.2 c/kWh) and high (70.8 c/kWh) grid-purchase costs. The resulting central PV installation was observed to be approximately 2.5 times higher as the grid-purchase tariff increased from medium to high. Furthermore, the cost optimal capacity of central PV installation increased 8.6 times as the assumption in the electricity feed-in tariff was varied from low (3.77 c/kWh) to high (21.75 c/kWh). The total annualized costs were found to be reduced with an increase in the feed-in tariff. This is due to higher revenues earned by feeding the excess PV electricity into the grid, also thanks to higher installed PV capacities which become economical as the feed-in tariff increases.

SGSW case study

The case study from SGSW examines the optimal energy system designs for a diverse-use district in St. Gallen. The district comprises 56 buildings with various usage types. Two scenarios are analyzed: the first focuses on 12 multi-family houses connected to a CHP plant (at the actual installation site), optimizing energy conversion and storage technologies individually and grouped for different cluster sizes; the second considers all 56 buildings, optimizing them individually and grouped while comparing the optimal system configuration to existing technologies and inspecting the share of energy demand supplied by renewable energy sources.

A central CHP plant of 404 kWth capacity, along with central storages for DHW (1.3 m^3 capacity) and space heat (28 m^3 capacity), was found to be the most promising technology design for the group of 12 MFH buildings (Scenario 1) based on a cost minimization. While the current on-site installation for these buildings is as well a CHP plant, the capacity of this plant is 242 kW_{th} (40 % lower than the cost optimum sizing) with decentral gas boilers of overall 564 kW capacity for meeting the remaining heating demand. Therefore, by increasing the capacity of the CHP plant, it would be possible to completely replace the decentral gas boilers. Moreover, the use of non-renewable fuels could be avoided if renewable gas is used as the primary energy source of the CHP plant, in future, instead of natural gas.

Installing a central CHP plant became the cost optimum choice when a cluster (or group) of at least 7 MFH buildings were optimized collectively. The size of central CHP plant in this case was evaluated as 224 kW_{th}. For cluster sizes up to 5 MFH buildings, a central ASHP along with small electric heating rods to cover the peaks was concluded as the optimum heating technology. Based on our assumptions, an ASHP costs 30 % lower per kWth capacity than a CHP plant. In addition, ASHPs benefit from higher performance efficiency and as a result, despite the grid electricity being more expensive than natural gas, the operational cost of an ASHP is relatively lower. Therefore, for the CHP to become more economical over an ASHP installation, the benefits from the combined production of heat and electricity would need to overcome these cost and performance gaps. Since the assumed installation cost of a CHP plant in this case study was already lower than those used by the SGSW project planners, we decided not to study the impact of a further reduction in the CHP installation cost. We, therefore, investigated the influence of lowering the gas price on the choice between an ASHP and a CHP installation. A central CHP installation of 180 kW_{th} was determined as the cost optimum choice for the group of 5 MFHs if the gas price is reduced by 20 % (6.9 c/kWh) or more up to 50 % (4.3 c/kWh). If the gas price is lowered by 30 % (6.1 c /kWh) or more then installing a central 117 kW_{th} CHP plant becomes the economical solution even for the cluster of 3 MFHs. Whereas a CHP plant was not an economical choice for a single MFH or 2 MFHs even at 50 % lower gas prices.

Delving into the topic of environmental optimization of the group of 12 MFHs from the first scenario, we found that solar thermal collectors (STC), ASHP (supported by electric rods) and PV were selected instead of a CHP plant. Electrical batteries were employed to store PV electricity during low sunshine hours, which led to a 54 % decrease in grid electricity consumption compared to the cost optima. This was achieved by choosing a very high capacity for the electrical batteries (capable of storing 6.7 h of peak PV power), which reduced the LCA impact but increased the cost significantly. Furthermore, in case of cost optimization, about 70 % of the annualized cost resulted from system operation, i.e. the use of grid electricity and natural gas. While the operation of the systems contributed towards a mere 5 % of the total annualized cost in the environmental optimum resulting only from the use of grid electricity. Nonetheless, the annualized cost of the environmental optimum design was found to be nearly 3 times higher than that of the cost optimum design. A major contribution (about 58 %) here comes from the large batteries installed in the environmental optimum. Moreover, about 95 % of the GHG emissions in the cost optimum design arise from the system operation. Therefore, optimization of system operation would be quite relevant for obtaining the highest benefits from the cost optimum design. This could be achieved, in reality, by implementing a smart control to optimize the use of grid electricity and natural gas during the operation of the system. The contribution of GHG emissions resulting from the system operation in the environmental optimum design were found to be around 38 %.

In the second scenario (Scenario 2), all the 56 heterogenous-use buildings were considered. PV, ASHP and CHP plant were selected in the cost optimization both when the buildings are optimized together as a group and individually. Central solutions appeared when the buildings were optimized together, while decentral installations of the said technologies were chosen for individual building optimization. In collective optimization, the installed capacity of the central CHP plant was found to be 2.5 times higher, while that of the central ASHP was reduced to half compared to individual building optimization. Furthermore, the total installed thermal energy storage capacity in the cost optimum design was reduced by 5 % by incorporating district heating in the collective building optimization. The total annualized cost of the cost optimum designs in individual optimization was found to be 19 % higher than that in collective building optimization (excluding the cost of district heating and microgrids). Therefore, the centralized cost optimum setup in collective building optimization could be considered economical if the network costs do not exceed 19 % of the total annualized cost. In terms of the share of technologies in the total electricity production, we observed that the contribution from PV and CHP increased by 11 % and 4 %, respectively, when the buildings were optimized collectively leading to centralized system installations. As a result, the grid electricity consumption was found to be lower in collective building optimization. Additionally, in collective building optimization the share of DHW demand covered by the CHP plant is higher when compared to the share covered by an ASHP. This is due to higher operation temperature and consequently, a lower COP of ASHP for DHW than for space heat production. Based on the same reasoning, the production from ASHP is higher for space heat than for DHW in the cost optimum both when the buildings are optimized individually and as a group.

Moreover, in the environmental optimum all the technologies except CHP plant (i.e. ASHP, GSHP, STC and PV) were chosen in both individual and grouped building optimization for Scenario 2. The selection of STC in the environmental optimum is expected, however, the selection of both GSHP and ASHP technologies might not be that apparent. GSHPs have a large LCA impact from the installation of boreholes (2.7 times higher per unit installed capacity than an ASHP), but they have better efficiency especially at lower ambient air temperatures. Therefore, in the environmental optimum GSHPs operate during the periods with high GHG emissions and low ambient air temperatures. The overall installed capacities of STCs and DHW storages in the environmental optimum are 39 % higher and 3 times higher, respectively, if the buildings are optimized individually. Moreover, the cost of the environmental optimum is significantly higher than the cost optimization (and the intermediate optimization runs) both in individually and collectively optimized buildings. This is due to the inclusion of large electrical batteries to reduce the grid electricity consumption during high CO_2 emission periods. The grid electricity consumption in the environmental optimum solutions is reduced to about 39 %, from 61 % in individual cost optimization and 46 % in grouped cost optimization. Furthermore, in the intermediate optimization runs, the optimum decentralized system designs for individual buildings were found to be 23-38 % more expensive than the optimum system designs in group optimization (cost of district heating and microgrids links excluded). Thus, in these runs, the central installation setups suggested by optimizing the buildings together could be considered economical if the links don’t cost more than 23-38 % of the total annualized cost.

Conclusions

The project OPTIM-EASE allowed the development of the open-source python framework optihood for optimizing energy systems at the neighborhood scale. Built upon the oemof framework[2], it offers several enhanced features, including a simplified scenario/problem definition using config or excel files, multi-objective optimization based on cost and GHG emissions criteria, technology models for HP, individual or group building optimizations, and an option to improve computational speed through day clustering. Optihood's versatility extends to optimizing a diverse range of energy systems, encompassing district heating, microgrids, and neighborhoods with a mix of residential, commercial, and industrial buildings. Optihood is an open-source framework readily available on GitHub[3] and accompanied by comprehensive online documentation[4].

The conclusions drawn from specific case studies are expected to be extrapolated to similar neighborhoods but not to cases with strong differences in energy demand and buildings with other shape factors or internal gains. The shape factor changes mostly the roof area available per square meter of heated floor area and thus the size of the potential PV system.

Grouping buildings within an energy community is seen to be beneficial in terms of cost as well as for mitigation of environmental impacts. If only electricity is shared within a microgrid, electricity price is seen as the main driver of the potential benefit allowing a larger share of heat being delivered through heat pump. Then if heat flows are allowed to be shared between buildings, more gain can be expected if the infrastructure for the thermal grid was less than 7% to 40% of the equivalent annual cost.

Based on the cost and greenhouse gases emissions assumption, photovoltaic is the preferred technology to be installed on roofs. However, for small buildings, installation of photovoltaic array is not suggested at the cost optimum. For larger buildings and for energy communities, photovoltaic panels are almost always installed.

Results are subject to the hypothesis in the cost and emissions parameters. GSHP is impeded by the emissions factor for the borehole heat exchanger. It was updated in the KBOB in 2023 to half the previous value, this could change the competitiveness of GSHP in the investigated studies. To generate robust results, uncertainty of the cost and emissions parameters should be considered in future research. Uncertainty evaluation infers higher calculation burden and should be resolved in future work.

2 https://oemof.org/
3 https://github.com/SPF-OST/optihood
4 https://optihood.readthedocs.io/

1 Introduction

1.1 Background information and current situation

The Swiss Energy Strategy 2050 relies on a strong modification of the national energy system so as to reduce greenhouse gas emissions down to net-zero or even to net-negative values. In these 30 years forecast, it is expected that fossil energy consumption will be dwarfed, while flattening the electricity demand's growth. In addition, renewable energy sources should cover largely the electricity demand as well as the demand for heating and cooling [2].

In order to meet these objectives, the energy demand of buildings needs to be drastically reduced and rationalized, as it represents a large share of the national energy demand [3]. However, the buildings' heterogeneity (construction period, usage, user behavior, etc.) increases the complexity in achieving this objective. Current trends to tackle the CO_2 footprint of buildings are to renovate the building stock (to limit the demand) and to use heat pumps or district heating instead of decentralized fossil heating systems to cover the heat demand, as well as to use photovoltaics to cover part of the electricity demand [4] However, the consumption of fossil fuels by the building stock needs to be reduced quickly to meet the national objectives. Innovative solutions are thus needed to meet these goals.

In parallel, the production of renewable energy, especially renewable electricity, should be strongly increased in order to compensate for the phasing out of nuclear power generation while at the same time provide enough electricity for increasing electrification of mobility and the heating sector (via heat pumps), thus limiting imports. So far, a massive deployment of photovoltaic technologies is observed in Switzerland [5]. While this is positive in terms of climate change mitigation, it is at the same time obvious that the decentralized electricity production from PV installations at the building level with all the electricity produced during daytime and most of it in summer, does not perfectly match the daily (Figure 1) or seasonal demand of heat and electricity of the buildings.

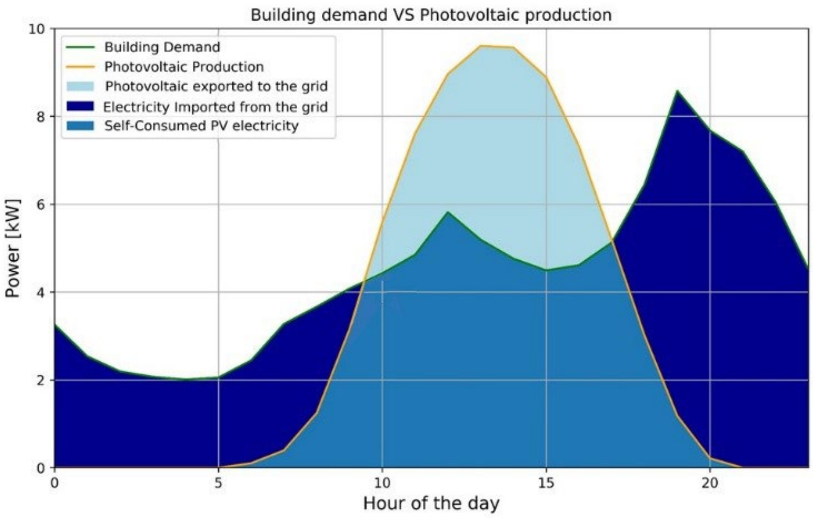

Figure 5 Building electricity demand compared to photovoltaic production for a typical day.

Therefore, regarding the energy demand of buildings, there is a special need to bridge the gap between demand and supply. At the building level, there are several solutions that are currently implemented or under investigation (load shifting, energy storage, etc.). However, for individual buildings, many of them are still expensive and are unfortunately not yet widely implemented in practice [6]

One of the promising solutions, regarding the demand/supply gap, is to enhance the system boundaries and to consider several buildings together as a whole system, i.e. grouping buildings within an energy community. By doing so, three benefits can be obtained:

1. It fosters the exchange of energy between buildings and reduces the total energy cost compared to individual buildings by improving among others the self-sufficiency of the group of buildings. [7]
2. The heterogeneity of the building load profiles eases the energy balance between the supply and demand sides. Moreover, inefficient part-load operation can be reduced.
3. Larger and different energy conversion units (cogeneration, storage, etc.) can be considered with higher energy generation efficiencies and lower specific investment costs.

These solutions for energy control, conversion and storage strategies are called "decentralized multi-energy systems" (DMES). The concept of DMES aims at defining adequate energy management and conversion strategies that encompass demand and supply aspects (energy management, storage, different energy production options, etc.) for a group of building instead of developing individual building solutions. The energy management strategy at the neighborhood level is indeed not necessarily equal to the sum of the optimal solutions for each single building, such as represented in Figure 2, and grouping buildings can be of interest to reduce the environmental impact and cost related to building energy demand. It is necessary to assess the influence of aggregating buildings within an energy community to define optimal energy control, conversion and storage strategies for groups of buildings.

Figure 6: OPTIM-EASE project hypothesis: the optimum energy management for a group of buildings is not equal to the sum of the "optimal" solutions of each building looked at in isolation.

Decentralized multi-energy system (DMES) solutions are emerging in Switzerland especially because of the law on energy (SR 730.0 Art. 16-18 & SR 730.1 Art. 14-18) which allows creating energy communities since 2018. The possibility to create energy communities offers a large potential for the deployment of decentralized production and optimization of the produced energy while bringing new business opportunities for energy service companies (ESCOs [2]). These concepts have the potential to reduce the energy consumption, cost and environmental impact of the building sector such as confirmed by several studies [8,9]. Thereby, energy communities and DMES could play a significant role in the Swiss energy transformation. Nevertheless, so far, no quantitative comparisons between the cost and environmental impacts of DMES for groups of building (i.e. pooling their energy production, management and control strategies), compared to the sum of individual DMES for buildings considered separately, have been performed. The interest in grouping buildings has therefore not been quantified compared to individually optimized solutions.

To make this quantitative comparison possible, it is necessary to identify suitable DMES for groups of buildings and for single buildings when considered separately. However, the reliable definition of such energetic concepts is a complex task. On the one hand, from the supply side perspective, it requires to consider a large set of technologies to harvest energy (decentralized systems such as photovoltaic, solar thermal, ground source, air source, etc.), store energy (thermal and electrical in a short or long-term perspective) and convert energy (heat pumps, CHP, gas boilers, etc.) as well as the available networks (electrical, gas, thermal). In addition, these systems interact with each other, and they can be mixed. On the other hand, from the demand side perspective, the heterogeneity of the buildings' load profiles (related to various typologies, construction periods, etc.) and eventually Demand Side Management (DSM) concepts need to be considered. Moreover, both demand and supply aspects are closely interacting and need to be addressed consistently for the proper definition of the separate buildings or grouped buildings performance. Finally, the definition of the Key Performance Indicators (KPI) that characterize the performance is a key issue since it is necessary to consider economic and environmental performance so as to propose solutions that will comply with the future energy landscape. Thus, developing an appropriate DMES concept, either at the group of buildings level or at the individual scale (buildings considered separately) implies the use of advanced computational methods that consider all the above presented variables (type of production and conversion technologies, storage solutions, energy demand profiles of buildings, etc.).

Indeed, the improvement process generally currently used in the building energy sector follows the rule of "step by step configuration assessment" (i.e. only few scenarios considered), which leads to sub-optimal energy concepts (local optimum for example) implying higher cost or non-minimized environmental impacts. Thus, it is necessary to encompass a large set of possible technical configurations (energy harvesting and conversion technologies, storage, etc.), including their cost and environmental impacts, which requires to develop a specific framework in order to avoid an extensive and time-consuming approach of calculating many variants manually in a pre-study.

In this context, the following questions need to be answered:

4. What are the most appropriates methods and means to identify and design DMES for individual buildings and groups of buildings in order to minimize the cost and environmental impacts?
5. How are different and sometimes opposite cost and environmental objectives handled together?
6. To which extend can grouping buildings reduce the cost and environmental impacts of their energy demand by exploiting their synergies compared to individual considerations?

1.2 Purpose of the project

These challenges can be dealt with by multi-objective optimization methods (MOO) combined with energy simulation tools. In MOO, cost and other KPIs (such as environmental, cost or energy indicators) are calculated for various configurations, including various decentralized energy production systems (type and size), energy management strategies, short- and long-term storages (thermal and electrical), the number of buildings to consider, the various buildings load profiles and their interconnection. Based on these results it is possible to identify the most suitable solutions for DMES for grouped and single buildings by characterizing a Pareto front between investment, operation costs and environmental impacts that gives a set of optimal solutions that cannot be modified without making one criterion worse. These methods have shown a large interest in particular when designing DMES. However, until recently, most studies have considered only the supply side (i.e. the decentralized energy integration) and only few studies have addressed both supply and demand size (considering the energy performance of buildings) [10]. Thus, considering demand and supply side together is essential, especially with the increasing use of heat pumps and thermal storage solutions.

Thereby, MOO approaches are of strong interest since they allow for the identification of optimal solutions while considering a broad range of possible configurations. This approach could serve as a basis for ESCOs or public authorities to develop strategies that minimize the cost and the environmental impacts regarding the building energy demand over a given district (letter of support and co-fundings for the OPTIM-EASE provided by private companies confirm such needs). However, in such optimization approaches, two main aspects need to be considered:

- Adequate and realistic models for the energy conversion and storage management,
- Key Performances Indicators (KPI) and adequate data base for their calculation,

In order to identify optimal energy systems, control and management strategies within an MOO framework, the definition of the energy model is a key aspect. First, technological models for each of the technical systems need to be defined. They need to encompass a wide range of possible technical systems (including DSM, supply technologies, etc.). For each of them, their characteristics (for example nominal power for the production systems) have to be varied and the statistical variability of the energy demand has to be considered (building characteristics, grouping characteristics for DMES, etc.). These technological models need to:

- Encompass dynamically energy, cost and environmental aspects,
- Be reliable and representative for the technologies' performances[5] (for example by including part load efficiencies),
- Be simple enough in order to be further integrated and aggregated for larger systems.

The partners involved in OPTIM-EASE have developed such type of simple but accurate and fast calculating technological models within research projects [11,12] and for educational purposes, and these can now be used for the OPTIM-EASE project. The integration into larger systems while enabling to operate different technologies synergistically together has to be developed. The interactions of the technologies between each other into energy systems and their integrated performances estimation including the energy control and management strategies is a key aspect that has been identified as a key issue regarding the DMES [13]. Finally, the MOO model has to be defined in order to identify the optimal solution that will minimize (or alternatively maximize) the chosen KPI. Different MOO methods have been developed and applied within the building energy context such as Mixed-Integer Linear Programming (MILP), genetic algorithm, etc. [14]. However, it appears that within these works, the energy models were always very simplified (for example considering a constant COP of heat pump performance no matter the heat demand profile or the external temperature for air/water devices), in order to allow for a fast and thorough resolution of the optimization problem [15].

Furthermore, within the existing published research, the cost, energetic and sometimes environmental gains are quantified between the optimized DMES system and the initial situation of the buildings (ex-ante situation) [13–16]. The cost and environmental benefits include both the use of newly implemented technical systems (decentralized electricity production systems, storage, etc.) mixed with the synergy effect of aggregating the buildings. However, the assessment of the benefits between individually optimized solutions (each building separately) and the energy community optimized solution (i.e. optimization of the group of buildings) has not been quantified in these studies. Characterizing separately both effects, i.e. new technical solutions and grouping of buildings, by performing optimization for each building separately and comparing the results with the optimized DMES of a group of buildings, is thus of high interest. Only this method allows to decompose the contributions from grouping and from new technologies and characterizes the key factors that drive the interest in grouping buildings so as to justify the deployment of more complex technologies for the coupling of buildings.

The choice of the KPIs to be selected for the decision process is a key issue. While cost is always of interest because it drives the investment decision, it can be necessary to distinguish between investment cost (CAPEX), operational cost (OPEX), and annuities or net present value (NPV). Considering different metrics can indeed lead to different optimal design solutions since they serve different objectives. The environmental aspects are also of strong interest since the developed solution needs to contribute efficiently to the reduction of impacts of the building energy supply. However, a proper assessment of multi-criteria environmental impacts (using Life Cycle Assessment, LCA methods) is only rarely considered. In addition, when taken into account, there are often two limitations. First, it considers generally one single KPI indicator, mostly the Global Warming Potential (e.g. GWP100), while there are different indicators that can be assessed such as the non-renewable primary energy consumption. Secondly, when dealing with electricity consumption, actual environmental KPIs assume a constant value for its environmental impacts, no matter when the electricity is consumed. However, the

[5] Performances are characterized with the energy conversion efficiencies and GHG emissions.

environmental impacts of electricity consumed from the Swiss grid (GWP, non-renewable energy consumption, etc.) are dynamic, as they vary depending on the hour of the day or period of the year because of availability of national production and imports as shown in the Figure 3.

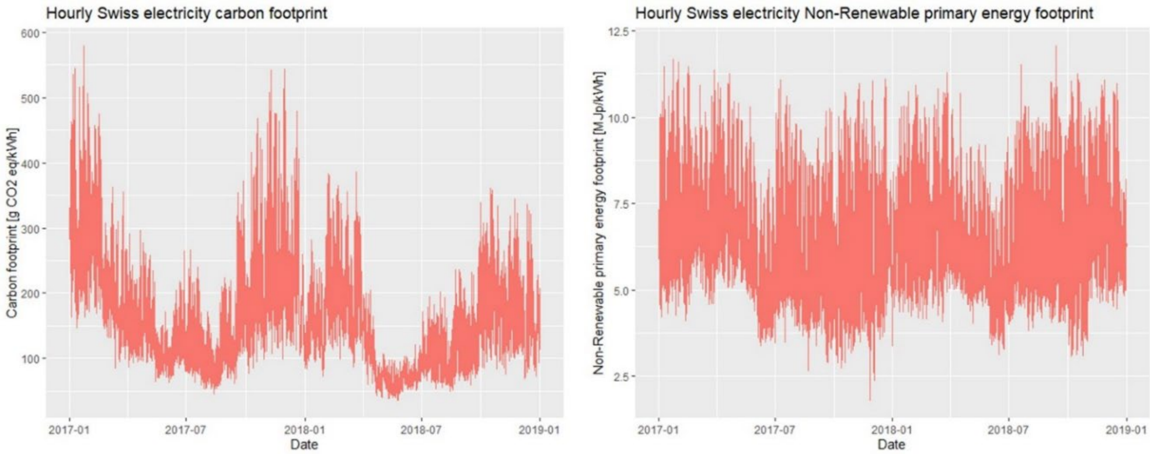

Figure 7: Hourly dynamic carbon and non-renewable energy footprints of the Swiss consumed electricity according to [17,18]

In [17,18], the dynamic environmental impact was highlighted as necessary when considering MOO approach. It can indeed modify the optimal configuration choice. While the dynamic considerations regarding the energy balance of the supply and demand of the building is addressed in current MOO via the energy models used, it has not been implemented yet for the environmental impacts of electric energy for optimal system identification. Therefore, promoting the use of dynamic environmental indicators in building energy optimization processes and providing a reliable framework to encompass their dynamic aspects is a key requisite for reliable results that aim at supporting strategical decisions. Associated with cost assessment, this approach will enable professionals and decision-makers to identify optimal solutions for DMES and management strategies for the building sector. It will also highlight what is the benefit of considering energy communities rather than individual buildings separately.

1.3 Objectives

The OPTIM-EASE project focuses on three goals:

1. To mitigate the cost and environmental impacts of building energy systems by enhancing and optimizing the synergies between energy needs (thermal & electrical), decentralized energy production and grid electricity
2. To study the influence of dynamic and multi-criteria environmental impact considerations on the optimal energy concepts definition for buildings and group of buildings.
3. To assess the influence of grouping buildings compared to individual solutions from cost and environmental KPIs.

To achieve these goals, the OPTIM-EASE project needs to develop a framework for data, enhanced simulation and MOO based on the previous research work in this field. This includes cost and dynamic environmental impact assessment for the identification of optimal solutions regarding the energy control, conversion and storage strategies for single buildings and groups of buildings (of various typologies), and within energy communities. Thereby, different options for existing short-term energy storage solutions as well as prospectively future long-term energy storage options shall be considered.

The OPTIM-EASE project will apply an enhanced and adapted MOO framework in order to identify optimal energy systems in terms of cost and dynamic environmental impacts. This includes the energy control, conversion and storage strategies of buildings and groups of buildings. This framework will serve to quantify the benefits of optimal DMES solutions for groups of buildings compared to optimal individual solutions, which is schematically represented by the different Pareto-fronts in Figure 4.

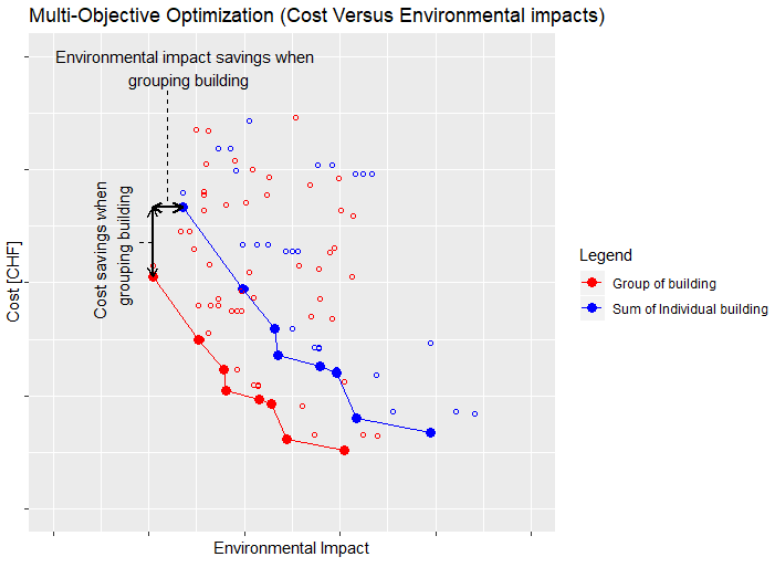

Figure 8: Schematic representation of the OPTIM-EASE project output (unscaled example developed by HEIG-VD)

The schematic of Figure 4 represents a possible outcome of the OPTIM-EASE project. It shows the environmental impacts and costs of a groups of buildings together (red dot in Figure 2) and for the sums of all buildings separately (blue dots). Visibly, the Pareto fronts for the groups of buildings considered together (red line) and for the sums of the optimal solutions of each individual building considered separately (blue line), is quite different. The difference between the two lines thus quantifies the cost and environmental savings related to the building synergies.

2 Procedures and methodology

2.1 Requirements for OPTIM-EASE and existing MOO framework

The relevant specifications and requirements needed to fulfill the project's goals have been identified by means of functional analysis. In order to choose the approach and tools to carry out the work in OPTIM-EASE a review and comparison of suitable existing tools and frameworks was carried out. Finally, as none of the reviewed framework fulfilled all the requirements, the selected framework was extended with new features in a new tool called optihood. These are detailed in the following sections.

2.1.1 Specifications

The following specifications were defined, which are shortly presented hereafter and in Figure 5:

- Read input parameters: energy demand profiles (thermal and electrical), weather data, energy converters and storage parameters (efficiency, cost and environmental impacts)
- Pre-processing of data: generate hourly energy demand (thermal and electrical)
- Investment optimization, including technology selection with optimal capacity and their hourly optimal operation by minimizing cost and/or environmental impact. This can be applied to single buildings or to a group of buildings.
- Dispatch optimization: optimization of the operation of a defined energy system where the capacities of the technologies are known.
- Results and outputs: display and render the results to be analyzed by a user. For example, through Sankey diagrams and Pareto fronts.

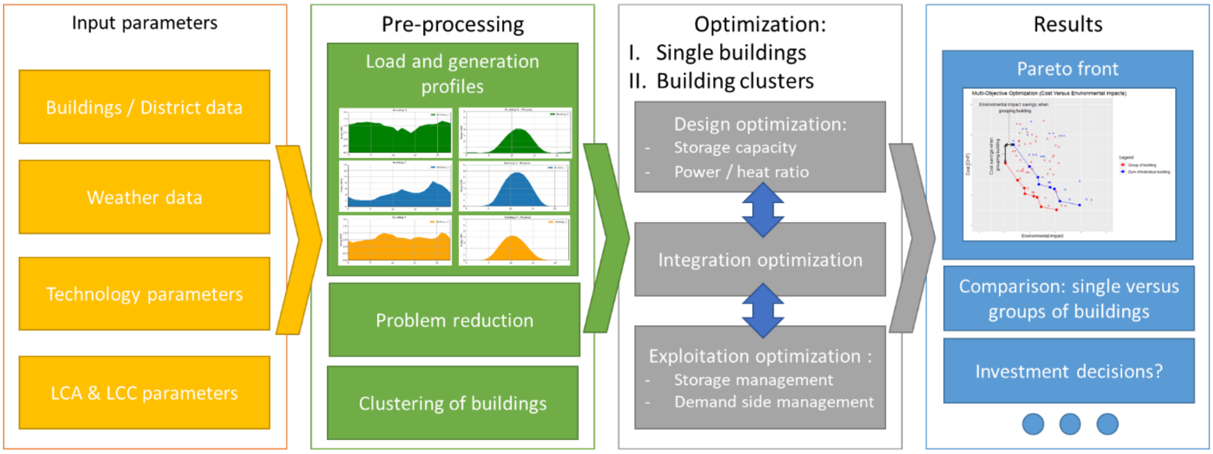

Figure 9: Summary of the specification of the solution.

2.1.2 Requirements

These specifications are also subject to many requirements. First, the functional (technical) ones, which define the basic system behavior, are defined:

- Provide environmentally and economically optimal energy systems.
- Respect hourly demand for each building (excess energy production is allowed if it can be stored locally or sold to the grid)

- Respect technologies’ constraints (temperature level, efficiencies, minimum loads, …)
- There are also non-functional requirements that must be taken into account. They specify how the solution will perform and fulfil functional requirements:
- fast and accurate enough models for energy, cost and environmental impact calculations
- Modularity in terms of solver and models choice
- Adaptability: modification of the code possible for future needs
- Acceptable computation time: A few days of calculation is the maximum for the most complex systems. For the first case studies, with a limited number of technologies and buildings, few minutes is expected.
- Interpretation and visualization of the results for a general accessibility
- Open-source or freely distributed solver
- Only one optimization, integration, size and operation all together
- Provide interface at minima with excel for inputs and outputs.

2.1.3 Optimization method and programming language

To fulfil the specification and requirements defined for the framework, two general optimization methods exist: non-linear programming and linear programming. Non-linear programming methods although allow precise representations, especially in case of thermal technologies (such as solar thermal, thermal energy storage and heat pumps) which are highly non-linear, the computational time and solver stability in such programming methods pose an issue when dealing with complex problems. Mixed Integer Linear Programming (MILP) is an effective modelling approach (with a fast and guaranteed convergence) commonly used to solve complex optimization problems, however at the cost of reduced accuracy. Since the project involves optimization of multiple technologies (in terms of both operation and capacity) at a community scale, the computation time of the selected optimization method is highly critical. Consequently, a highly simplified modelling approach should be undertaken. Moreover, the optimization method needs to be fast and robust enough to perform multiple optimizations with different cost and environmental targets to permit multi-objective analysis. The selected optimization method should also facilitate a comparison between groups of buildings (coupled through electricity grid) and buildings taken individually. Therefore, due to its fast, robust and effective characteristics, the MILP approach was chosen.

To reduce the development time and coding effort, a high-level modelling language was thought to be of great benefit. Several options are available and widely used for the optimization of DMES, for example: AIMMS, AMPL, GAMS. However, in order to facilitate the dissemination and adaptability of the tool, the language has to be open-source and redistributable without or with little restrictions. Pyomo[6] fulfilled these requirements and is coded with python, a well-known programming language used in many fields today. Moreover, it was found to be used in several existing frameworks for the optimization of DMES. As well an important feature of pyomo is that it enables the use of several solvers (commercial and open-source), which fulfils the OPTIM-EASE requirements. This ensures the possibility to choose between high performance and broad distribution capabilities.

2.1.4 Platform comparison

After setting the specifications and requirements, available tools were reviewed and tested. In the end the best suited option was selected avoiding a completely new development started from scratch. Four frameworks for the modeling and optimization of distributed energy systems were identified:

[6] http://www.pyomo.org/

- python-ehub from the HUES platform, https://hues-platform.github.io/
- URBS - https://urbs.readthedocs.io/
- FINE - https://vsa-fine.readthedocs.io/
- oemof - https://oemof.org/

It is relevant to compare what each platform could do and how some of their characteristics could be used in OPTIM-EASE.

The first platform is python-ehub. This software was developed for the HUES platform (a repository of open-source models and algorithms for the study of urban DMES). Python-ehub is a python transcription of the well-known energy hub concept [19] which was originally programmed with the commercial software AIMMS and Matlab. The python platform has very little documentation, only three case-studies and one Notebook. In the latter, a class is defined; it provides clear access to data needed to implement an energy hub model. Then, the model is specified, with its sets, variables, parameters, constraints and objective function. All the platform is defined inside this .ipynb file. The platform uses Pyomo, the python-based modeling language previously covered. Ehub-python was coded 3 to 4 years ago, which makes it hard to work with today, as every package used has been upgraded since then. Moreover, the energy models are very simple and do not provide sufficient accuracy for the objective set in OPTIM-EASE. For these reasons, it was decided not to continue with ehub-python.

The Technical University of Munich (TUM) developed the code of the second platform, URBS. The modeling of the optimization problem is simplified with the use of Pyomo, like in ehub-python. The platform benefits from a large documentation on readthedocs.io and diverse example studies. Several Python scripts are available on github, but only one has to be run. This one calls the inputs and sets different scenarios, which will be compared. The model and its characteristics are specified in a different script. URBS presents a more accurate energy performance modeling, closer to the one required in OPTIM-EASE compared to ehub-python. However, like ehub-python, the development was a little out of date, and upgrading the deprecated libraries is time intensive. Thus, Urbs was ruled out, but the visualization tools were kept in mind. They offer well-made specific graphics that could be used in OPTIM-EASE.

The FINE platform, stands for Framework for Integrated ENergy system assessment, is a python package providing a framework for modeling and optimizing energy systems. Developed by Jülich Forschungszentrum, a research center in Germany, it offers a simple modeling of every energy system possible for their optimization by minimizing the total annual cost of the system. The platform is interesting as everything is well defined and explained; also, the workflow is intuitive. FINE has many objectives similar to OPTIM-EASE, like the single optimization for the choice of the technologies, their size and their operation over the horizon defined. However, some aspects are different. A single objective function is defined, and it is used inside every class. This means it is difficult to introduce a second one or adapt it, as every single class already created will have to be updated. Another important limit is the simplicity of the models. Here, a heat pump is similar to a cogeneration, and a hot water tank to a battery. It is not enough for the project. However, new classes could be easily introduced, some were identified in the next describe framework.

The last framework is the oemof framework. oemof (Open Energy Modelling Framework) is an open-source collection of libraries for energy system modelling and optimization. It was pioneered by RLI (Reiner Lemoine Institut) Berlin in collaboration with the Center for Sustainable Energy Systems (ZNES – University of Applied Sciences Flensburg) and Magdeburg University. It is very similar to FINE, but with a major difference: oemof is a community-driven framework, containing ten packages, with a team of developers actively maintaining the offered packages for modeling, optimization or simulation tasks. For example, there is oemof.solph, used to optimize multi-regional energy systems considering power, heat and mobility, oemof.thermal, for modeling thermal energy components, or oemof.visio, for plotting the results. The main aspects that were attractive for using this framework are the following: oemof has a stratified storage model, as well as a solar thermal collector, and different kinds of CHP technology.

These possibilities reduce development time that was dedicated to improving more complex models such the heat pump. Moreover, the platform was found to have scope for improvement. Classes were clearly defined, and the large documentation allows efficient modification of the framework.

For all these reasons, the oemof framework was chosen for the OPTIM-EASE project. A comparison between all the frameworks tested can be found in table 1.

	Projet	URBS	EHUB	FINE	OEMOF
MILP	x	x	x	x	x
Optimal sizing and use	x	x	x	x	x
Hourly-spaced time step	x	x	x	x	x
Multi-objective optimization	x				
Choice between cost/emission optimization		x	x		x
Trade with external market	x	x	x	x	x
Predefined networks		x	x		
Input scenarios		x			
Max environmental output		/h /y	/y	/y	
Max stock supply		/h /y	/h		
Max sell limit		/h /y			/y
Max buy limit		/h /y			/y
Switching speed limitation	(x)	x			x
Part load behavior	x	x	x	x	
Intertemporal optimization		x			
Losses considered on the network	x	x	x	x	x
Simple network modelization		x	x		
Complex network modelization	x			x	x
Simple models (PV, CHP...)		x	x	x	
More complex models	x				x
Plot source of electricity or heat /h		x		x	x
Plot energy production /h			x	x	x
Plot cross-scenario comparison		x			
Good documentation		x		x	x
Latest packages				x	x
Adaptability					x

Table 3: Comparison of the platforms reviewed.

2.2 Optihood framework

The optihood framework was implemented within this project and extended within the SFOE-sponsored project SolHOOD[7]. It is written in Python programming language and based on oemof (open energy modelling framework). In oemof, an energy system is defined as a combination of linear component models of different types namely, sources, transformers, sinks, and buses. The components models are linked together using flow objects which may have associated costs (optional) to formulate the target function to optimize. Then, Oemof makes use of pyomo, an open-source modelling language for optimization solutions, to define a MILP optimization problem. The framework optihood offers a flexible and easy-to-use environment with several useful features for a neighborhood beyond what oemof can provide. The basic construct of oemof is modified in a sense that the components are grouped by buildings and the results (time series of energy production/consumption, costs, emissions, etc.) can be obtained per building. Moreover, optihood uses a config or excel file for a simplified definition of the scenario/problem to be optimized. Additionally, optihood provides additional features such as: (i) multi-objective optimization based on two target criteria, (ii) more advanced models for technologies, (iii) optimizations of individual buildings or as a group, and (iv) the option to improve the computational speed by clustering days. The optihood framework was published as open source on GitHub[8] along with a supporting online documentation[9].

2.2.1 Software architecture of optihood

The scenario consisting of the energy network (including buildings and links, if any) to be optimized can be defined using either a configuration (or config) file or an excel file. The input config/excel file defines the available energy conversion and storage technologies. The associated parameters and sizing limits of the technologies are also defined within the input scenario file, along with the cost and environmental impact assumptions per technology, a path to the demand profiles and weather data files. The purchased electricity cost as well as the emissions of the grid electricity can either be a time series or a constant value. The demand profiles for space heating can be defined statically or alternatively by means of a dynamic linear building model. After preparing the config/excel file, an energy network can be defined in a Python script for optimization. Figure 1 shows the architecture of the optihood framework.

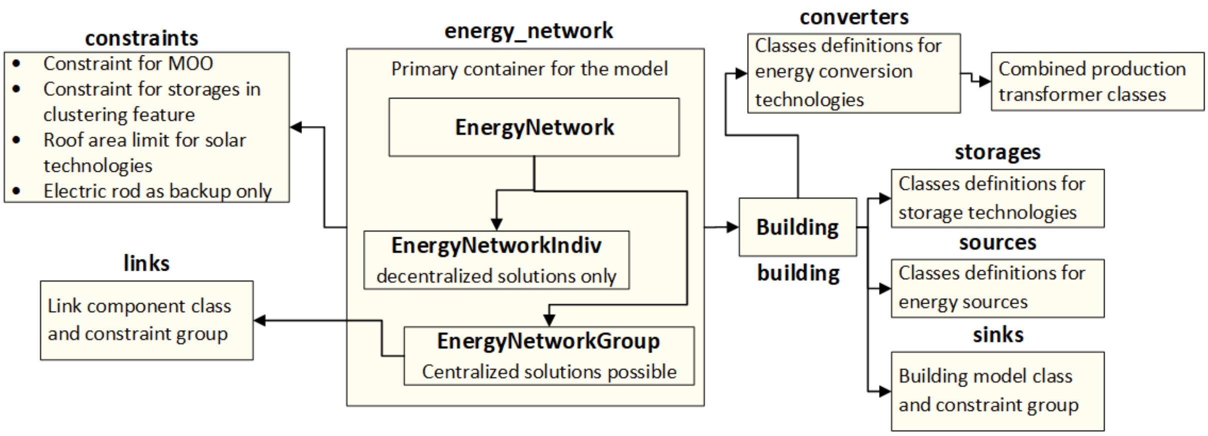

Figure 1: Architecture of the optihood framework.

Grid electricity, natural gas, or any other form of energy consumed by the system can be considered as energy sources. An energy source is modelled simply as a “Source” from oemof solph. An energy demand can be related to electricity, space heat and domestic hot water, and is modelled as a “Sink”

[7] https://www.aramis.admin.ch/Grunddaten/?ProjectID=49313
[8] https://github.com/SPF-OST/optihood
[9] https://optihood.readthedocs.io/

from oemof solph. In terms of energy conversion and storage technologies, the following are presently implemented: air-source heat pump (ASHP), ground-source heat pump (GSHP), combined heating and power (CHP), solar thermal collector, PV, electric heating rod, gas boiler, electrical battery and thermal storage. A description of the models used for different technologies is presented next.

2.2.2 Modelling of energy system components

The energy system components can be classified into energy converters and storages. We use constant efficiency models for CHP, gas boiler and electric heating rods, where a fixed efficiency is pre-defined. Heat pumps (ASHP and GSHP) are modelled based on a bi-quadratic polynomial fit of the condenser heating power ($\dot{q}_c$) and the electrical consumption power of the compressor ($\dot{w}_{cp}$) proposed by [20].

$$\dot{q}_c = bq_1 + bq_2 \cdot \overline{T}_{e,in} + bq_3 \cdot \overline{T}_{c,out} + bq_4 \cdot \overline{T}_{e,in} \cdot \overline{T}_{c,out} + bq_5 \cdot \overline{T}^2_{e,in} + bq_6 \cdot \overline{T}^2_{c,out} \quad (1)$$

$$\dot{w}_{cp} = bp_1 + bp_2 \cdot \overline{T}_{e,in} + bp_3 \cdot \overline{T}_{c,out} + bp_4 \cdot \overline{T}_{e,in} \cdot \overline{T}_{c,out} + bp_5 \cdot \overline{T}^2_{e,in} + bp_6 \cdot \overline{T}^2_{c,out} \quad (2)$$

where, $T_{e,in}$ and $T_{c,out}$ are fluid temperatures at the inlet of the evaporator and the outlet of the condenser, respectively. $\overline{T}$ denotes the normalized temperature and is defined as $\overline{T} = \frac{T[°C]}{273.15}$. bq_i and bp_i are the polynomial coefficients calculated from the catalog heat pump data using multidimensional least square fitting. A detailed description of the heat pump models has been documented in Appendix A.

The condenser fluid outlet temperature $T_{c,out}$ was fixed to 35 °C and 65 °C, respectively, for space heating and domestic hot water. For the evaporator fluid inlet temperature $\overline{T}_{e,in}$, a ground temperature profile with seasonal variation (section 2.2.3) was considered for GSHP, while ambient air temperature was used for ASHP. For the additional components, we use models provided by oemof-thermal[10] . Solar thermal collectors and PV modules production profiles are pre-calculated before the optimization. For batteries, a simple model is used that accounts for fixed charging and discharging efficiencies and a loss parameter. For thermal storages, a stratified thermal storage model with two temperature zones is used.

2.2.3 Ground Source temperature profile.

The COP of the heat pump is calculated with the same model as for the ASHP. New coefficients were derived to account for the higher performances. The BHE is too complex to be modelled in MILP. Therefore, the hourly outlet temperature of the heat transfer fluid from the ground to the heat pump is pre-processed according to the following assumptions:

- The borehole fluid temperature is independent from heat flow rate extracted from the ground.
- The annual temperature profile is sinusoidal.
- The minimum is at the end of February.
- The probes are designed to have a minimum flow temperature of 0°C to avoid freezing of the ground.
- The maximum temperature corresponds to the annual average soil surface temperature according to the Swiss building’s norm SIA 384/6 (chapter 7.2.2) for the region north of the Alps (11°C).

Under these assumptions, we can draw the temperature profile of the outlet temperature of the BHE (Figure 10) that will be used to evaluate the COP of geothermal HP.

[10] https://oemof-thermal.readthedocs.io/

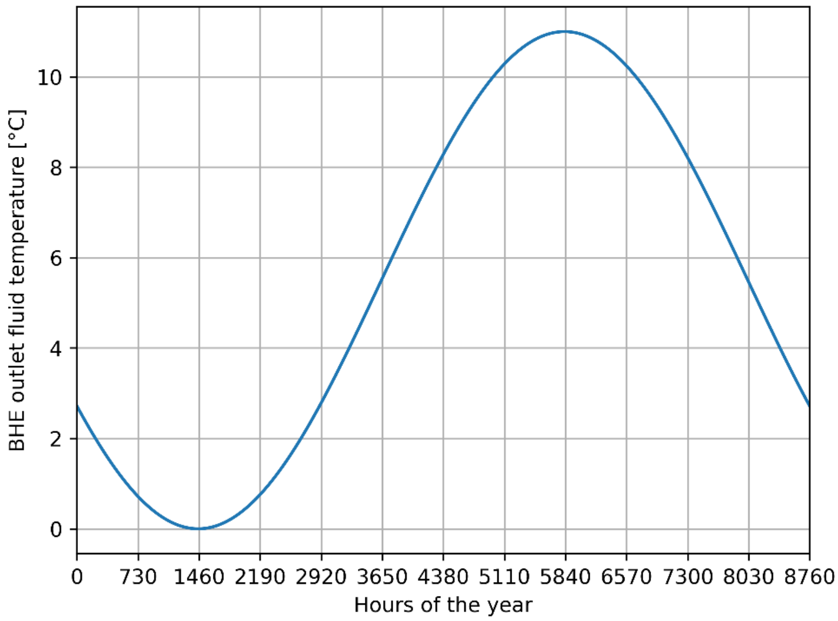

Figure 10: Ground source temperature profile

2.2.4 Combined production transformer

A new transformer called combined production transformer which extends the features of oemof "Transformer" was defined. Since some transformers like HP can have different efficiencies for SH and DHW production (DHW needs a higher temperature than SH), this transformer offers the possibility to consider those different efficiencies. It allows to produce both space heating (SH) and domestic hot water (DHW) during the same timestep while respecting the input/output balance constraint.

$$P_{input}(t) = \frac{P_{DHW}(t)}{\eta_{DHW}} + \frac{P_{SH}(t)}{\eta_{SH}}, \forall t \qquad (3)$$

where, *P* denotes the operating power for inputs (for example, electricity used by HP) and outputs (SH and DHW), η denotes efficiency of the transformer and *t* denotes the time step.

Physically the converters cannot supply both SH and DHW at the same time. However, if we consider a timestep of 1 hour it can be considered to be sub-divided into smaller intervals to produce SH and DHW both within 1 hour. The combined production transformer was used for the implementation of heat pumps (ASHP, GSHP), CHP, gas boiler and electric heating rod.

2.2.5 Roof area constraint

Previously, ST and PV arrays were implemented such as to respect only a minimum and a maximum installation size defined in the scenario. This means that the maximum size for each technology chosen by the optimizer does not consider the roof utilization of one technology versus the other. For example, if the maximum size of each technology is set to correspond to a roof utilization of 50 %, then if the optimizer does not install the full capacity of ST, the rest of the area is lost and cannot be used for PV panels. Therefore, a constraint (Eq. (16)) was implemented to evaluate the area needed by each panel based on its size and tilt. The distance between rows is calculated to avoid mutual shading (Figure 11) at the lowest solar zenith height. For now, it only works with south oriented panels.

$$\frac{P_{PV}}{\eta_{PV}} \times \frac{\sin(\alpha_{PV}+\beta)}{\sin(\beta)} + S_{ST} \times \frac{\sin(\alpha_{ST}+\beta)}{\sin(\beta)} \leq S_a \qquad (16)$$

- With,
- P_{PV} : capacity of PV panels installed.
- η_{PV} : efficiency of PV panels (~20%)
- S_{ST} : surface of solar thermal panels installed.
- α : tilt of panels
- β : solar height
- S_a: roof area available for solar panels

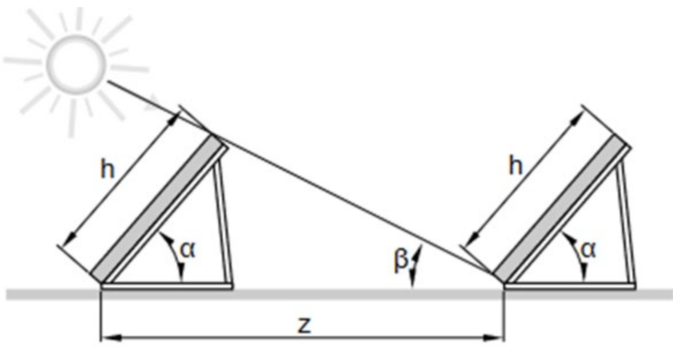

Figure 11: Distance between two rows of solar panels (source: Viessmann, 2017. Vitosol - Notice pour l'étude).

2.2.6 Electricity and thermal links

In order to allow the buildings to share the produced energy in grouped optimization, space heat, domestic hot water and electricity links were implemented. A new component class, called Link, was defined with a new constraint group. A link is modelled as a new component where all the relevant input/output flows of the buildings connect. The implementation of links adds complexity to the optimization problem and affects the convergence speed. In order to improve the speed of optimization, an option to merge the respective buses, i.e. energy flows (electricity, space heating and domestic hot water), of all the buildings to be linked was added into the framework. This option can be used to perform optimization in two steps. In the first step, links could be used without the merge buses feature, which allows the optimizer to select whether connecting the buildings is the best solution or not. Once it has been established that connecting the buildings is the best solution, the new option to merge buses could be used to produce additional optimizations' results faster.

2.2.7 Multi-objective optimization

The existing transformer and storage classes within oemof were extended to allow multi-objective optimization (MOO). The two targets of MOO are defined as total annualized cost and total annualized environmental impact of the system. The first and second optimization runs within MOO determine the two extremes where either cost or emissions are minimized. The remaining solutions of MOO are obtained by finding the curve of pareto optima between cost and environmental optimum using epsilon constraint method [21].

2.3 Objective functions

The last challenge of the optimization problem remains in the modelling of the objective functions; it is where the complete mathematical problem will be solved. In our project, we want to minimize both costs and carbon emissions. Two functions are thus necessary. These rely on input data that will be gathered for each technology considered.

2.3.1 Objective function for costs

To evaluate the economic performance of the system, the cost for a defined year is evaluated. The total cost originates from 3 items:

- CAPEX, which is the annualized investment cost to install each technology chosen by the optimizer. To account for interest rates and the lifetime of the technology, the investment is discounted. The CAPEX consists of a “base cost” that is independent of capacity, i.e. constant, and a “capacity cost” that is proportional to the nominal capacity of the installed technology. Installation and planning costs are accounted as a percentage of the investment costs.
- OPEX: are the operational costs of the system and therefore comprises of the cost to buy the necessary energy inputs (fuel, grid electricity, etc.) and the cost for the maintenance of the system.
- Feed in revenue: the revenues earned from the selling of surplus electricity to the local grid.
- To optimize the economic performance of the system, the following equation is minimized:

$$Cost = \sum_{t\ in\ technologies} V[use\ binary]_t \cdot (CAPEX_t + OPEX_t)$$
$$- \sum_{f\ in\ flows} feed\ in\ tariff_f \cdot V[quantity\ feed-in]$$

With:

- $CAPEX_t = V[use\ binary]_t \cdot Base_{cost_t} + V[capacity]_t \cdot Cost\_capacity_t$
- $OPEX_t = \sum_{i\ in\ inputs}\left(Cost_i \sum_{f\ in\ flows} V[quantity\ of\ inputs]_{i,f}\right) + Cost\_maintenance$
- V is a vector of the optimization variables that will be calculated during the optimization.

2.3.2 Objective function for environmental impacts

To evaluate the environmental impacts optimality, we use LCA data of each energy vector and technology. The main life cycle impact assessment method considered in this study is the Global Warming Potential (GWP) over 100 years from IPCC [22]. It quantifies greenhouse gases (GHG) emitted to the atmosphere as kilogram of CO_2 equivalent effect on global warming potential over 100 years (kg CO_2-eq.). The GHG emissions of a technology (t) is calculated for a year accounting for the manufacturing, the use stage and the recycling/disposal at end-of-life. The use stage is calculated by summing the hourly energy vectors consumptions and productions (i) over a year. The impacts of manufacturing and end-of-life are added, yearly amortized by the infrastructure lifetime. Therefore, the following quantity of interest is used in the environmental objective function of the optimization:

$$GHG\ emissions = \sum\left(GHG\ emissions_i \sum_{f\ in\ flows} V[quantity\ of\ i]_f\right)$$
$$+ \sum_{t\ in\ technology} V[capacity\ of\ t] \cdot \frac{GHG\ emissions_t}{lifetime_t}$$

- with V elements describing optimization variables that will be calculated during the optimization.

2.4 Technologies: cost, environmental impact and nominal performances

The technologies are classified in three categories:

- Energy inputs: all energy vectors that are energy sources for the systems, e.g. fuels, grid electricity, energy from the environment like solar radiation, etc.
- Energy converters: equipment that converts inputs into usable energy (heat or electricity) for the end consumers.
- Energy storages: device to store electricity or heat locally in order to be consumed later.

Inputs	Converters	Storages
Electricity grid	Heat pumps	Batteries
Natural and bio -gas	Boilers	Hot water daily storage (HWS)
Ambient and ground heat	Solar thermal	Domestic hot water storage (DHWS)
Solar irradiation	Photovoltaic	
	CHP-ICE*	

* Combined heat and power with internal combustion engine

Table 4; list of the technology defined within OPTIM-EASE

For the GHG emissions of energy inputs, grid electricity has an hourly profile as documented in WP1 deliverable [23], the one for natural gas is constant at 0.230 kgCO_2eq/kWh. Cost and GHG emissions for the technology considered are taken equal for each investigated case study. They are summarized in Table 5.

The nominal performances of the technologies considered within all case studies are presented in the Table 6. For the GSHP, the BHE is sized considering a nominal specific heat extraction rate of 20W/m corresponding to a compact borehole filed with low regeneration ratios.

Important information:
According to the SFOE's heat strategy 2050, fossil gas is banned from the energy sector and synthetic and renewable gases are used to cover heat requirements at high temperatures for industrial processes and not for buildings. These energy inputs are considered in the OPTIM-EASE project in specific case study where for example the technology was already installed and for CHP systems. CHP installations are heat driven; this means that the heat must be consumed on site.

	unit	Lifetime	CAPEX		O&M costs [% CAPEX/y]	GHG emissions
		[y]	per capacity [CHF/unit]	base [CHF]		[gCO_2eq/unit]
Converters						
ASHP	kW	20	2153	16678	2	281
GSHP + *BHE*	kW	20	3052	22257	2	772
Gas Boilers	kW	30	164	8832	1.5	93
Solar thermal	m^2	20	820	5500	0.5	127
Photovoltaic	kWp	30	1103	17950	2	1131
CHP-ICE	kWh	20	1153	24879	3	360
Energy storages						
Batteries	kWh	20	981	5138	0	29
HWS	L	20	1.41	1092	0	0.49
DHWS	L	20	6.88	2132	0	0.49

Table 5 : summary table of costs and GHG emissions parameters for the considered technologies.

	Performance indicator and nominal conditions	Nominal Performance
Converters		
ASHP	COP @A7/W35	3.5
GSHP + BHE	COP @B0/35 and specific extraction heat rate	4.65, 20 W/m
Gas Boilers	Conversion efficiency over lower heat value	0.9
Solar thermal	Conversion efficiency for a global irradiation of 800 W/m2; an ambient/fluid temperature difference of 40K	0.61[11]
Photovoltaic	Conversion efficiency	0.2
CHP-ICE	Conversion efficiencies for electricity, space heating and DHW preparation	0.25, 0.6, 0.6
Energy storage		
Batteries	Input and output flow efficiencies	0.9, 0.86
HWS	Insulation thickness, conductivity	100 mm, 0.03 W/(m.K)
DHWS	Insulation thickness, conductivity	100 mm, 0.03 W/(m.K)

Table 6 : list of the nominal performances of the considered technologies.

[11] With $\eta_0 = 0.73,\ a_1 = 1.7, a_2 = 0.016$

2.5 Case studies

The case studies have the objective to apply the developed framework (see https://optihood.readthedocs.io/) to generic and real case studies, illustrate its applicability and answer general research questions. More precisely, the results of the case studies will:

- Characterize the range of environmental and cost benefits generated by grouping buildings together compared to the sum of individual solutions.
- Identify the drivers that influence the environmental and cost benefits (group size, building typologies, etc.) of energy communities.

The applicability of the framework will be presented in case studies provided by three companies from the field that have expressed their interest (Romande Energie, Energie360 and SGSW). They will also drive the on-going development of the tool. Input data and boundary conditions, such as climate, resource availability and restriction will be based on the actual site of the case study. The selection of the case study is conducted between the research partner (HEIG-VD or SPF) and the partner from the field based on interest and the following list of criteria.

- Group of several buildings close enough to be interconnected in a microgrid.
- Total floor area higher than 10 000 m^2
- Heterogeneous building usage (residential, offices or shops) and/or typology (Insulation class, construction year, …)
- Availability of the data
- Shown interest in the possible results (from the field and the academic partners)
- These criteria are not mandatory and were set according to the estimated capabilities of the tool and the interest of the partners: The number of buildings is not defined because the buildings with similar demand profiles can be aggregated together and therefore reduces the complexity of the optimization problem.

2.5.1 Case study from Romande Energie

The one from Romande Energie is a new real estate development in the region of Lausanne commissioned between 2019 and 2020. The objective of the investors was to build an ecological, durable, and innovative area in an urban context. It comprises of six Minergie A buildings with:

- Households for a total heated floor area of 26’000 m^2 representing approximately 350 flats,
- One supermarket of 500 m^2,
- Retail shops for 2’900 m^2.

All the buildings have PV panels and produce SH with GSHP. The building 4 which supplies also with heat building 5 and 6 also produces DHW with a GSHP whereas buildings 123 use ST panels for DHW production with a fossil gas backup boiler. Table 9 summarizes the areas and equipment installed in each of the four buildings.

Buildings	Nb of dwellings	Dwellings area (m²)	Shops area (m²)	Available roof area (m²)	GSHP (kW)	Gas boiler (kW)	PV (kWp)	Solar thermal (m²)	DHW storage (L)	SH storage (L)
1	76	7 751	1 003	1100	188	320	~50	88	3 500	3 000
2	72	6 883	932	1100	170	300	~47	73	3 500	3 000
3	44	3 940	516	630	92	200	~30	37	2 500	1 000
4 (5&6)	92	8 237	810	1650	220	-	107	-	6 000	2 000
TOTAL	284	26 811	3 261	4 480	670	820	234	198	15 500	9 000

Table 7: Buildings areas and actual installed energy system in the Romande Energy case study

In addition, equipment for cooling and refrigeration needs for the supermarket are owned and operated by the company. No information is available on the actual equipment, only the electricity consumption is accounted for with the rest of the electricity consumption of building 4. Also, the condenser heat of the cooling and refrigeration equipment for all the building is rejected in the borehole heat exchanger (BHE) and thus participates in balancing the heat source for the HPs.

This case study is well suited for OPTIM-EASE and fulfils several of the set criteria even if the typology of the buildings is similar. Romande Energie owns the electrical and thermal contracting for the facilities, which guarantees good access to the data. Moreover, the buildings were commissioned in two phases, firstly buildings 1, 2 and 3 in April 2019 and then 4, 5 and 6 in October 2020. This fits well the planning of the project, as at least a year of measurement will be available at the beginning of WP3 in January 2022.

Main interests lie in an ex-post optimization and a sensitivity analysis on energy prices of the building group with the optihood framework. Based on the actual monitored demand of the buildings and on-site boundary conditions, optimal designs (Pareto front) in term of technology choice, sizing and operation of the energy system will be identified according to the objective functions defined (see 2.3).

Analysis of the results will be carried out by comparing optimal solutions (Pareto front) with the actual energy concept to access the benefits of using the framework compared to state-of-the-art planning methods. To do so the reference is the result of both objective functions evaluated with the actual performances of the installed energy system and associated investment and operation costs. These results will then be compared graphically and numerically with the optimal solution identified on the Pareto front.

Definition of the scenarios and boundary conditions

a) Scenario 1: optimization of private consumption community vs individual

In this scenario, 3 optimizations are carried out with different price schemes, one for PCC ("group") and two individual optimizations. In the "group optimization", we consider that the buildings can share locally produced electricity (PV and CHP) with one another through the local grid (microgrid). The group works as an energy community for the tariffication, this means that since it is a large consumer it has his own medium voltage/low voltage transfer station and therefore it is granted with a price for electricity of 19 c./kWh during peak hours and 12 c./kWh during off-peaks. In the case of individual optimization, each building is considered individually. Locally produced electricity is either directly consumed on site or sold to the local electricity provider. Here two electricity prices are considered. Firstly, peak/off-peak price of respectively 22 and 12 c./kWh are considered and represent the price for a large MFH with electricity-based heating system. Secondly, a constant price 22 c./kWh corresponding to the price paid by small consumers. These considerations are summarized in Table 8.

Cost Hypothesis	Group Optimization	Individual Optimization with Peak/Off-peak prices	Individual Optimization with constant prices
Gas	8.7 c./kWh	8.7 c./kWh	8.7 c./kWh
Electricity	19 – 12 c./kWh	22 - 12 c./kWh	22 c./kWh
Electricity feed-in	7.2 c./kWh	9.5 c./kWh	9.5 c./kWh
Interest rate	5%	5%	5%

Table 8 summary of energy prices and interest rate considered for each investigated scenario in the Romande Energy case study.

b) Scenario 2: Natural gas, electricity price ratio sensitivity:

The aim of this scenario is to consider 2023 price conditions and assess the variability of the ratio of electricity price over natural gas prices. The microgrid is contractually obligated to purchase electricity on the free market. Romande Energy purchase strategy is to estimate the load curve of the neighborhood and establish a fix selling price for the year. For 2023, the price was set to 44 c./kWh. For natural gas, it is then assumed to have half then one third of the electricity price respectively, 22 c./kWh and 14.7 c./kWh (Table 9)

Cost Hypothesis	2-1	3-1	4-1
Gas	22 c./kWh	14.7 c./kWh	11 c./kWh
Electricity	44 c./kWh	44 c./kWh	44 c./kWh
Electricity feed-in	18.3 c./kWh	18.3 c./kWh	18.3 c./kWh
Interest rate	5%	5%	5%

Table 9 summary of energy prices and interest rate considered for each investigated scenario in the Romande Energy case study.

c) Scenario 3: HP Operation optimization

This scenario focuses on the optimization of the operation of the energy system for both heat and electricity. The system itself is fixed with the installed set of equipment given for this test case. Therefore, no optimization of the selection of technologies or capacity is done here. As additional input the gas price is set at 8.7 c./kWh and the electricity price from the power grid varies with 19 c./kWh for peak and 12 c./kWh for off-peak periods. This corresponds to the group price scheme used for scenario 1 (bullet a))

d) Scenario 4: electric mobility

The aim of this scenario is to evaluate the influence of electric mobility in the design and operation of DMES for groups of buildings and PCC. To carry out this study, electric consumption of a pool of EV was retrieved from another project provided by Romande Energie and scaled to fit the case study investigated here. In total, it was decided to have a pool of 250 EV. The dataset is comprised of the aggregated monitoring data of two groups of charging sockets, the first has 7 sockets and the second 5 sockets. 15min consumption index for a whole year from the 15 mars 2022 to 15 March 2023 was provided.

2.5.2 Energie360 case study

This case study was provided by Energie360 and refers to the new building project Stockacker in Reinach BL[12]. The site consists of 4 newly constructed residential buildings with a total of 77 apartments (2.5-5.5 rooms). They meet the characteristics set out by MINERGIE-ECO® and SIA-Effizienzpfad Energie. The aim of the Energie360 project was to exploit the synergies between energy consumption for heating, cooling, electricity and electromobility by means of:

- Geothermal heat pumps for heat generation and free cooling via boreholes.
- PV system for the generation of electricity to supply the heat pump, car charging stations and cover the household electricity demands of the buildings.
- Charging infrastructure for electric vehicles with plug-and-play principle.
- A centralized energy system instead of 4 individual energy systems for each building.

The installation site has PV panels of 205 kWp capacity which produce electricity for all the four buildings. The capacity was chosen in order to maximize the local electricity production while providing a profitable case to the building investors by installing PV panels over the entire available roof area. Furthermore, two centralized geothermal heat pumps along with two large thermal storages provide space heat and domestic hot water to the apartments. In normal operation, one of the heat pumps produces heat primarily for domestic hot water the other only for heating. If the former stops working, then the second heat pump could also produce domestic hot water. The site also has two charging stations for electric vehicles, which are supplied by the PV system. Table 10 gives an overview of the technologies installed in each of the four buildings in the case study. The hourly measurement data from 15-06-2021 to 14-04-2022 (10 months), after linearly interpolating the missing values if any, was used as demand profiles within the simulations. The total demands for electricity, e-mobility, space heat and domestic hot water in the group of buildings for the considered analysis period are listed in Table 10.

Buildings	Usage type	Dwellings	Gross floor area (m^2)	Demand				GSHP		PV (kWp)	Storage	
				Electricity (MWh)	Mobility (MWh)	DHW (MWh)	SH (MWh)	DHW (kW)	SH (kW)		DHW (L)	SH (L)
4	Residential	77	10 300	143.6	2.69	170.2	259.7	125	129	205	4 000	3 760

Table 10: Overview of the buildings, demands and actual installed energy systems in the Energie360 case study.

The key interest lies in highlighting the benefits of linking the energy systems to supply the demands of the buildings. The optimal capacities of the installed technologies will be evaluated using the optihood framework and compared with the installations at site. In addition, recommendations will be made on the alternative technologies which could be more optimal in terms of the two objectives functions defined in section 2.3.

Definition of the scenarios

Firstly, a scenario with heat pumps (GSHP and ASHP) and PV as optional energy conversion technologies and sources was defined in order to investigate the competitiveness between the alternative technologies for both: i) grouped optimization and ii) individual optimization. In grouped optimization, the buildings were allowed to share locally produced electricity, space heat and domestic hot water. While, in individual optimization each building was responsible for its own consumption, i.e. locally produced energy could either be stored, consumed, or in the case of electricity, fed into the grid to generate revenue. Furthermore, a sensitivity analysis was carried out to determine the impact of cost

[12] https://emonitor.ch/neubauprojekt-stockacker/

of GSHP relative to ASHP and grid purchase tariff on the optimization results. Next, a multi-objective analysis based on the two target criteria, cost and CO_2 emissions, was performed for both individual and grouped optimization of the considered scenario. Finally, we elaborated the case study by performing a comparison between the cost optimum design configurations of energy conversion and storage technologies in five cases, namely:

- GridGSHPi: In this case, the optimal sizing of GSHP and energy storage technologies is determined in individual optimization (i.e., decentralized installations). The electricity demand of the buildings is supplied by the grid.
- PVGSHPi: This case represents the individual optimization of PV, GSHP and energy storage technologies to meet the energy demands of the four buildings. As it is a case of individual optimization like GridGSHPi, all solutions are decentralized, including PV production (electricity links not possible).
- PVGSHPg: The systems considered here are the same as in PVGSHPi, but instead of individual optimization we optimize the buildings collectively (i.e., grouped optimization). Therefore, a centralized solution might come up as an economically optimum design.
- PVGSHPg_split: In the cases described above, GSHP can produce both space heating and domestic hot water. However, there are two separate centralized heat pumps (one mainly for DHW and the other for space heat) in the actual installation on site. We, therefore, investigate a case with separate heat pumps for space heat and domestic hot water production within grouped optimization.
- DesignOptimalOperation: This case represents the actual installation on site. Unlike in the other cases, we fix the capacities of PV, GSHPs and thermal energy storages to those installed on site and optimize the collective operation of the system components. The capacities are therefore based on the design values from the planning process and not the measured data from the operational system.

The five cases mentioned above were compared in terms of the installed technology capacities, costs, GHG emissions and grid electricity consumption. Furthermore, two additional KPIs namely, self-sufficiency and self-consumption factors, were evaluated for these cases as per the following relations:

$$self\ sufficiency = \frac{\sum_b \sum_t (P_{pv,b}^t - P_{feedin,b}^t)}{\sum_b \sum_t P_{cons,b}^t}$$

$$self\ consumption = \frac{\sum_b \sum_t (P_{pv,b}^t - P_{feedin,b}^t)}{\sum_b \sum_t P_{pv,b}^t}$$

where, $P_{pv,b}^t$, $P_{feedin,b}^t$ and $P_{cons,b}^t$ stand for the electricity generated from PV installations, PV electricity fed into the grid and the total electricity consumption, respectively, of building b at the t^{th} time step. The term $\sum_b \sum_t (P_{pv,b}^t - P_{feedin,b}^t)$ therefore represents the total PV electricity which is used for in house consumption (to meet the electricity demand, mobility demand or in power-to-heat conversion devices).

Table 11 summarizes the cost assumptions for the different technologies. The costs pertaining to electricity and thermal links between buildings are neglected in the study. The costs for technologies are annualized within the framework by considering the lifetime of each component and an interest rate of 5%. The annualized costs for each technology are then used in the objective function if the target is to find the economically optimum solution.

	unit	Lifetime	CAPEX		O&M costs [% CAPEX/y]	GHG emission
		[y]	per capacity [CHF/unit]	base [CHF]		[CO_2eq/unit]
Converters						
ASHP +electric rod	kW	20	1725	13126	5	
GSHP + *BHE*	kW	20	4053	19700	0	
Photovoltaic	kWp	30	1158	18848	5	
Energy storages						
Batteries	kWh	15	681	276	0	207
HWS	L	20	1.4	1092	0	0.01
DHWS	L	20	6.9	2132	0	0.04
Energy inputs						
Grid electricity	kWh	0.20	-	-	-	-
Electricity feed-in	kWh	0.09	-	-	-	-

Table 11: Summary of cost assumptions considered in the investigated scenario for Energie360 case study.

The climatic conditions for Reinach BL, namely ambient temperature, global and diffuse solar radiation on a horizontal plane were obtained from MeteoSwiss. A fixed purchase tariff of 20 c/kWh was assumed during optimizations along with dynamic hourly carbon emissions for grid electricity as defined in WP1 deliverable [23]. The hourly emissions are based on lifecycle impact assessment, i.e. global warming potential over a span of 100 years. Moreover, the mobility demand of the neighborhood was modelled as an additional electricity demand within the optihood framework.

2.5.3 SGSW case study

The case study from SGSW (St. Galler Stadtwerke) refers to a district in Winkeln Ost, St. Gallen, consisting of 56 buildings. The district incorporates a blend of seven different sectors namely, residential (single-family and multi-family houses), office, shop, school, hotel, trade and sport. Most of the buildings (41 out of 56) have boilers (gas-fired, oil-fired or electric) installed to meet the space heating and domestic hot water demands, while 3 buildings (two offices and a sports complex) operate with geothermal heat pumps. A CHP generation plant (with natural gas) with a total of 120 kW_{el} and 242 kW_{th} supplies 12 multi-family houses with gas boilers as additional heat sources. Moreover, three buildings have rooftop PV installations: one building with 93 kWp capacity, and two buildings with 26.3 kWp each. The building with 93 kWp is a sports complex which uses the PV installation for its own electricity consumption. The two buildings with 26.3 kWp each PV installations are hotel and office buildings and supply electricity to one additional nearby building (belonging to the same office/hotel). Therefore, the electricity produced by rooftop PV installations is consumed by a total of 5 buildings (two hotels, two office and one sport complex buildings), while the rest of the buildings rely on the grid for their electricity needs. Table 12 provides an overview of the installed technologies for heating in the SGSW case study.

Number of Buildings	Usage type	Energy Converters

		Space heat	Domestic hot water
2	Office	GSHP	GSHP
1	Office	Gas boiler	Electric boiler
3	Single-family house	Gas boiler	Gas boiler
3	Single-family house	Oil-fired boiler	Oil-fired boiler
6	Single-family house	Oil-fired boiler	Electric boiler
1	Single-family house	Gas boiler	Electric boiler
10	Multi-family house	Gas boiler	Gas boiler
12	Multi-family house	CHP plant, Gas boiler	CHP plant, Gas Boiler
3	Multi-family house	Oil-fired boiler	Oil-fired boiler
3	Hotel	Gas boiler	Gas boiler
1	Hotel	Oil-fired boiler	Electric boiler
1	Sports	GSHP	GSHP
3	School	Gas boiler	Electric boiler
1	Shop	Oil-fired boiler	Electric boiler
1	Shop	Gas boiler	Gas boiler
1	Shop	Gas boiler	Electric boiler
1	Shop	Electric boiler	Electric boiler
2	Trade	Oil-fired boiler	Electric boiler
1	Trade	Oil-fired boiler	Oil-fired boiler

Table 12: Overview of the building usage and actual installed energy systems for heating in the SGSW case study.

The total annual consumption of each building was provided by SGSW, however, the hourly profiles for the consumption of electricity, domestic hot water and space heat had to be generated. The python package Demandlib[13,14], which is a part of the oemof framework, was used to generate the hourly profiles of each building. Demandlib creates the electricity and heating (including and excluding domestic hot water consumption) profiles by scaling the gas consumption data from BDEW (Bundesverband der Energie- und Wasserwirtschaft) to the desired annual demand. Demandlib considers different types of buildings based on the usage and has a building category defined for each. Table 13 summarizes the different building types in the case study and their respective building categories from oemof demandlib. A description of residential buildings, a building class also needs to be defined (from 1–11), which is calculated from the proportion of buildings constructed before 1978 in the total building stock. The building class for the residential buildings in the case study was identified as 1, with 89.5 % of single and multi-family houses constructed before 1978.

Building type	Number of buildings	Demandlib category (electricity)	Demandlib category (heating)
Office	3	G1	GHD
Single-family house	13	H0	EFH
Multi-family house	25	H0	MFH
Hotel	4	G2	GBH
Sports	1	G2	GHD
School	3	G1	GHD
Shop	4	G4	GHA
Trade	3	G0	GHD

Table 13: Number of buildings and identified building categories of demandlib for different building types in SGSW case study.

13 https://github.com/oemof/demandlib
14 https://demandlib.readthedocs.io/

Definition of the scenarios

In this case study, we investigated the optimal energy system designs for the buildings within the heterogeneous-use district by considering two scenarios:

- Scenario 1: Here, we consider the 12 MFH buildings which are connected at the physical installation site by a CHP plant. The energy conversion and storage technologies for the 12 buildings were optimized individually as well as collectively (as a group) from the cost perspective. Furthermore, we examined the cost optimum system designs for building clusters or groups of different sizes, namely 1 building, 2 buildings, 3 buildings, 5 buildings, 7 buildings and 12 buildings. The sizes of clusters were defined based on the geographical nearness of the buildings within the real district. For each cluster size, the optimal choice and capacities of the energy conversion and storage technologies were identified. The aim here was to identify the group size (or cluster size) of the buildings for which installing a CHP plant becomes an economical solution. Finally, we also performed an optimization of the energy system design for the 12 buildings based on the environmental target and a comparison with the cost optimum was made.
- Scenario 2: In this case, we consider all the 56 buildings within the mixed-use district and perform multi-objective optimization with the two optimization targets of costs and emissions. The buildings were optimized both individually and collectively as a group in order to find out the optimal system design configurations in both cases and compare them against the existing technologies installed on site. The share of energy demand supplied by renewable energy technologies, as a result of optimization, was also inspected in each case.

In both the cases described above, the choice between technologies was left open, i.e. the framework could choose among all the available energy conversion and storage technologies (given in section 2.4). The weather data for St. Gallen was obtained from MeteoSwiss and the hourly GHG emissions of the grid electricity based on life cycle assessment [23] was used within the analysis. The cost assumptions for energy inputs, energy conversion and storage technologies are summarized in Table 11. Similar to the Energie360 case study, the buildings were allowed to share locally produced electricity, space heat and domestic hot water in grouped optimization.

2.5.4 Renewable gas assessment

Disclaimer: As an additional research question, the FOGA (Research, Development and Promotion Fund of the Swiss Gas Industry) analysed the impact of using renewable gas. According to the SFOE's heating strategy, the use of renewable gas for heating purposes should be avoided.

This study aims to evaluate the potential of renewable gas to meet the energy needs of both individual buildings and groups while minimizing costs and carbon emissions. The study addresses four key questions:

4. Under what conditions is biomethane use relevant, considering building load profiles, the number of buildings, and construction periods?
5. How do the renewable gas share, carbon footprint, and specific cost influence optimal energy systems?
6. Which devices are most effective for utilizing renewable gas to meet energy demands?

Based on the hourly energy demand of three reference MFH under the climatic conditions of the Lausanne region, the study was conducted considering a variation share of biomethane in the gas supply as well as corresponding pricing. The following section details these specifics assumptions. Choice of technology and their corresponding cost and GHG emissions are taken from section 2.4.

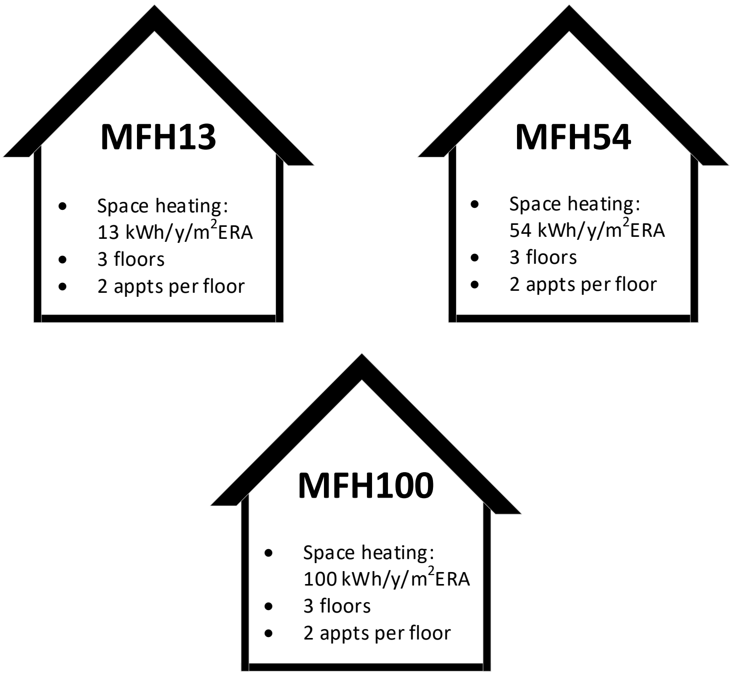

Figure 12 MFH main data summary

Three theoretical buildings from [24]have been selected for the study. The three of them are multifamily houses (MFH) from different decades, as they are meant to represent different geometries, insulation standards and ventilation levels prevalent in the Swiss residential sector. They were developed and used within several SFOE and Horizon2020-sponsored projects by SPF for application in simulation tasks. Each MFH is named according to their annual surface heating per m2 ERA demand. They were originally simulated in TRNSYS18 with Zürich climate but, as specified before, we work with Pully weather data, hence the name changes. MFH25, MFH85 and MFH 145 [19]from [24] are in this study called MFH13, MFH 54 and MFH100. They share a very close geometry, which is depicted in Figure 13 and Figure 14. There are 4 levels, one basement which holds a parking and cellars, and the three others are divided into apartments. MFH13 and MFH54 have 2 apartments per level and MFH100 3. These mains facts are summed up in Table 14. MFH13 can be seen as a modern building, MFH54 as a renovated building and MFH100 as a non-renovated building.

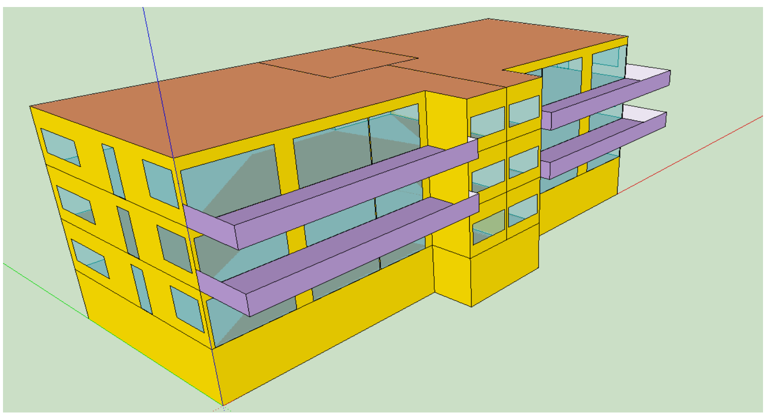

Figure 13 3D building model of [19]MFH13 [24]

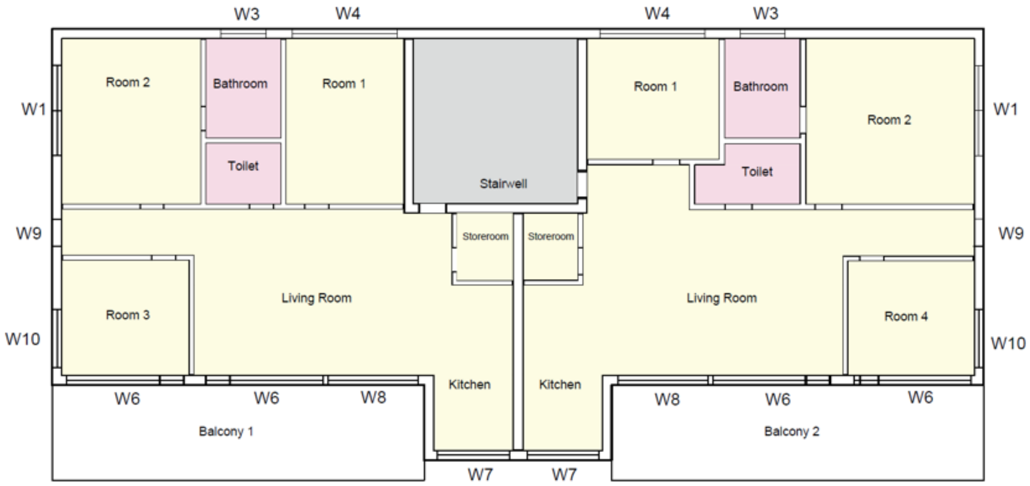

Figure 14 Apartment floor plan for the building MFH13 [24]

The energy reference area (ERA), the thermal envelope and the building envelope factor of the three buildings are detailed in the following table:

Floor	height,m			ERA, m2			Thermal envelope, m2			Building envelope factor		
	MFH13	MFH54	MFH100	MFH13	MFH54	MFH100	MFH13	MFH54	MFH100	MFH13	MFH54	MFH100
1	-2.97	-2.97	-2.81	35	37	36	0	0	0	1.39	1.45	1.57
2	0	0	0	388	379	377	701	706	748			
3	2.867	2.86	2.86	388	379	377	291	308	352			
4	5.734	5.72	5.71	388	379	377	678	685	727			
Total	-			1199	1174	1167	1670	1699	1827	-		

Table 14 Floor height, ERA, thermal envelope and envelope factor for MFH13, MFH 54, MFH100

The energetic consumption of the buildings is decomposed into 3 items: electricity, heat for domestic hot water and heat for space heating. The numbers are presented in Table 15.

	MFH13	MFH54	MFH100
Electricity (kWh/m^2/year)	13	17	32
DHW (kWh/m^2/year)	16	17	24
SH (kWh/m^2/year)	13	54	100
Total (kWh/m^2/year)	42	87	156
Energy reference area (m^2)	1 199	1 174	1 167
Electricity (kWh/year)	16 163	19 396	37 147
DHW (kWh/year)	19 456	19 456	28 255
SH (kWh/year)	15 335	63 818	116 397
Total (kWh/year)	50 954	102 669	181 798

Table 15 Energy consumptions for MFH13, MFH54, and MFH100

As MFH100 is supposed to be an older building, the temperature of the water used for space heating is set to 60° whereas MFH13 and MFH54 use low temperature heating system at 35°C. The DHW heat is the same for MFH13 and MFH54 but raises substantially for MFH100 as it has more apartments and thus more occupants. For electricity, the consumption rises from MFH13 to MFH54 because MFH54 is an old, renovated building with smaller windows and thus a larger consumption for electrical lighting.

As the most important energy carrier studied in this work, particular attention is paid to biomethane. To perform optimizations, a mean value of 124 $gCO_2eq./kWh$ HHV is first used. Taken from the KBOB database [25], this average can indeed be challenged, as the definition of the biogas supply chain and its boundaries for a life cycle analysis are numerous. To study this matter, a sensitivity analysis will be realized on the basis of a study carried out by the Empa on the plant in Werdhölzli, Zürich [26]. In this analysis, different allocation options are tested. The general model detailed illustrated in Figure 15 shows that we find two sources of biogas, the anaerobic digestion of bio-waste and the sewage sludge. Moreover, different functional units (FU1, FU2, FU3) are represented, but we set our focus on FU3 as it encompasses the production of raw biogas, its treatment to biomethane and its transportation on the gas network. Nevertheless, the conversion to heat considered in the results will be subtracted to obtain values useful in the context of our study.

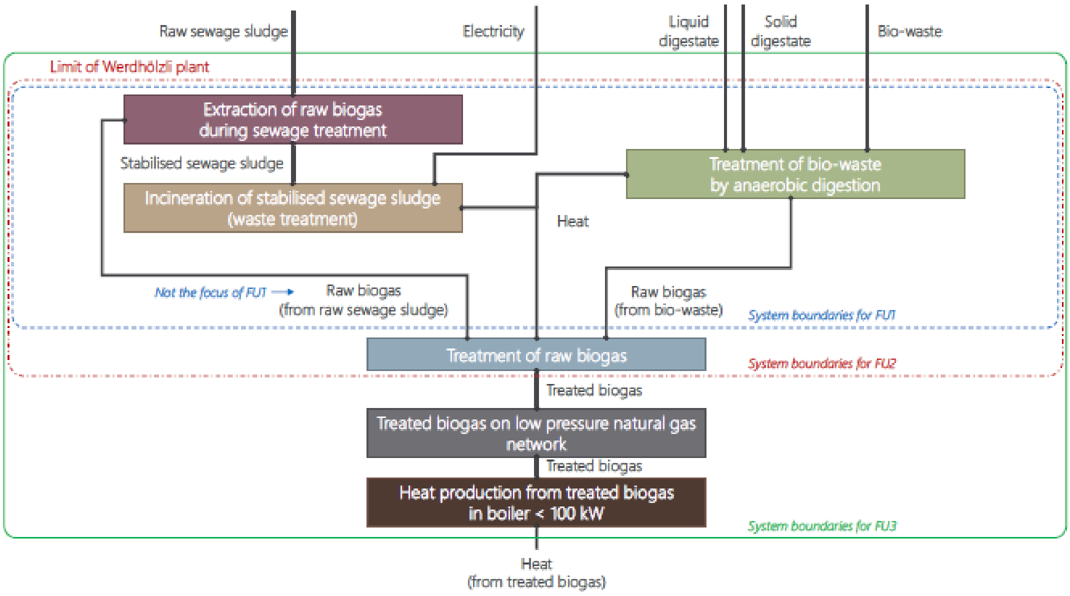

Figure 15 General model of the processes included in waste treatment [26]

The following 4 allocation models are used:

- Cut-off system modelling: the initial production of materials is consistently allocated to their primary users. When materials are recycled, the primary producer does not receive recognition for providing the recyclable materials. As a result, recycled materials are made available to recycling processes without any associated burdens. The impacts of recycling processes are solely borne by the secondary (recycled) materials. For instance, when paper is recycled, it only carries the impacts of wastepaper collection and the recycling process, without being burdened by the forestry activities and processing required for its primary production. In our case, this means that raw biogas from sewage treatment and anaerobic digestion are burden-free.
- Causal allocation: in this approach, the fact that the biowaste goes through fermentation to generate biogas is treated as a choice, which in comparison to composting leads to more methane production. The same logic applies to the raw sewage sludge treatment. Therefore, the GHG emissions of the biomethane rises with this consideration, in comparison to the cut-off system modelling.

- Economic allocation: the total emissions are allocated to the waste treatment process and its by-products which have an economic value. The split is done by comparing the prices of waste disposal and the prices of the by-products. In this case, 22% of the impacts are allocated to the raw biogas and 78% to the treatment.
- Avoided burden: lastly, this method counts the total emissions of the treatment process but subtracts the "avoided burdens", which here represents the use of anaerobic digestion instead of and industrial composting, the production of digestate that prevents the production of home composting and the avoidance of raw sewage sludge incineration.

The results of the emissions for each allocation method are presented in Figure 16, where each component of the analysis is detailed. The "heat from boiler" emissions need to be deducted since we input statistics of final energy and not useful. Moreover, the kWh of useful heat can be converted to kWh HHV, using the assumption given in the report that the boiler has a 99% HHV efficiency. The final values of biomethane carbon footprint which will be used as input for optihood are presented in Table 16.

	Cut-off	Causal	Econ Alloc	Avoided
Heat from boiler	2.7	2.7	2.7	2.7
Gas network	2.7	2.8	2.7	2.7
Raw biogas treatment	6.8	22.3	33.4	64.0
Anaerobic digestion	0.0	12.2	7.9	44.7
Avoided impacts	0.0	0.0	0.0	-78.4
Total	12.3	40.0	46.7	35.8

Figure 16 Climate change impact of the heat from the Werdhölzli biomethane [26]

	Werdhölzli, Zürich plant			
	Cut-off	**Causal**	**Economic**	**Avoided**
Emissions (g C02 eq. /kWh HHV)	9.5	36.9	43.6	32.8

Table 16 Biomethane carbon footprint values used as inputs for optihood.

As for the price, the natural gas price 9.9 ct/kWh HHV (Table 17) is the base, on which 0.3 ct/kWh are added per 10% of biomethane in the mix. This value is taken from the Energie 360° gas tariffs[15]. For the different mixes studied, the prices are the following:

biomethane %	0%	10%	30%	50%	100%
Price (ct/kWh HHV)	9.9	10.5	11.7	12.9	15.9

Table 17 Natural gas and biomethane mix prices used as inputs in Optihood.

[15] Gas prices | Energie 360°

3 Results and discussion

3.1 Case study – Romande Energie

3.1.1 Comparison between individual solution versus group energy community

General conclusions can be taken based on the Figure 17 presenting the pareto front of the all the investigated price scenarios. The pareto front reveals a clear benefit of the group optimization compared to individual optimization in terms of costs.

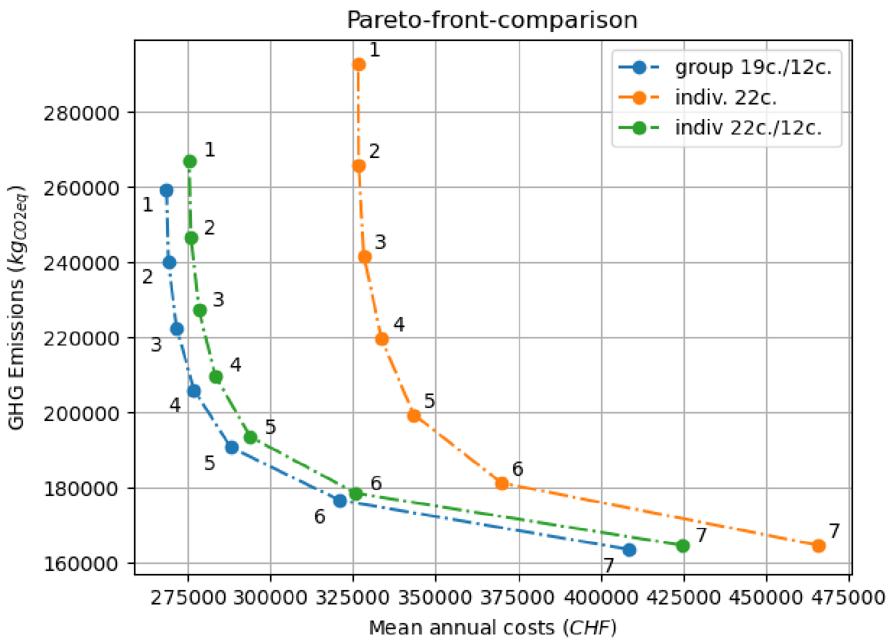

Figure 17 : Pareto front representation of the 3 scenarios investigated in the Romande Energie case study: orange line: individual optimization of the building with constant electricity prices of 22c./kWh, green-line: individual optimization of the buildings with peak/off-peak prices, blue-line: grouped optimization with peak/off-peak prices.

1. Scenario individual building with constant electricity at 22c./kWh

Figure 18 presents the evolution along the pareto front (Figure 17 – orange line) of the installed capacities per technology for all the 4 buildings. The cost optimum (optimization 1) relies on a combination of gas boiler and ASHP for the SH and DHW needs with capacities of respectively 350 kW and 153 kW for a total capacity of about 503 kW. By looking at the buildings individually, the same energy concept is found with about the same capacity distribution. On the other side of the pareto (optimization 7), the environmental optimum relies only ASHP for heat and PV for local electricity production. The total heating capacity is 529 kW. A value very close to the energy system chosen for the cost optimum.

In terms of local electricity production capacities (see Figure 19), PV is maximized from the cost optimum and on with 433 kWp installed. i.e. 14.4 Wp/m^2.SRE, this means that the whole roof is used. However, in terms of heat generation the ASHP covers 1234 MWh against 539 MWh for the natural gas boiler, while for electricity, the PV 601 MWh including 263 MWh fed-in to grid; grid purchase accounts for 911

MWh. The resulting electricity self-sufficiency rate[16] is 22%. The self-sufficiency rate corresponding to the electric energy from CHP and PV compared to the electrical energy consumed by the buildings.

Figure 20 shows the installed energy storage capacities along the pareto front. Electric batteries are installed only on reaching the 6th optimization and are maximized at the environmental optimum. As well thermal energy storage from SH and DHW are maximized at the environmental optimum. However, capacities are constant between points 1 and 4, this means that there is no clear benefit in terms of GHG emission reductions (certainly because a large of heat need is produced with gas boiler).

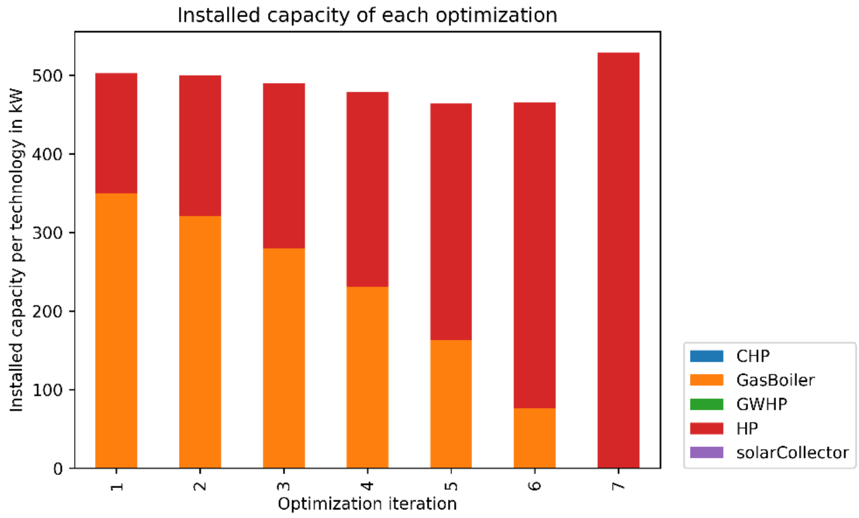

Figure 18: Evolution along the pareto front (optimization iteration) of the installed capacities in all buildings for space heating and DHW for individual buildings and constant electricity price of 22 c./kWh.

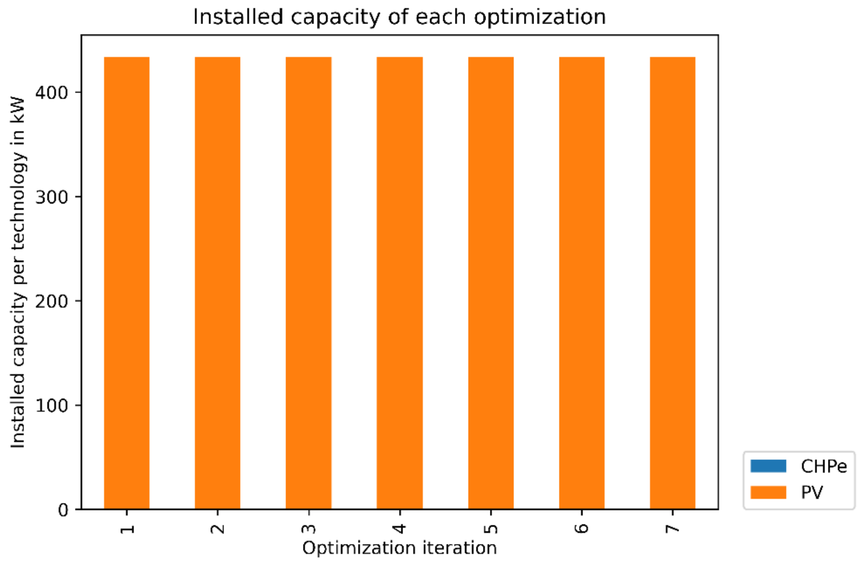

Figure 19: Evolution along the pareto front (optimization iteration) of the installed local electric production capacities in all buildings and constant electricity price of 22 c./kWh.

16 Ratio between the electricity demand covered with local electricity production over the total electricity demand.

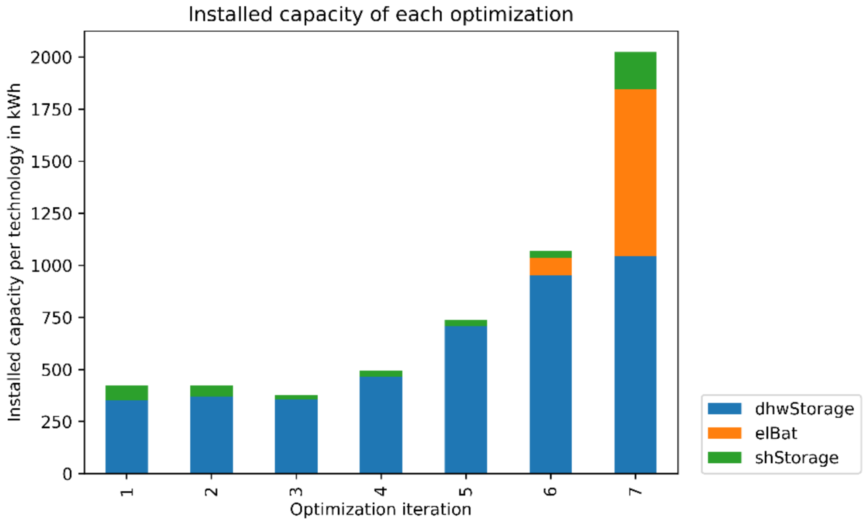

Figure 20: Evolution along the pareto front (optimization number) of the installed storage capacities for all buildings for individual building and constant electricity price of 22 c./kWh,

The evolution of the pareto front between optimization 1 and 5 reveals the cost of reducing GHG emissions can be competitive with 180 CHF/tCO_2eq but still higher than the actual carbon tax of 120 CHF/tCO_2eq[17]. This decrease as shown in Figure 20 is achieved by substituting natural gas technology with electricity through a higher use of the ASHP. One should note that here natural gas price is already penalized with the carbon tax of 120 CHF/tCO_2eq.

Figure 21 presents the evolution along the pareto front (Figure 17 – green line) of the installed capacities per technology for all the 4 buildings. The cost optimum (optimization 1) relies on a combination of gas boiler and ASHP for the SH and DHW needs with respectively capacities of 319 kW and 178 kW for a total capacity of about 497 kW. Which is very similar to the scenario with constant electricity price. By looking at the buildings individually, the same energy concept is found with about the same capacity distribution.

In terms of local electricity production (Figure 22), PV is maximized from the cost optimum and on with 433 kWp installed, i.e. 14.4 Wp/m^2.SRE. Concerning energy production at the cost optimum, on the heat side the ASHP accounts for 1356 MWh and the gas boiler 416 MWh. On the electric side, PV system produces 601 MWh including 254 MWh fed-in to the grid; grid purchase accounts for 939 MWh.

Lastly, Figure 23 show gradually increased storage capacities, especially for DHW. Electric batteries are installed to further reduce the GHG emissions from optimization 6 but comes at a greater cost. On the other side of the pareto, the environmental optimum relies as well on ASHP and PV for local electricity production. The energy storage capacities are also maximized. The total heating capacity reaches 529 kW, which is slightly higher (6%) than at the cost optimum. As before, this reveals under the given GHG emissions assumptions, that increasing storage capacities is here not capable of reducing substantially the capacity of non-intermittent heat producers.

The evolution of the pareto front between optimization 1 and 6 reveals that a reduction of GHG emissions can be cost effective, as the front is very steep achieving a slope of 252 CHF/tCO_2eq. This decrease as shown in Figure 21 is achieved by substituting natural gas boiler usage with ASHP.

[17] https://www.bafu.admin.ch/bafu/en/home/topics/climate/info-specialists/reduction-measures/co2-levy.html

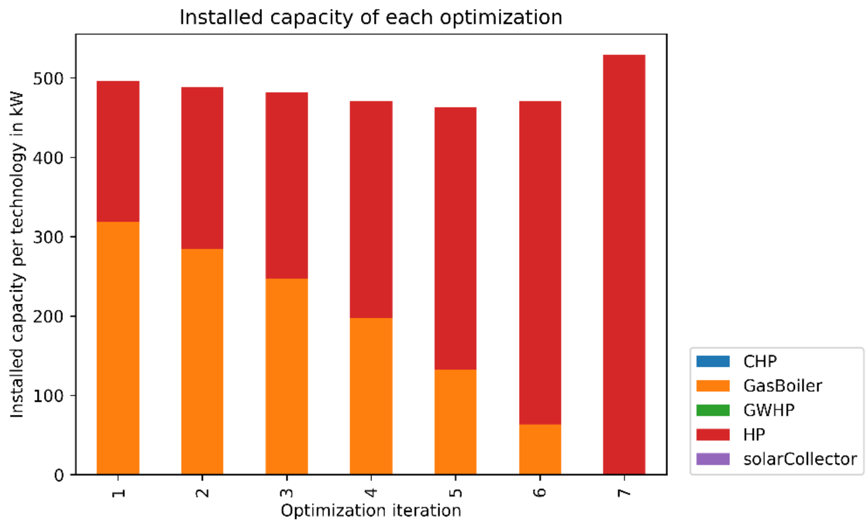

Figure 21: Evolution along the pareto front (optimization iteration) of the installed capacities in all buildings for space heating and DHW for individual buildings and on/off peak electricity price of12-22 c./kWh.

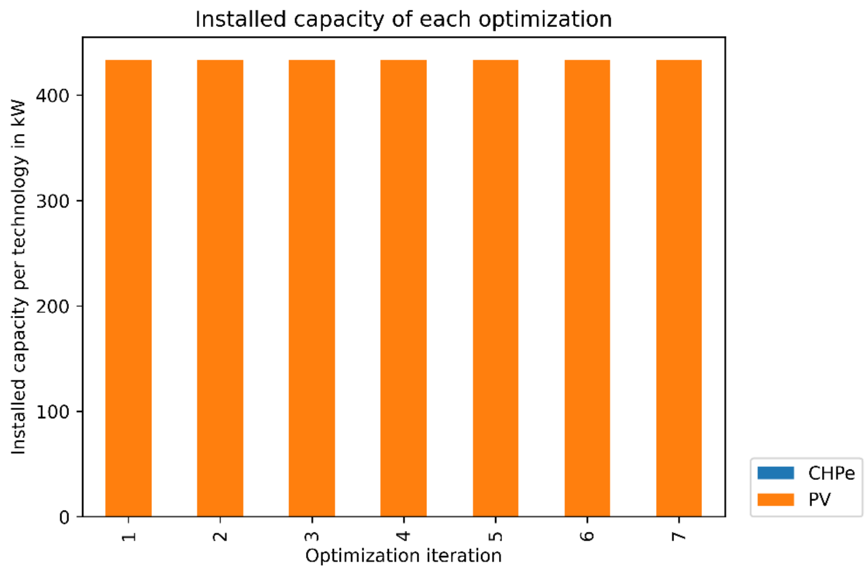

Figure 22: Evolution along the pareto front (optimization iteration) of the installed local electric production capacities for individual buildings and on/off peak electricity price of 12-22 c./kWh.

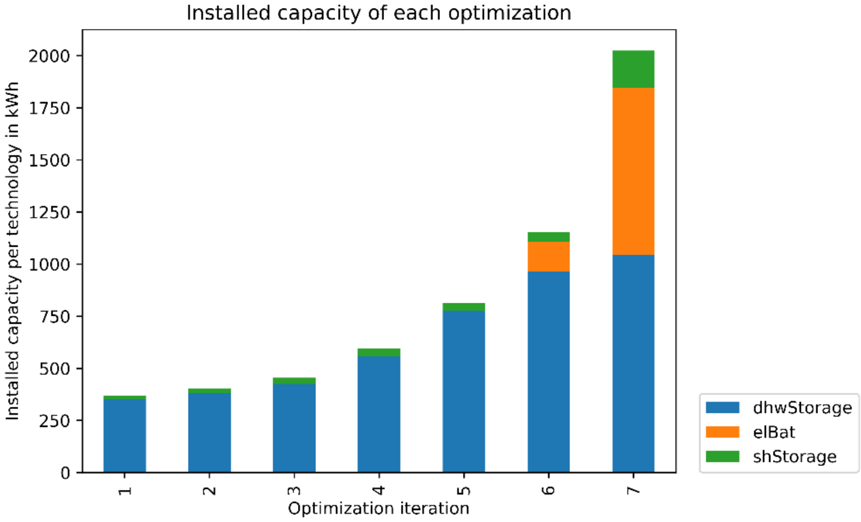

Figure 23: Evolution along the pareto front (optimization number) of the installed storage capacities for all buildings for individual building and on/off peak electricity price of12-22 c./kWh.

Figure 24 presents the evolution along the pareto front (Figure 17 – green line) of the installed capacities per technology for all the 4 buildings. The cost optimum (optimization 1) relies on a combination of gas boiler and ASHP for the SH and DHW needs with respectively capacities of 309 kW, 186 kW for a total capacity of about 495 kW. By looking at the buildings individually, the same energy concept is found with about the same capacity distribution. In terms of local electricity production (Figure 25), PV is in this case not maximized until optimization 6. However, the PV installed capacities between optimization point 1 and 5 ranges between 404 and 412 kWp. It corresponds to a variation of 8 kWp respectively around 42 m^2 of panels. Which is not significant.

Lastly and as seen before, storage capacities (Figure 26) are gradually increased, especially for DHW. Electric batteries are installed to further reduce the GHG emissions from optimization 6 but comes at a greater cost.

On the other side of the pareto, the environmental optimum relies only on ASHP for heat and PV for local electricity production. The energy storage capacities are also maximized. The total heating capacity reaches 529 kW. This is higher than the energy system chosen for the cost optimum.

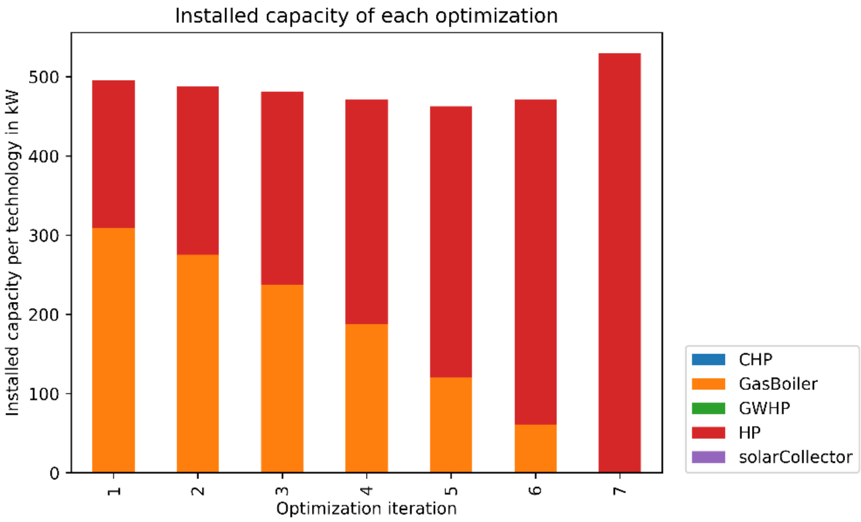

Figure 24: Evolution along the pareto front (optimization iteration) of the installed capacities in all buildings for space heating and DHW for individual buildings and on/off peak electricity price of 12-19 c./kWh.

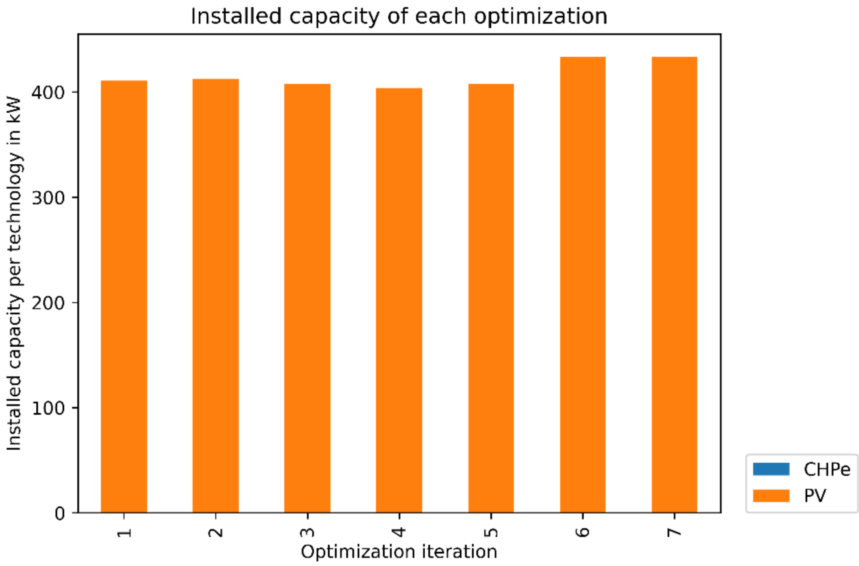

Figure 25: Evolution along the pareto front (optimization iteration) of the installed local electric production capacities for individual buildings and on/off peak electricity price of12-19 c./kWh.

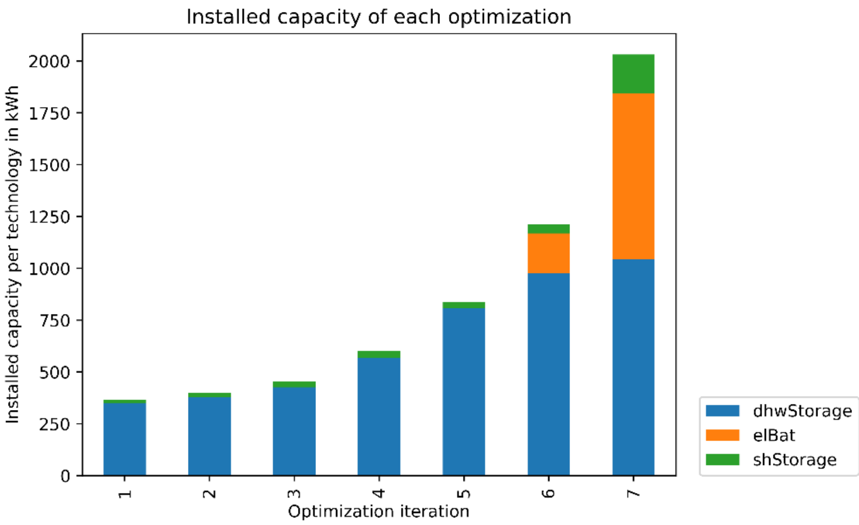

Figure 26: Evolution along the pareto front (optimization number) of the installed storage capacities for all buildings for individual building and on/off peak electricity price of12-19 c./kWh.

The evolution of the pareto front between optimization 1 and 5 reveals that a reduction of GHG emissions can be cost effective, the cost of reducing GHG emissions is 283 CHF/tCO_2eq. This decrease as shown in Figure 20 is achieved by substituting natural gas technology with HP.

Grouped buildings have decreased costs and GHG emissions respectively by 18% and 11% at the cost optimum compared with the scenario individual buildings with electricity price of 22 c./kWh. This decrease in GHG emissions is due to a greater use of HPs and a lesser use of gas boilers because the grid electricity is cheaper in the grouped optimization. In the environmental optimum, costs have decreased by 12%, while GHG emissions remain in the same range with a decrease of less than 1%. This proves the benefit of grouping building together; however, the benefits seem to be driven by the cost of the electricity as it suggested by the results of the on/off peak prices scenario. Scale effects in terms of CAPEX cost are not taken into consideration, if these exists for microgrids and when pooling projects for several buildings additional gain in cost is to be expected.

The scenario with peak/off-peak electricity prices for individual buildings have decreased costs and GHG emissions respectively by 16% and 9% at the economic optimum compared with the individual buildings' scenario with electricity price of 22 c./kWh. This decrease in GHG emissions is due as previously to a greater use of HPs and a lesser use of gas boilers because the grid electricity is on average cheaper than with a constant price. In the environmental optimum, costs have decreased by 9%, while GHG emissions remain in the same range.

3.1.2 Energy price sensitivity

General conclusions can be taken based on Figure 27 presenting the pareto front of the all the investigated price scenarios. The Pareto fronts show that the optimal solutions in terms of cost are influenced greatly by the electricity/gas price ratio. However, for GHG emissions lower than about 210 000 kgCO_2eq, the cost and GHG emissions falls within the same range. Finally, as one could predict, the environmental optimum is uninfluenced by energy price differences.

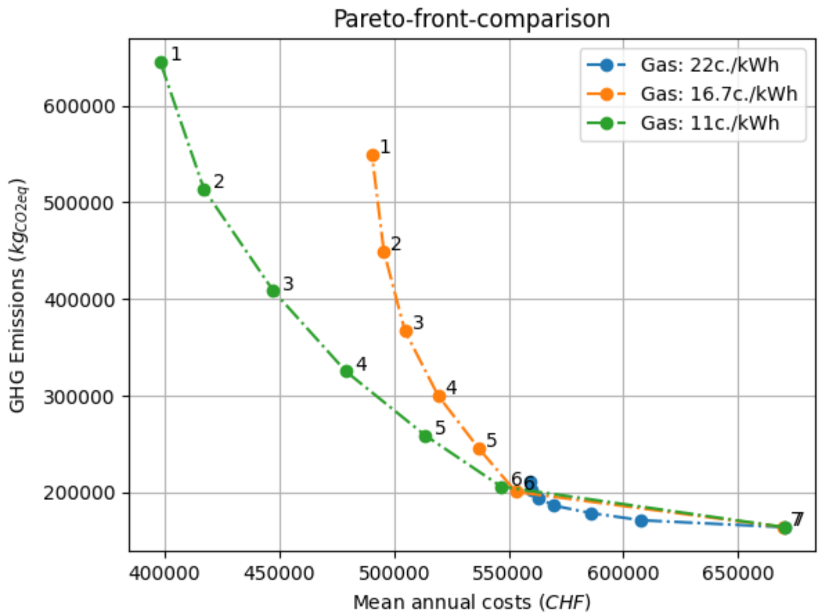

Figure 27 : Pareto front representation of the 3 price schemes investigated: blue-line: Gas 22 c./kWh (ratio 2-1); orange line: Gas 16.7 c./kWh (ratio 3-1), green-line: Gas 11 c./kWh (ratio 4-1). (all for an electricity price of 44c./kWh)

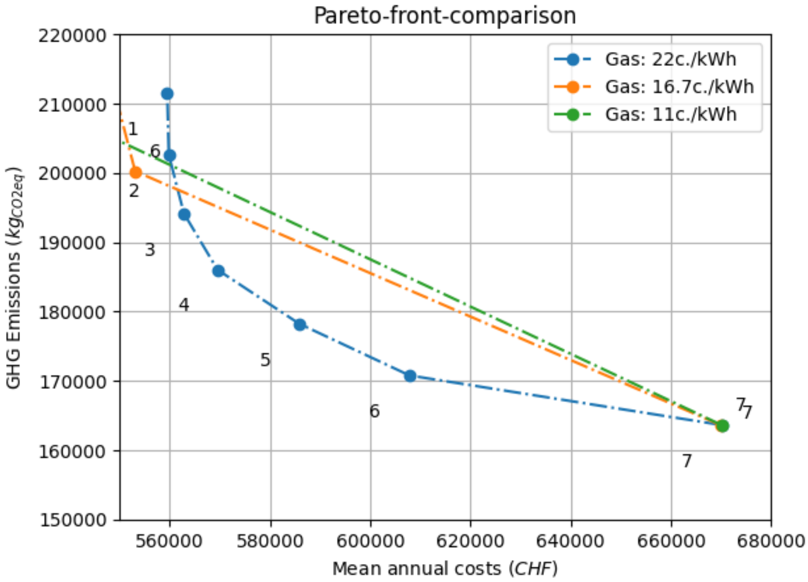

Figure 28 : Zoom of Pareto front representation of the 3 price schemes investigated: orange line: Gas 22 c./kWh (ratio 2-1) ; orange line: Gas 16.7 c./kWh (ratio 3-1), green-line: Gas 11 c./kWh (ratio 4-1). (all for an electricity price of 44c./kWh)

Figure 29 presents the evolution along the pareto front (Figure 27 – blue line) of the installed capacities per technology for all the 4 buildings. The cost optimum (optimization 1) relies on a combination of gas boiler and ASHP for the SH and DHW needs with respectively capacities of 215 kW, 264 kW for a total capacity of about 479 kW. The GHG emissions are reduced by substituting the gas boiler with ASHP capacities.at the GHG emissions optimum the energy concept relies only on ASHP with a total installed capacity of 529 kW. In terms heat production at the cost optimum, the gas boilers cover at the most 8.4 % of the heat demand. This share is gradually decreased on to the optimization 6 with an irrelevant share smaller than 1% and is suppressed. In terms of on-site electricity production, the PV system is also maximized at 433 kWp and only PV is used. Concerning the electricity production and grid purchase and feed in, the grid purchases remain mostly constant at an average of 992 MWh (variation of 3%). Excess PV production is sold for economic reasons at the beginning then gradually decreased in favor of self-consumption enabled by energy management, additional thermal storage capacities followed by the installation of electric batteries.

Figure 30 shows that the electric batteries are not installed until optimization 5. The total storage capacity is minimum at optimization 1. The DHW storage increases proportionally as the GHG emissions are optimized. Between optimization 6 and optimization 7, storage capacities are greatly increased from 1482 kWh to 2030 kWh installed with only limited reduction in GHG emissions.

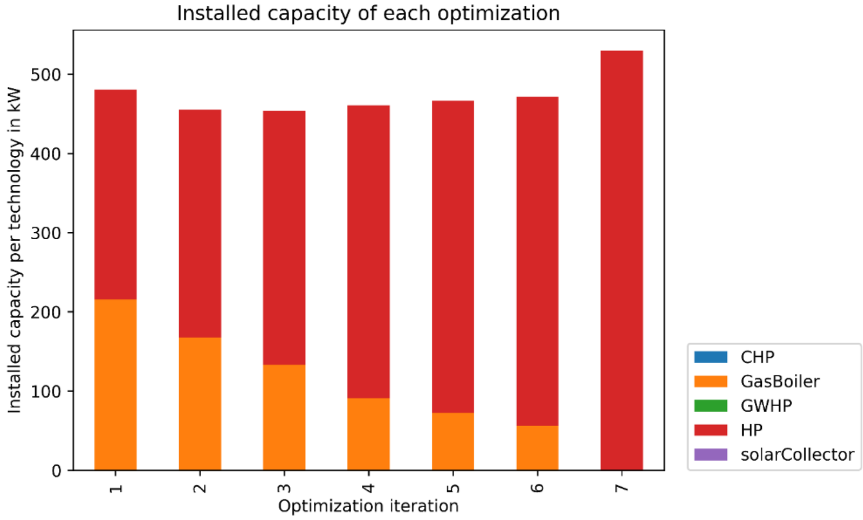

Figure 29: Evolution along the pareto front (optimization iteration) of the installed capacities in all buildings for space heating and DHW for an electricity gas price ratio of 2/1 (44 c./kWh – 22 c./kWh).

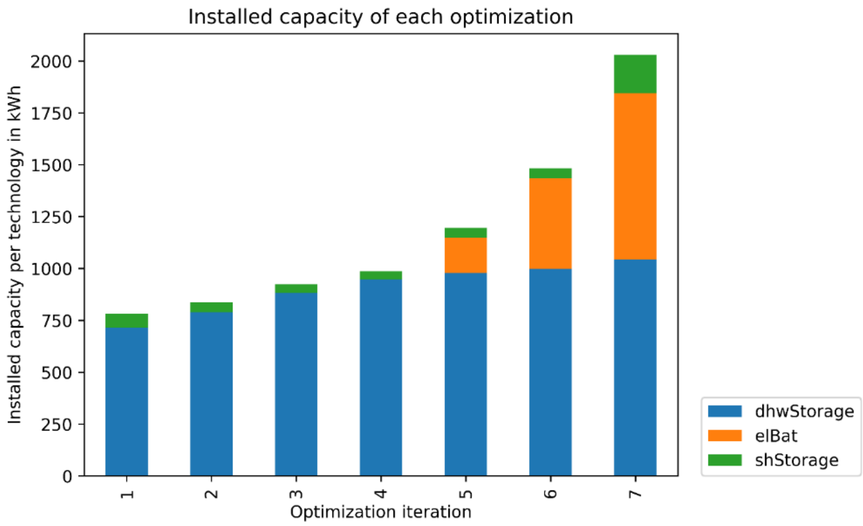

Figure 30: Evolution along the pareto front (optimization number) of the installed storage capacities for all buildings for an electricity gas price ratio of 2/1 (44 c./kWh – 22 c./kWh).

Figure 31 presents the evolution along the pareto front (Figure 27 – orange line) of the installed capacities per technology for all the 4 buildings. The cost optimum (optimization 1) relies on a combination of gas boiler, CHP and ASHP for the SH and DHW needs with respectively capacities of 135 kW, 266 kW, 83 kW, for a total capacity of about 484 kW. Along the Pareto front, the installed capacity for a boiler is almost constant before being suppressed at the GHG emission optimum. The GHG emissions are reduced by substituting the CHP with ASHP capacities.at the GHG emissions optimum the energy concept relies only on ASHP with a total installed capacity of 529 kW. The capacity of the gas boiler is non-negligible, however its share in the heat production is less than 5%.

In terms of electric capacity installed (Figure 32), PV is also maximized with 433 kWp but is supported by the CHP with 111 kW at the cost optimum. The photovoltaic electricity production remains constant as we seek to optimize the GHG emissions while the CHP decreases proportionally. The grid purchases increase as the electricity generated by the CHP decreases. The PV electricity production is maximal (roof size constraint) and remains constant until optimization 6. Nevertheless, at the environmental optimum, the production of PV electricity is slightly reduced.

Figure 33 shows that the electric batteries are not used until optimization 7. However, at this optimization point, the electric batteries represent 39% of the installed capacity with 800 kWh electric batterie's. The storage has minimum capacity at optimization 2 which is rather unusual. This should be further investigated to find its cause. DHW storage capacity increases gradually as we optimize the GHG emissions. Between optimization 6 and optimization 7, storage increases from 907 kWh installed to 2030 kWh installed, which is more than double.

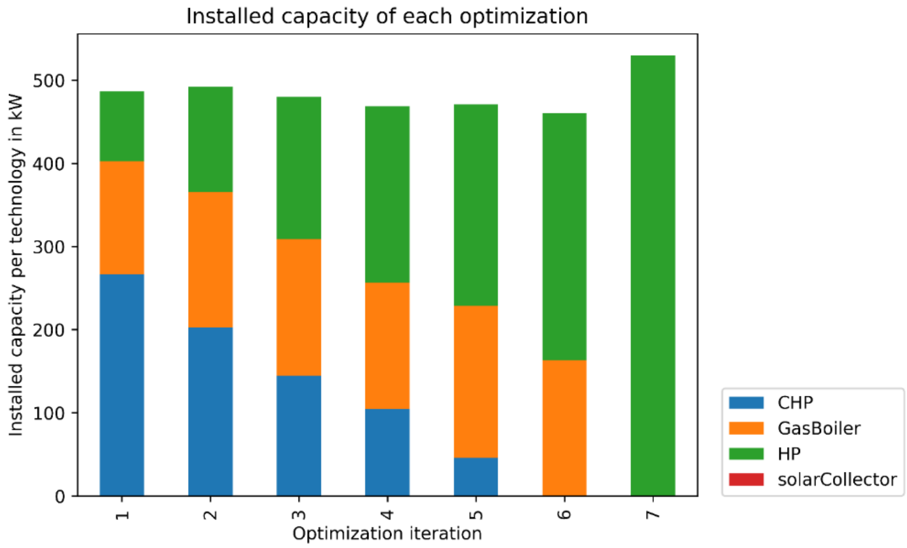

Figure 31: Evolution along the pareto front (optimization iteration) of the installed capacities in all buildings for space heating and DHW for an electricity gas price ratio of 3/1 (44 c./kWh – 14.7 c./kWh).

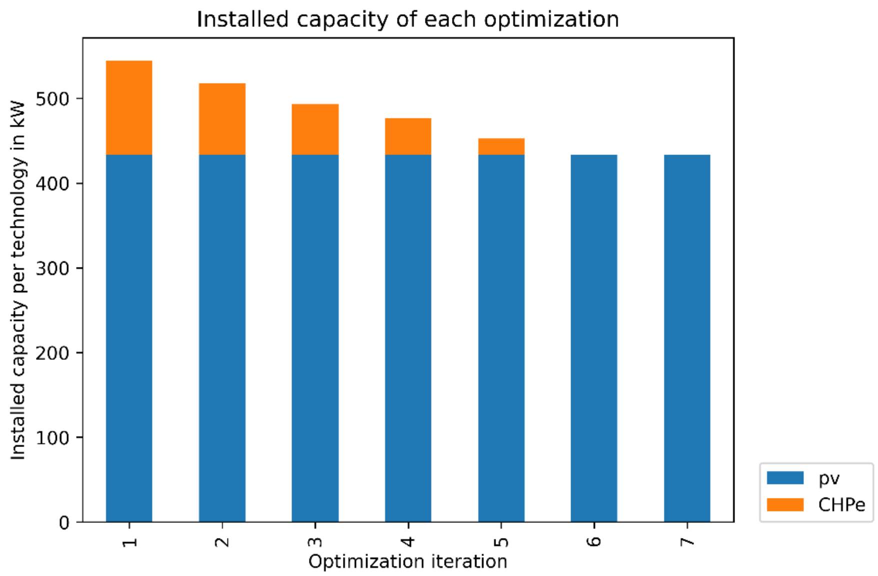

Figure 32: Evolution along the pareto front (optimization iteration) of the installed local electric production capacities for an electricity gas price ratio of 3/1 (44 c./kWh – 14.7 c./kWh).

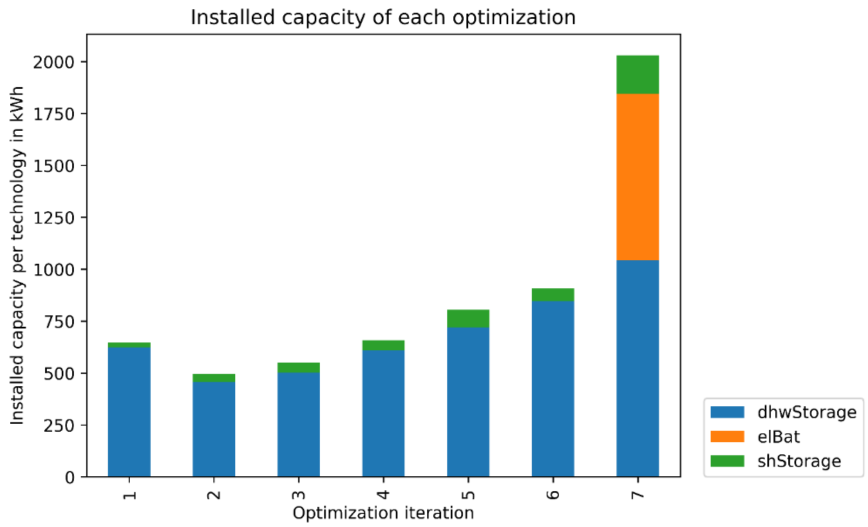

Figure 33: Evolution along the pareto front (optimization number) of the installed storage capacities for all buildings for an electricity gas price ratio of 3/1 (44 c./kWh – 14.7 c./kWh).

Figure 34 presents the evolution along the pareto front (Figure 22– blue line) of the installed capacities per technology for all the 4 buildings. The cost optimum (optimization 1) relies on a combination of gas boiler, CHP and ASHP for the SH and DHW needs with respectively capacities of 108 kW, 337 kW, 31kW, for a total capacity of about 476kW. As in the previous analysis, the installed boiler capacity is almost constant up to optimization 6 before being completely removed when seeking to optimize GHG emissions. Along the Pareto front during the first 6 optimizations, the installed CHP capacity is reduced, and it is replaced by ASHP. The GHG emissions are reduced by substituting the CHP with ASHP capacities. At the GHG emissions optimum the energy concept relies only on ASHP with a total installed capacity of 529 kW. As the CHP capacity is bigger than in the 3/1 scenario, the gas boiler covers a lesser share of the heat demand with 2% at the most.

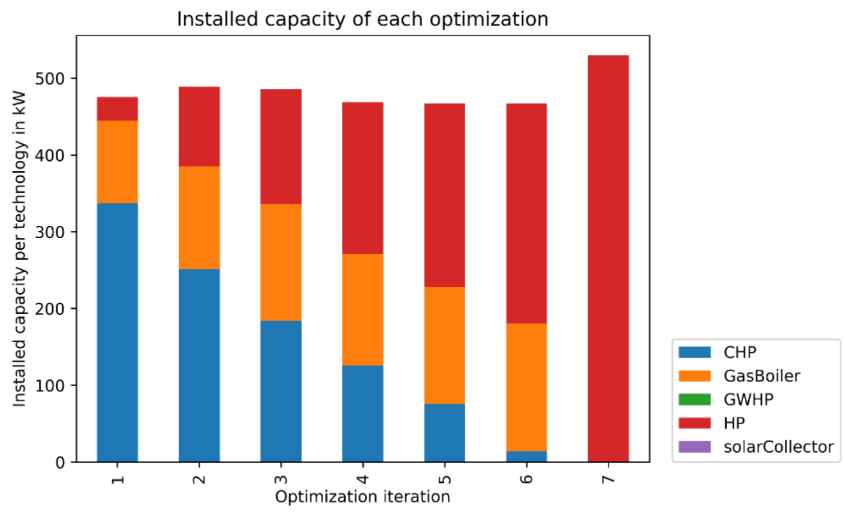

Figure 34: Evolution along the pareto front (optimization iteration) of the installed capacities in all buildings for space heating and DHW for an electricity gas price ratio of 4/1 (44 c./kWh – 11 c./kWh).

In terms of electric capacity installed (Figure 35), PV is also maximized with 433 kWp but is supported by the CHP with 140 kW at the cost optimum. Regarding photovoltaic electricity production remains constant as we seek to optimize the emission of greenhouse gases while the CHP decrease proportionally. The grid purchases increase as the electricity generated by the CHP decreases. The PV electricity production is maximal (roof size constraint) and remains constant until optimization 6. Nevertheless, at the environmental optimum, the production of PV electricity is slightly reduced (Figure 36).

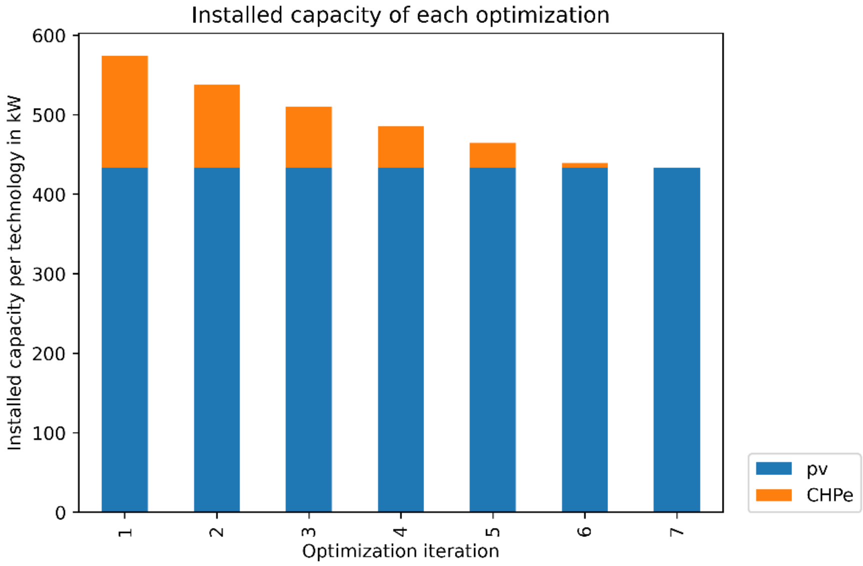

Figure 35: Evolution along the pareto front (optimization iteration) of the installed local electric production capacities for an electricity gas price ratio of 4/1 (44 c./kWh – 11 c./kWh).

Figure 37 shows that the electric batteries are not used until optimization 7. However, at this optimization point, the electric batteries represent 39.4% of the installed capacity. The storage has minimum capacity at optimization 3 which is rather unusual. There is an apparent economic benefit to invest in storage capacities when the capacity of the CHP is sufficient to maximized the electricity production. However, the storage capacity is then no longer beneficial to reduce the GHG emissions. Between optimization 6 and optimization 7, storage increases from 899 kWh installed to 2030 kWh installed, which is more than double.

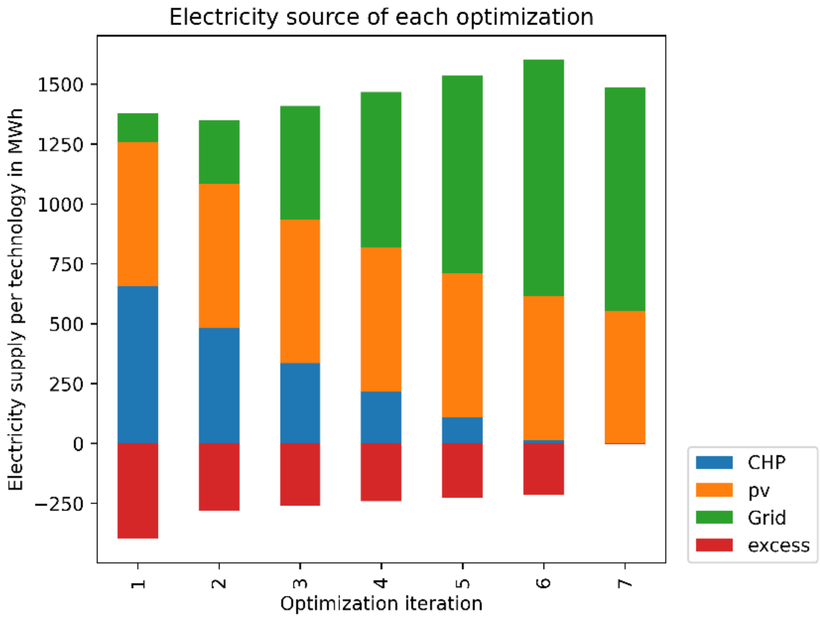

Figure 36 : Evolution along the pareto front (optimization number) of the electricity supply per technology for an electricity gas price ratio of 4/1 (44 c./kWh – 11 c./kWh.

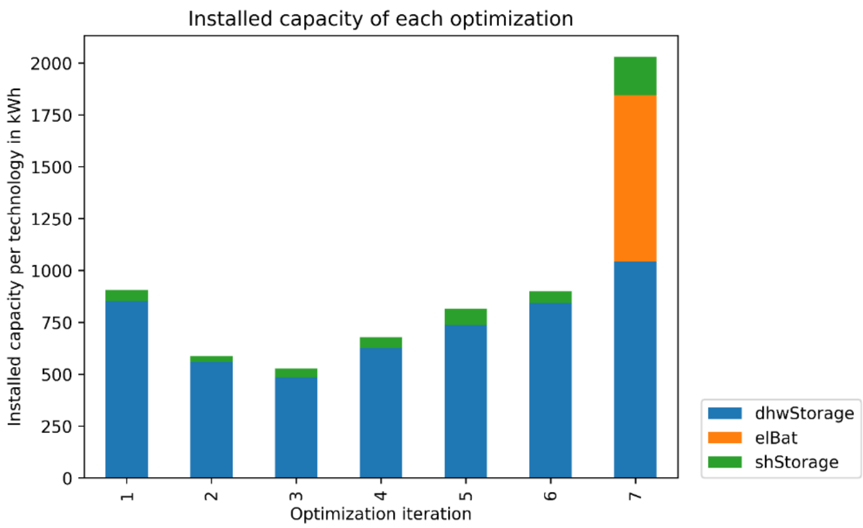

Figure 37: Evolution along the pareto front (optimization number) of the installed storage capacities for all buildings for an electricity gas price ratio of 4/1 (44 c./kWh – 11 c./kWh).

When analyzing the installed capacities according to the different optimizations for the 3/1 and 4/1 scenarios, the CHP is replaced first when seeking to optimize GHG emissions, followed by the gas boiler. At the environmental optimum, only the HP is installed regardless of the price scenario. In terms of heat production, the gas boiler is very useful to cover peak consumptions but represents only a small fraction of total heat demand (less than 5%). This heat producer is therefore used for all the price scenarios and for all the point of the Pareto front except at the environmental optimum (Figure 38). As the heat output of the gas boiler is correlated to the output of the CHP and HP, the optimums and minimums in the amount of heat generated are different in each scenario of prize.

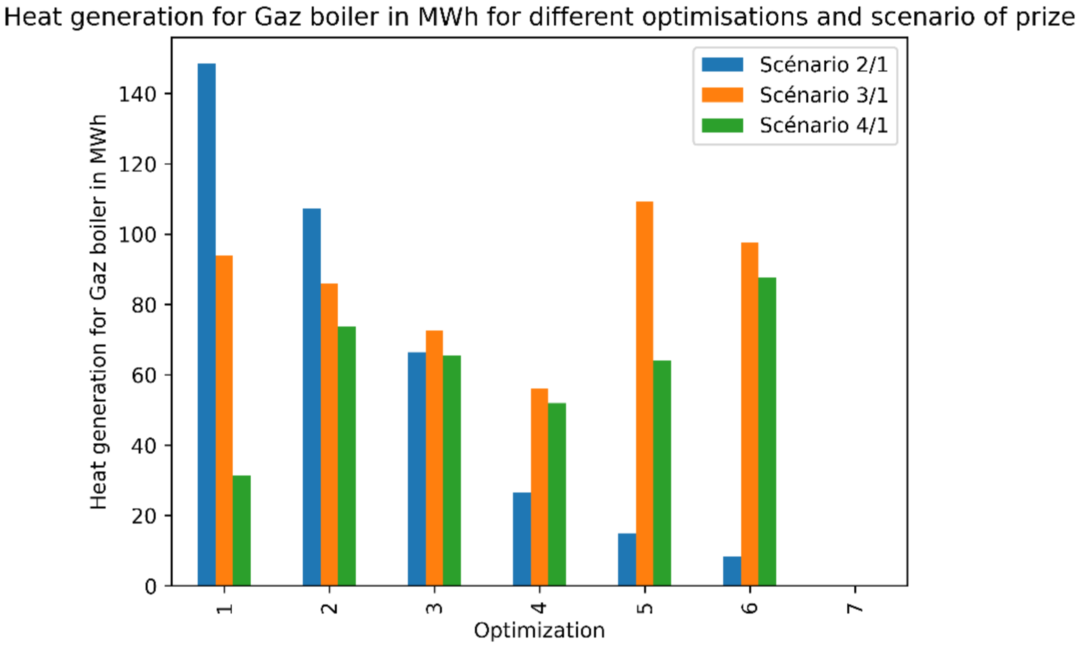

Figure 38 : Evolution along the pareto front (optimization number) of heat generation for gas boiler for all buildings and all scenarios of prize.

Concerning CHP, the investment in this technology is in the case study of Romande Energie mainly driven by the favorable natural gas prices compared to electricity (scenario 3/1 and 2/1). In the 2/1 scenario, the price of electricity being low, CHP is not installed even at the economic optimum. In terms of GHG emissions, the electricity produced with CHP has a higher carbon footprint than the grid and the PV installations.

With regard to storage, when electricity / gas price ratio is of 2/1, electrical storage is installed based on the optimization 5. For the other variants of the price ratio between gas and electricity, electric storage is only present at the environmental optimum. High gas prices (scenario 2/1) tend to favorize electric batteries.

The installed PV capacity remains constant for all price scenarios. Having only PV at the environmental optimum demonstrates that the electricity supply coming from grid is less carboned than all electricity producing technologies except PV.

3.1.3 Operation optimization of the actual energy concept:

In this scenario the case study - Romande Energie, which is described in section 2.5.1 , is analyzed based on its existing installed system by optimizing its hourly operation during one year based on two objective functions, on the annual GHG emissions and mean annual costs.

The system is designed in a way which gives little room for operational variation. Even between the cost optimum and the environmental optimum, only small variation can be expected as presented in Figure 39. Indeed, the observed absolute variations are around 1 600 CHF for costs and 2300 $kgCO_2eq$ for GHG emissions. .

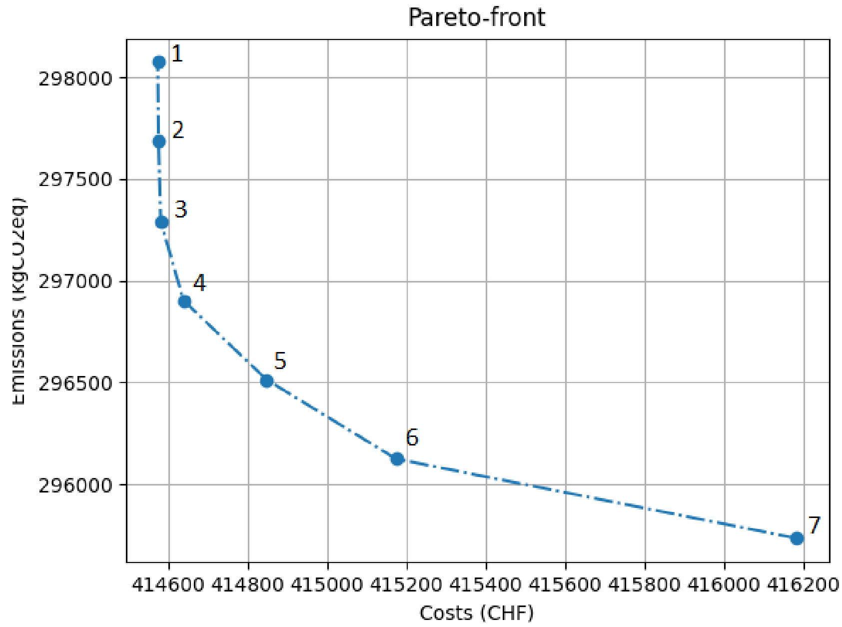

Figure 39 : Pareto-front with optimal solution describe by blue-line.

As already presented before the installed capacity for the heating system is illustrated in Figure 40 for all 4 buildings. Buildings 1-3 have solar collectors installed, which is favored at all times in all solutions for the production of domestic hot water based on its lowest operational costs and direct GHG emissions close to zero. Furthermore, the ground water heat pump (GWHP) in building 4 is capable of operating at low and high temperature and is fixed to generate all required space heating and domestic hot water. In building 1-3, the ground water heat pumps (GWHP35) only operate at low temperatures for space heating, while the gas boiler can be used for both space heating and domestic hot water. The gas boilers are therefore fixed to generate the required domestic hot water which is not covered by the solar collectors. The two sole operational decisions are:

how to generate space heating in building 1-3 by choosing between the gas boilers or heat pumps,

the optimal integration of heat storage for both space heating and domestic hot water to benefit from the varying GHG emissions of the grid and the use of electricity generated by the photovoltaic system.

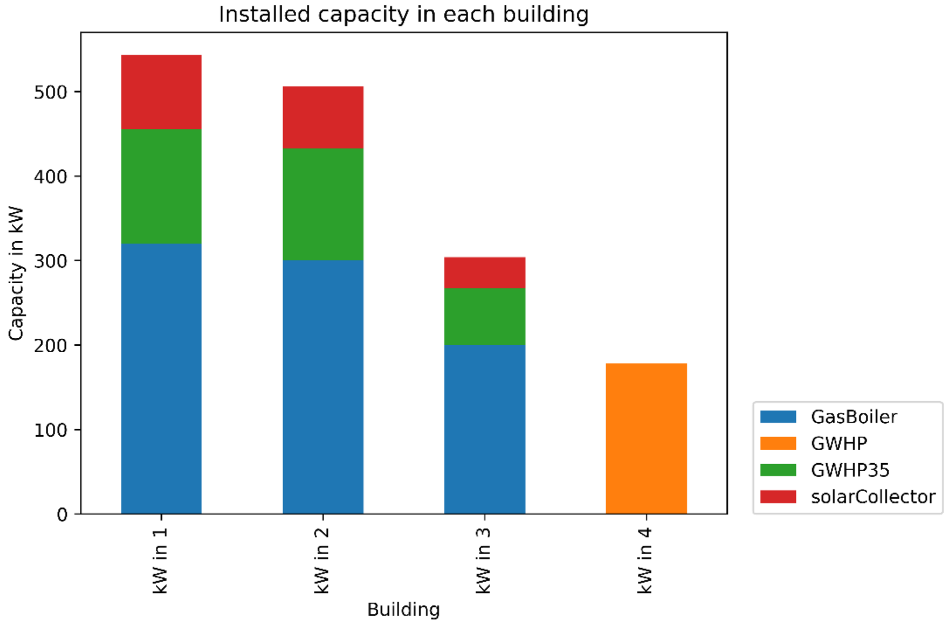

Figure 40 : Installed capacity for the heating system in four different buildings.

Based on the used input parameters, the optimization gives a clear answer to the first operational decision. Figure 41 shows the generation of space heating in the whole energy system for the 4th optimization solution, which is furthest to the lower left corner in the pareto optimal graph. However, in none of the 7 solutions is the gas boiler selected for the generation of space heating and all 7 solutions show a similar space heating production.

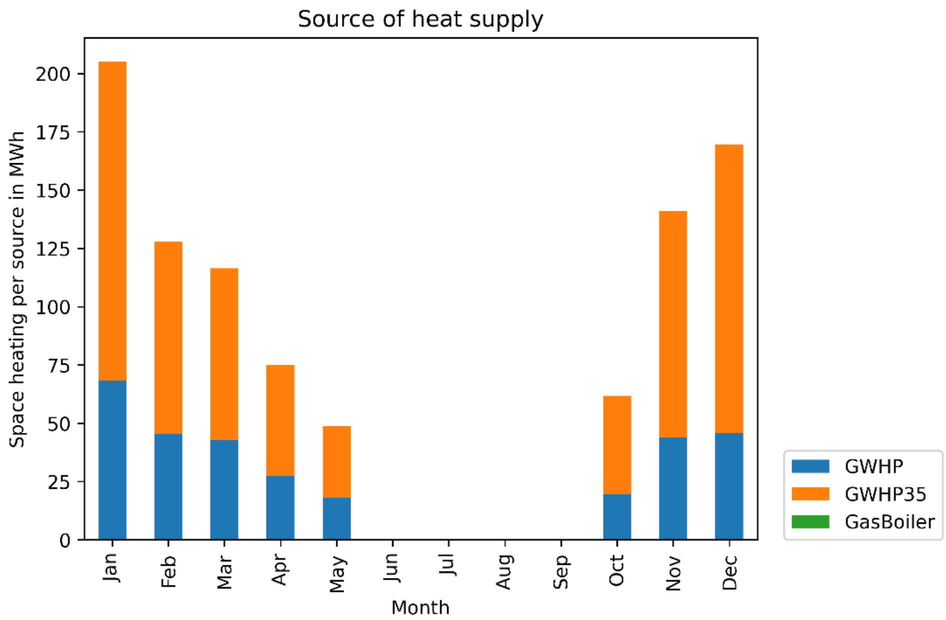

Figure 41 Monthly space heating generation by technologies in all four buildings combined.

Even though both space heating and domestic hot water is generated with the same technologies in all optimization iterations, the minor difference in operational costs and variable GHG emissions is due to shifting the generation of heat with the use of heat storages. In the cost optimized iteration (1), the production of heat with the ground water heat pump aligns with the production of photovoltaics and therefore the prices for electricity. From Figure 42 to Figure 45 the production of heat by groundwater heat pumps are plotted with the production of electricity by photovoltaic or the GHG emissions of the consumed electricity (from the grid and the PV installations) of the decision variable (electricity price and GHG emissions of electricity).

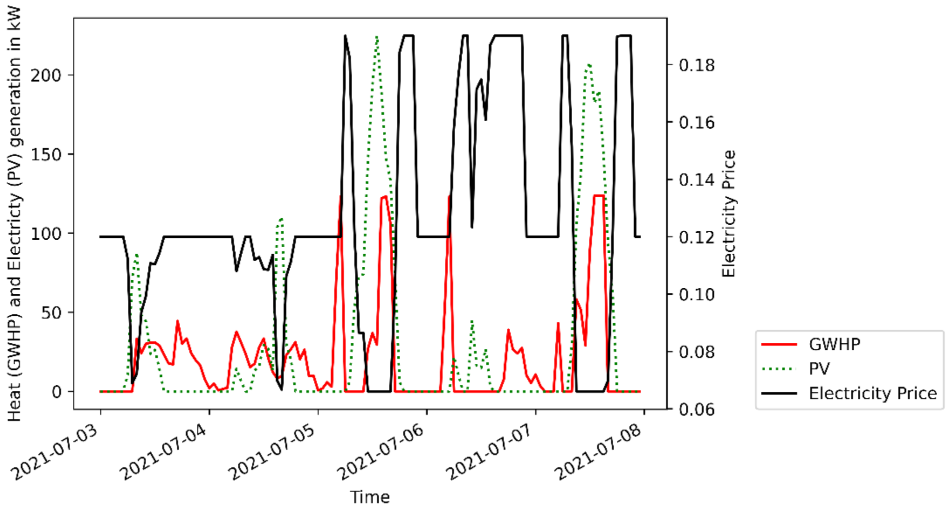

Figure 42 Domestic hot water generation by the GWHP in comparison to the real electricity price over a five-day period for the cost optimized control strategy.

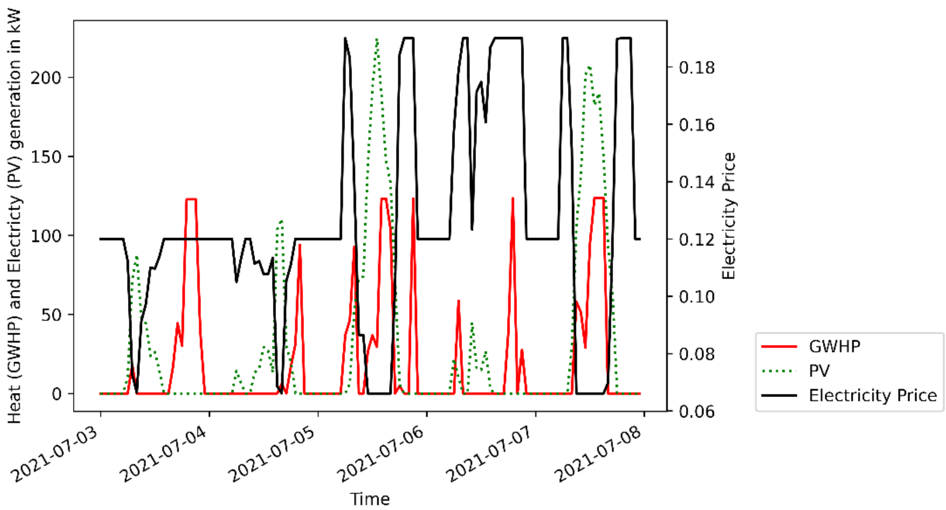

Figure 43 Domestic hot water generation by the GWHP in comparison to the real electricity price over a five-day period for the GHG emission optimized control strategy.

The electricity price shown in Figure 42 and Figure 43 represents the real price of electricity for the energy system. It is calculated by combining the levelized costs of the photovoltaic system with the electricity price of the grid. During high photovoltaic productions, the system does not require any additional electricity from the grid and the electricity price is in this time period fully determined by the levelized cost of the PV system. Comparing the GWHP production between the cost and GHG optimized iteration, it can be observed that only little heat is generated during high-cost periods and most peak production is during low-cost periods. The GHG optimized iterations shows in general a similar pattern, with the exception of a few peak productions during higher cost periods (e.g. end of 06.07).

In a similar manner to the electricity price, the GHG emissions of the energy system is shown in Figure 44 and Figure 45. By considering the GHG emissions, the previous shift noted in Figure 43 of the GWHP heat production gets obviously. At the environmental optimum, the GWHP tries to operate on periods with low GHG emissions for electricity. The similar pattern in both optimization iteration suggests that both price and the GHG emissions of electricity have some common dependences (e.g., the production with photovoltaic system with low levelized costs and low GHG emissions).

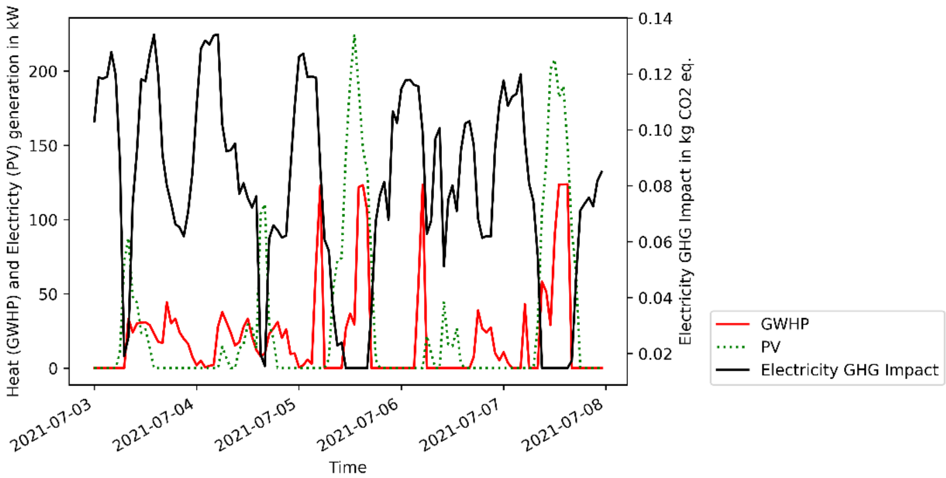

Figure 44 Domestic hot water generation by the GWHP in comparison to the electricity GHG emission impact over a five-day period for the cost optimized control strategy.

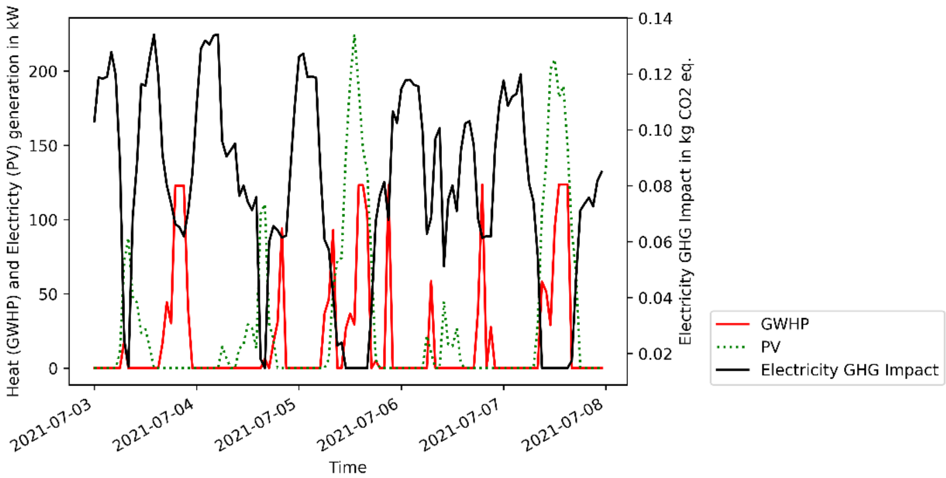

Figure 45 Domestic hot water generation by the GWHP in comparison to the electricity GHG emission impact over a five-day period for the GHG emission optimized control strategy.

3.1.4 Integration of electric mobility

General conclusions on the scenario integrating electric mobility can be taken based on the Figure 46 presenting the pareto front for two different electricity demand scenarios. Obviously, the Pareto front shows a clear advantage for the scenario without electric vehicle because the demand for electricity is lower. They are, however, not comparable since the energy demand in both cases is different. The shape of the Pareto front between the two scenarios is identical, and energy concepts are similar as explained in the sections below.

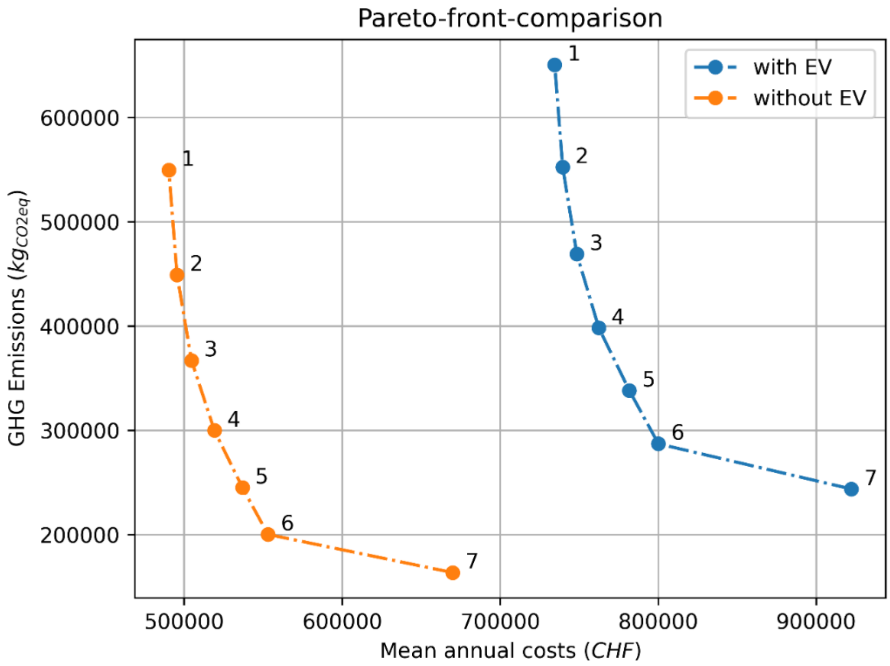

Figure 46 : Pareto front representation of the 2 scenarios: with or without EV: orange line: with EV, blue line: without EV.

1. Scenario Electricity / gas price ratio of 3/1 without electrical vehicle

The scenario without EV is modeled by the blue line in the Pareto front (Figure 46). This optimization is identical to the one described in chapter 3.1.2.

To compare the results with and without EV, it is necessary to complete the analysis of the results with the evolution along the pareto front (Figure 46– orange line) of electricity supply per technology. Figure 47 shows this evolution and at the cost optimum (optimization 1) the electricity demand are covered with a combination of PV, CHP, and Grid with respectively electricity supply of 601 MWh, 520 MWh, 212 MWh, for a total of 1333 MWh and with an excess of electricity of 291 MWh. The CHP is used up to optimization 5 and at the environmental optimum, there is no feed-in from the PV system to the grid.

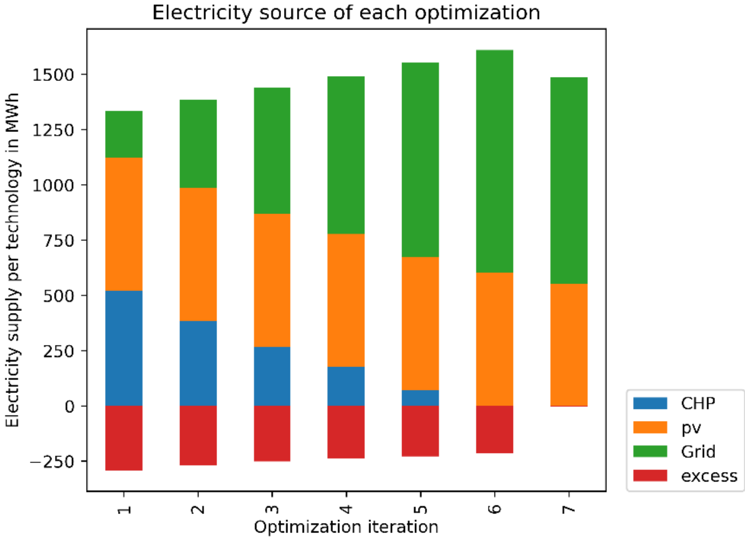

Figure 47 : Evolution along the pareto front (optimization number) of the electricity supply per technology for an electricity gas price ratio of 3/1 (44 c./kWh – 14.7 c./kWh) without EV.

2. Scenario Electricity / gas price ratio of 3/1 with electrical vehicle

Figure 48 presents the evolution along the pareto front (Figure 46– blue line) of the installed capacities per technology for all the 4 buildings. The cost optimum (optimization 1) relies on a combination of gas boiler, CHP and ASHP for the SH and DHW needs with respectively capacities of 138 kW, 278 kW, 73 kW, for a total capacity of about 489 kW. As in the previous analysis, the installed boiler capacity is constant up to optimization 6 before being completely removed when seeking to optimize GHG emissions. Along the Pareto front during the first 6 optimizations to reduce GHG emissions, the installed CHP capacity is reduced, and is replaced by ASHP. At the GHG emissions optimum the energy concept relies only on ASHP with a total installed capacity of 531 kW.

In terms of installed capacity of PV (Figure 49), is also maximized with 433 kWp but is supported by the CHP with 116 kW at the cost optimum cost.

Figure 50 shows that the electric batteries are not used until optimization 7. However, at this optimization, the electric batteries represent 39.4% of the installed capacity with 800 kWh electrical batteries (maximum capacity. The storage has minimum capacity at optimization 2 which was already observed in scenario on the energy price sensitivity (see section 3.1.2).

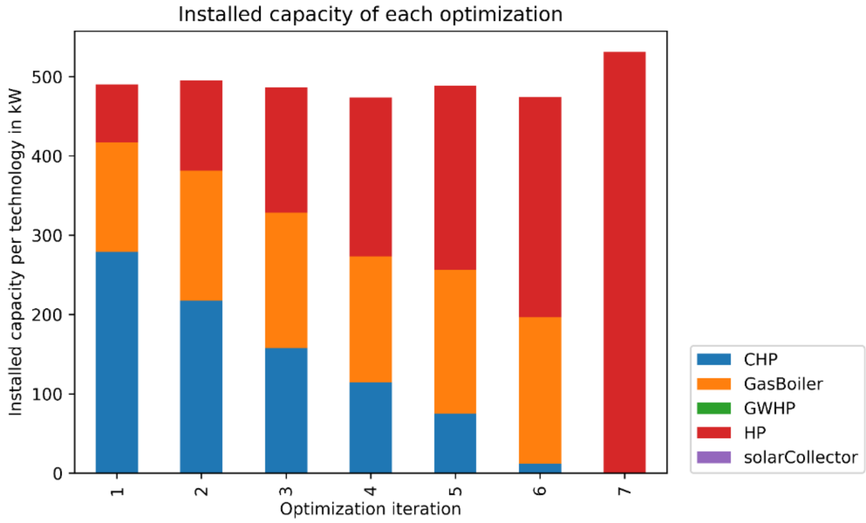

Figure 48 : Evolution along the pareto front (optimization iteration) of the installed capacities in all buildings for space heating and DHW for an electricity gas price ratio of 3/1 (44 c./kWh – 14.7 c./kWh) with EV.

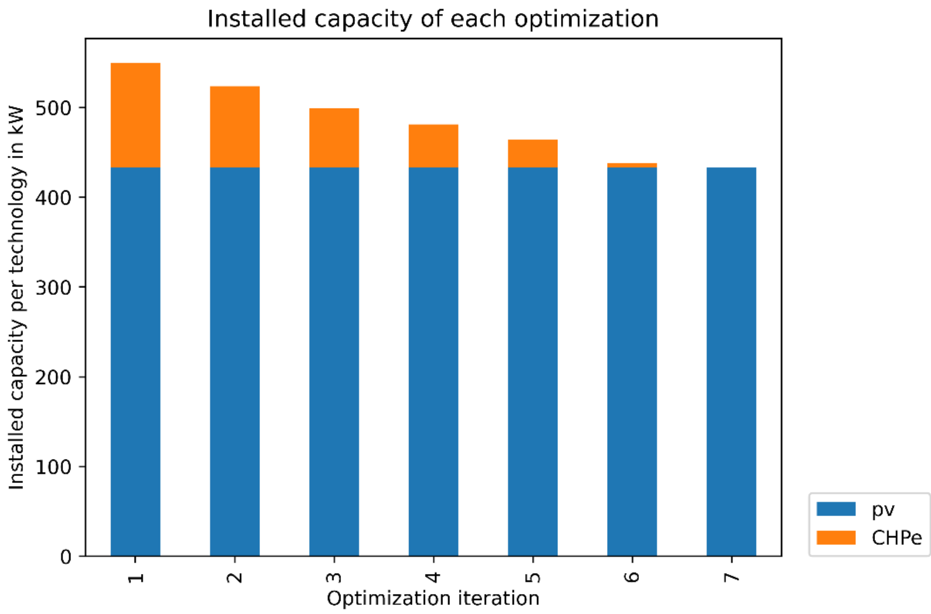

Figure 49 : Evolution along the pareto front (optimization iteration) of the installed local electric production capacities for an electricity gas price ratio of 3/1 (44 c./kWh – 14.7 c./kWh) with EV.

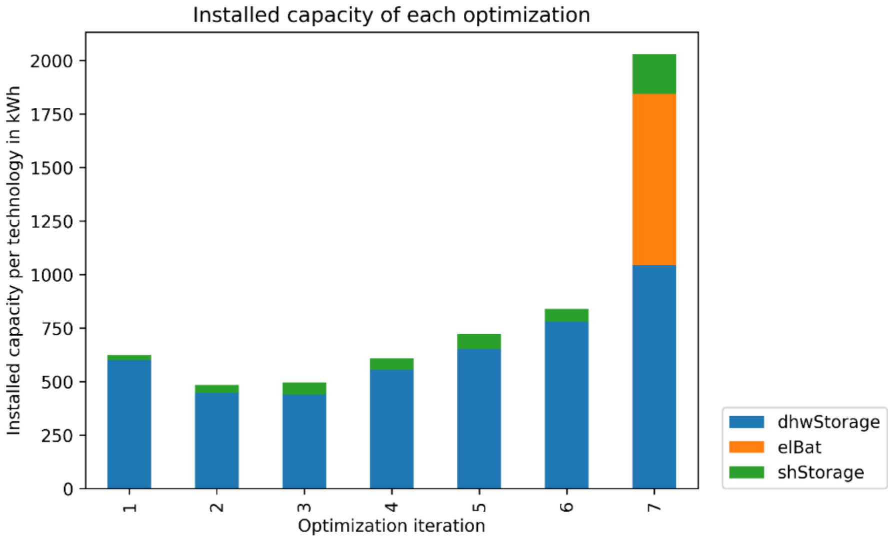

Figure 50: Evolution along the pareto front (optimization number) of the installed storage capacities for all buildings for an electricity gas price ratio of 3/1 (44 c./kWh – 14.7 c./kWh) with EV.

Figure 51 shows this evolution and at the cost optimum (optimization 1) relies on a combination of PV, CHP and Grid with respectively electricity supply of 601 MWh, 553 MWh, 704 MWh, for a total of 1858 MWh and with an excess of electricity of 240 MWh. The CHP is used up to optimization 6 and at the environmental optimum, there is no excess. The electricity supply by PV stays constant up to optimization 6 with 601 MWh before going down to 572 MWh at environmental optimum.

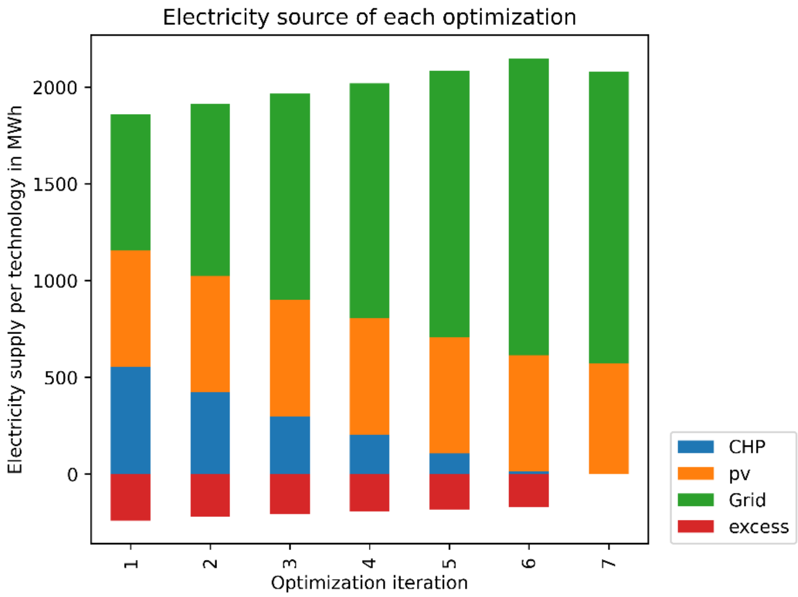

Figure 51 : Evolution along the pareto front (optimization number) of the electricity supply per technology for an electricity gas price ratio of 3/1 (44 c./kWh – 14.7 c./kWh) with EV.

3. Discussion

The additional electric consumption for the EV of 525 MWh (total electric of 1333 MWh without EV and 1858 MWh with EV) is covered with electricity from the grid. This can be seen in Figure 41 showing the self-sufficiency rate (local electricity consumption over total electricity consumption) for the scenario with EV in blue and without EV in orange. The self-sufficiency rate without EV is higher by more than 20 points at the economic optimum when there is no EV. This is explained by the fact that the PV installation is maximized in both cases therefore its production (601 MWh) cannot be increased. Moreover, the capacities of the CHP are only between 5 to 10% larger with EV than without because they are sized mostly according to the heat demand. Consequently, the additional electricity production from the CHP is limited relatively compared to the increase in electricity consumption (+40%). This comes from two causes: The heat from the CHP has to be used to cover some demand (no heat rejection is allowed), and there is the chosen technology for CHP (internal combustion engine) is not able to control the ratio of electricity to heat production. Therefore, additional CHP capacities would only be possible with additional heat demand. High use of the grid is therefore necessary.

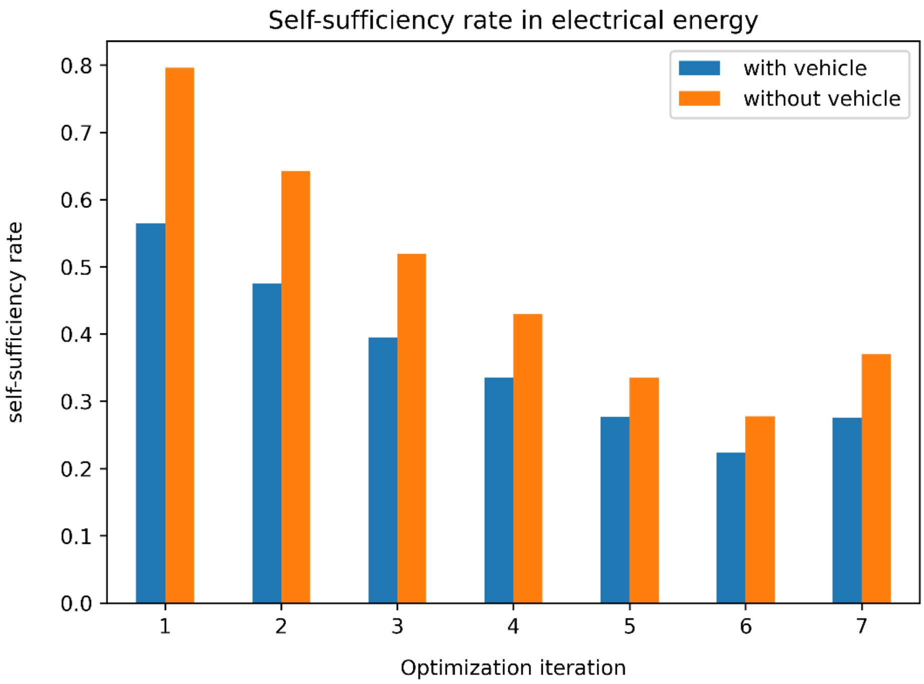

Figure 52: Comparison of the evolution along the pareto front (optimization number) of the electricity self-sufficiency rate in electrical energy for an electricity gas price ratio of 3/1 (44 c./kWh – 14.7 c./kWh) with and without EV.

3.1.5 Summary of case study and conclusions

This case study carries out a retrospective optimization applied to a real estate development in the Lausanne region of Switzerland. The development comprises six Minergie A buildings, each equipped with photovoltaic (PV) panels and utilizing ground source heat pumps (GSHP) for space heating (SH). Building 4 also provides heat to buildings 5 and 6 and generates domestic hot water (DHW) using a GSHP, while buildings 1, 2, and 3 use solar thermal (ST) panels and a backup gas boiler for DHW production. To simplify the optimization, buildings 4, 5, and 6 are considered as a single entity. Additionally, the cooling and refrigeration equipment for the supermarket is owned and operated by the retail company, with electricity consumption accounted for in building 4. It is noteworthy that the condenser heat from the cooling and refrigeration equipment contributes to balancing the heat source for the GSHPs through the borehole heat exchanger (BHE).

This configuration is used to study 4 main scenarios:

- Comparison between individual and energy community (group) solutions
- Price sensitivity in energy community context

- Optimization of the operational strategy
- Integration of electric mobility

1. Comparison between individual solution and energy communities (group)

The study investigates the energy tariffication boundaries. Large consumers benefit from lower energy prices due to scale effects, leading to variations between energy community and individual solutions. Three optimization scenarios are examined: one for the energy community and two for individual buildings with different electricity pricing schemes. The energy community, considered a large consumer, owns an electrical microgrid connecting buildings and a transfer station. The results highlight the cost and GHG emissions advantages of the grouped optimization over individual optimizations.

In terms of energy pricing, gas prices are consistent across all scenarios at 9.7 c./kWh, while electricity prices vary based on peak/off-peak schemes (12/19 c./kWh for energy communities and 12/22 c./kWh) and constant schemes (22 c./kWh). The Pareto front analysis reveals the superiority of the grouped optimization in terms of cost and greenhouse gas emissions. Notably as presented in , the cost-optimal solution for individual buildings with constant electricity prices involves a combination of gas boilers and air-source heat pumps (ASHP). On the other end of the Pareto front, the greenhouse gas emission optimal solution relies solely on ASHP for heat and maximization of the energy storage capacities.

For individual buildings with peak/off-peak electricity prices, the energy concepts are similar to constant electricity prices, with smaller natural gas boilers. Grouped buildings with on/off-peak electricity prices also exhibit comparable energy concepts, favoring ASHP over gas boilers. The analysis demonstrates that reducing GHG emissions incurs costs.

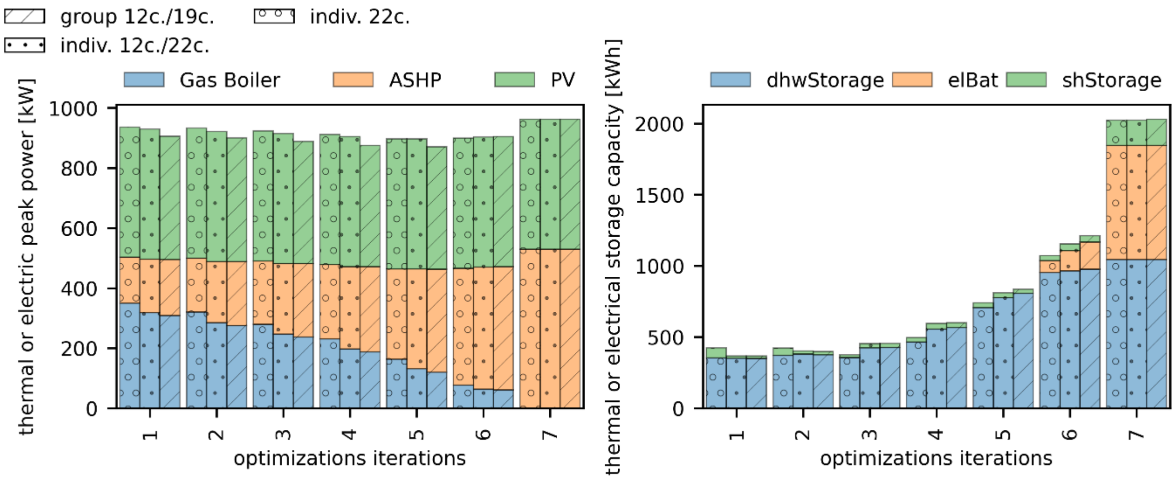

Figure 53 : Evolution along the pareto front (optimization iteration) of the installed converters' capacities (left) and energy storage capacities (right) in all buildings for space heating and DHW for grouped and individual buildings.

Grouped buildings exhibit at the cost optimum decreased costs and GHG emissions compared to individual scenarios. This reduction is attributed to greater use of ASHP and lower reliance on gas boilers, driven by the cheaper grid electricity in the grouped optimization. However, the benefits are tied to electricity costs. However, scale effects in CAPEX costs for microgrids and potential additional gains when pooling projects for multiple buildings are not currently considered.

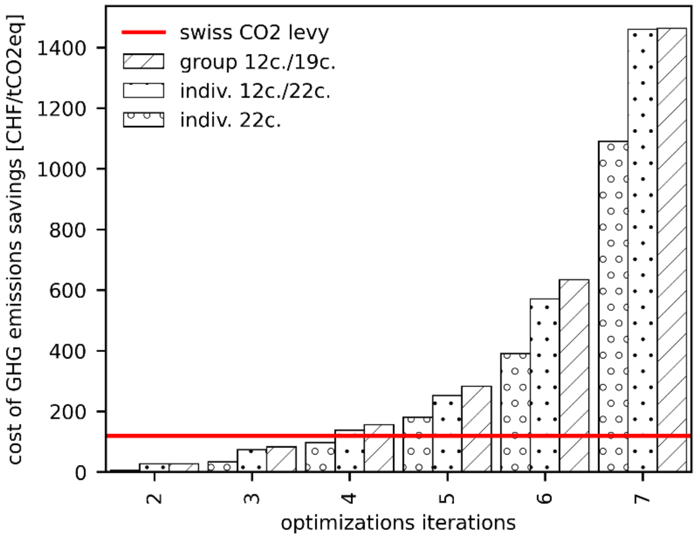

Figure 54 :

Figure 2 shows for all scenarios the cost differences per GHG emissions savings in tCO_2eq saved between the cost optimum and the other optimization iterations on the Pareto front and reveals the competitiveness of the decarbonations measures in relation to the CO_2 tax applied on fossil fuel in Switzerland set at 120 CHF/tCO_2eq (red line). From the 5th iteration, all scenarios present savings higher than the tax. Obviously, the scenario with the highest electricity cost shows the best potential of cost effective decarbonation.

2. Energy price sensitivity

In this study, various price scenarios are investigated for an energy community in relation to cost and GHG emissions optimization. The objective is to give trends of the optimal energy concept and sizing for different gas prices (22, 16.7, 11 c./kWh) with a constant electricity price 44 c./kWh, corresponding to price ratio (electricity vs gas) of respectively 2/1, 3/1, 4/1. illustrates the Pareto front for the given gas prices and electricity/gas price ratios, emphasizing the influence of these factors on optimal solutions. Cost-optimal solutions are significantly affected by the electricity/gas price ratio, while GHG emissions within a specific range exhibit similar cost patterns. The environmental optimum, however, is obviously not influenced by energy price differences. The Pareto fronts of the price scenarios investigated confound themselves under GHG emissions of 220 tCO_2eq.

 detail the evolution along the Pareto front for different scenarios, showcasing the installed capacities of technologies, such as gas boilers, ASHP, CHP, and PV, as well as storage capacities. The optimal combinations of technologies at different stages of the optimization process are depicted. Electric batteries, for instance, only come into play at a later stage (optimization 5-7) and in higher gas prices scenarios. Optimal energy storage capacities are influenced by the sizing of the CHP unit, as storage capacities are higher when CHP size is high. Low gas prices in relation to electricity (ratio 3/1 and 4/1) favors CHP systems in combination with heat pumps and gas boilers when cost is optimized. However, GHG emissions are higher than for scenarios where electricity is cheaper and where ASHP are preferred. Installation of CHP is complementary to PV systems, which are maximized in all cases and optimization's iterations.

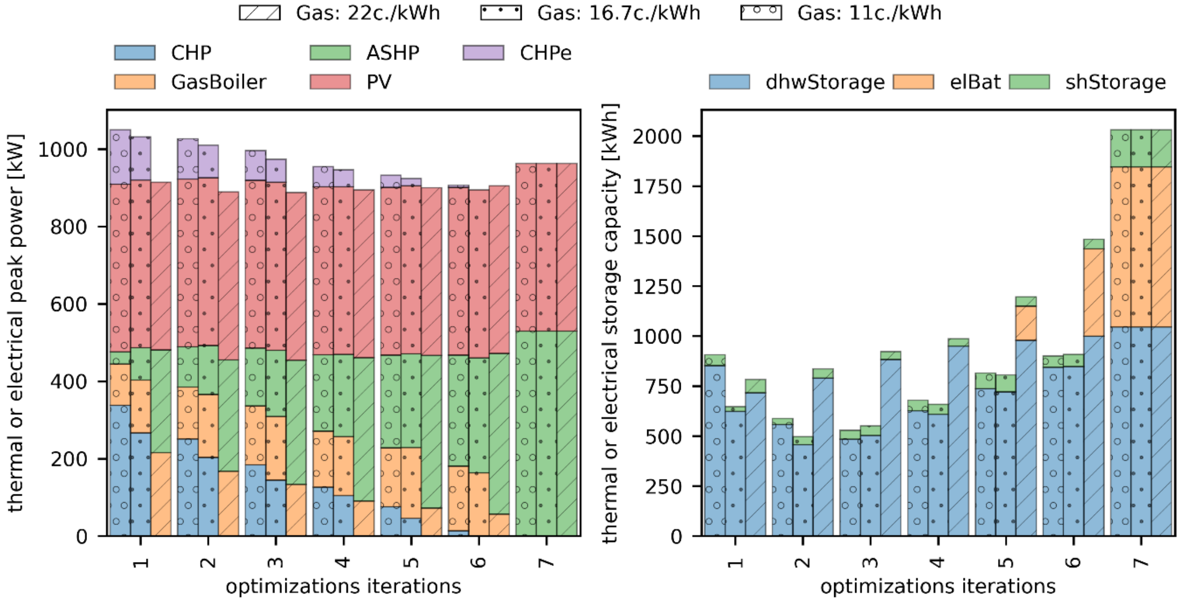

Figure 55 : Evolution along the pareto front (optimization iteration) of the installed converters' capacities (left) and energy storage capacities (right) in all buildings for space heating and DHW for different gas prices 22 c./kWh (ratio 3-1), 16.7 c./kWh (ratio 3-1), 11 c./kWh (ratio 4-1) (all for an electricity price of 44c./kWh)

3. Operation optimization

This scenario centers on optimizing the operation of the energy system in regards of heat and electricity use and production and dynamic prices and GHG emissions of the grid electricity. The system configuration remains constant, corresponding to the actual installed equipment of this test case. Consequently, there is no optimization carried out regarding the selection of technologies or their capacities. The energy pricing structure aligns with the group price scheme employed in scenario "group vs individual".

No obvious benefits in operation optimization were found for the space heating production in contrast with the DHW production where heat can be stored, and use shifted more efficiently. Figure 3 depict the DHW generation by groundwater heat pumps (GWHP) in comparison to the effective electricity price[18] over a five-day period for cost optimized control strategies. GWHP production occurs when possible and at full power during low-cost periods, while during high-cost period the GWHP load is rationally scaled to cover the demand.

In a similar manner GWHP operation optimization can be carried out considering dynamic GHG emissions calculated according to Ecodynelec tool [1] for the grid electricity and the locally produced electricity with PV. Same days as previously are shown in Figure 4. By considering the GHG emissions, the previous shifts noted in Figure 3 are now occurring when the GHG emissions are low. The GWHP tries to operate as much as possible on periods with low GHG emissions for electricity. The similar pattern in both optimization iteration suggests that both electricity price and GHG emissions have some common dependences (e.g., the PV production have low levelized costs and low GHG emissions).

4. Integration of electric mobility

This scenario investigates the impact of incorporating electric vehicles (EVs) into the energy system of the group scenario with the price boundary favorizing important local energy production, price scenario

[18] The price signal is calculated considering the price of the electricity bought from the grid and from the PV installation.

3/1. Based on the size of the settlement, 250 EVs were considered and account for an additional electricity consumption of 525 MWh representing 38% of the actual electricity demand. The hourly profile was derived from monitoring data and scaled to the assumed number of vehicles.

The results show that the higher electricity demand from EVs necessitates a greater reliance on the electricity grid. Without EVs, the self-sufficiency rate (local electricity consumption over total electricity consumption) reaches 45% at the economic optimum. With EVs, the self-sufficiency rate drops to 25% at the economic optimum. This is because the CHP capacity utilization remains relatively unchanged despite the increased electricity demand. This is because the CHP is primarily sized to meet the heat demand, and the additional electricity production from the CHP cannot keep pace with the increase in electricity consumption from EVs. As in previous scenario, electric batteries are not utilized until optimization 7, when the electric vehicle charging demand becomes substantial.

5. Conclusions

The following conclusions were drawn from the specific case study carried out for Romande Energie:

- Grouped solutions showed a 16% cost reduction and a 9% decrease in GHG emissions compared to individual solutions. This difference is only caused by the difference of 3c./kWh during peak hours granted as a large consumer.
- The energy concepts for both individual and grouped buildings are similar, relying on a bivalent system of natural gas boilers and ASHP. However, according to the federal energy policies and projections the use of fossil fuels in new buildings is prohibited, promoting decarbonization through ASHP and grid electricity.
- decarbonization can be cost effective (180 CHF/tCO_2eq) when electricity price is high (22 c./kWh) compared to natural gas (8.7 c./kWh). This is because large quantity of natural gas is substituted for electricity through heat pumps.
- PV is preferred over solar thermal panels for roof coverage, with installed capacity being maximized in all cases.
- Storage capacity is increased when GHG are reduced, with electric batteries being installed and maximized at the environmental optimum. However, investments in storage capacities reduce GHG emissions but incur higher costs compared to increasing ASHP size.
- Energy prices greatly influence the optimal energy concept and system operation, with higher electricity prices favoring CHP but leading to higher GHG emissions. CHP systems contribute to increased neighborhood self-sufficiency and grid security in case of electricity shortages.
- During the optimization of the controls, heat storages and electric batteries are utilized to shift heat production to periods of lower carbon intensity in the electricity grid.
- Electric mobility has a minimal impact on the optimal energy concept, with CHP capacities only increasing slightly (5 to 10%) despite a 40% increase in electric demand. Optimal CHP sizing is proven to be heat-led.

3.2 Case study – Energie360

As mentioned in section 2.5.2, the optimizer can choose among i) air-source heat pump (ASHP) ii) ground-source heat pump (GSHP) and iii) PV as available energy sources and converters in the considered scenario. Additionally, electric rods are available only as a backup to cover the peaks and enable the optimizer to meet the demands exactly. depicts the selected technologies along with annual energy flows between the components in grouped optimization. The leftmost components in the figure represent the energy sources, the rightmost are the energy demands, while those in the middle are energy converters and storages. Moreover, the annual electricity, space heating and domestic hot water flows are highlighted with the colors blue, magenta and red, respectively. This result shows the cost benefits of connecting buildings with thermal and electrical links. A centralized PV and a centralized ASHP were chosen as the cost optimal solution for the supply of electricity and heat in grouped optimization. The electricity grid is the primary electricity source, while about 18.4 % of the electricity demand is provided by the PV array. The leftmost block shows the two energy production sources resulting from the optimization.

Each of the four building A, B, C and D, have electricity, space heat (SH) and DHW demands, shown at the rightmost side under the demands block. While buildings B and C also have mobility demands (car charging stations) which is modelled as an additional electricity demand. All buildings except the one that has the centralized units (Building B to D) have electric rods of about 5 kW capacity (denoted using red color boxes with the label electric rod inside the converters and storages block) with a small, decentralized storage (SH and DHW inside the converters and storages block) to cover the peaks in space heating and domestic hot water demands. The decentralized electric rods and small thermal storage tanks are used by the optimizer to avoid over-dimensioning the centralized heat pump and thermal storages. There are two centralized large thermal storages for space heating (SH) and domestic hot water (DHW), which are located in this case in Building A and depicted under converters and storages block. The centralized storages are used to provide SH and DHW demands to the other buildings via the space heating (SH) and domestic hot water (DHW) links, respectively, which are located in the plot between the converters and storages, and demand blocks. Feed in on the rightmost region represents the excess PV electricity which is fed into the grid to earn economic incentives. The capacities of each technology selected by the optimizer in group optimization are given in Table 18.

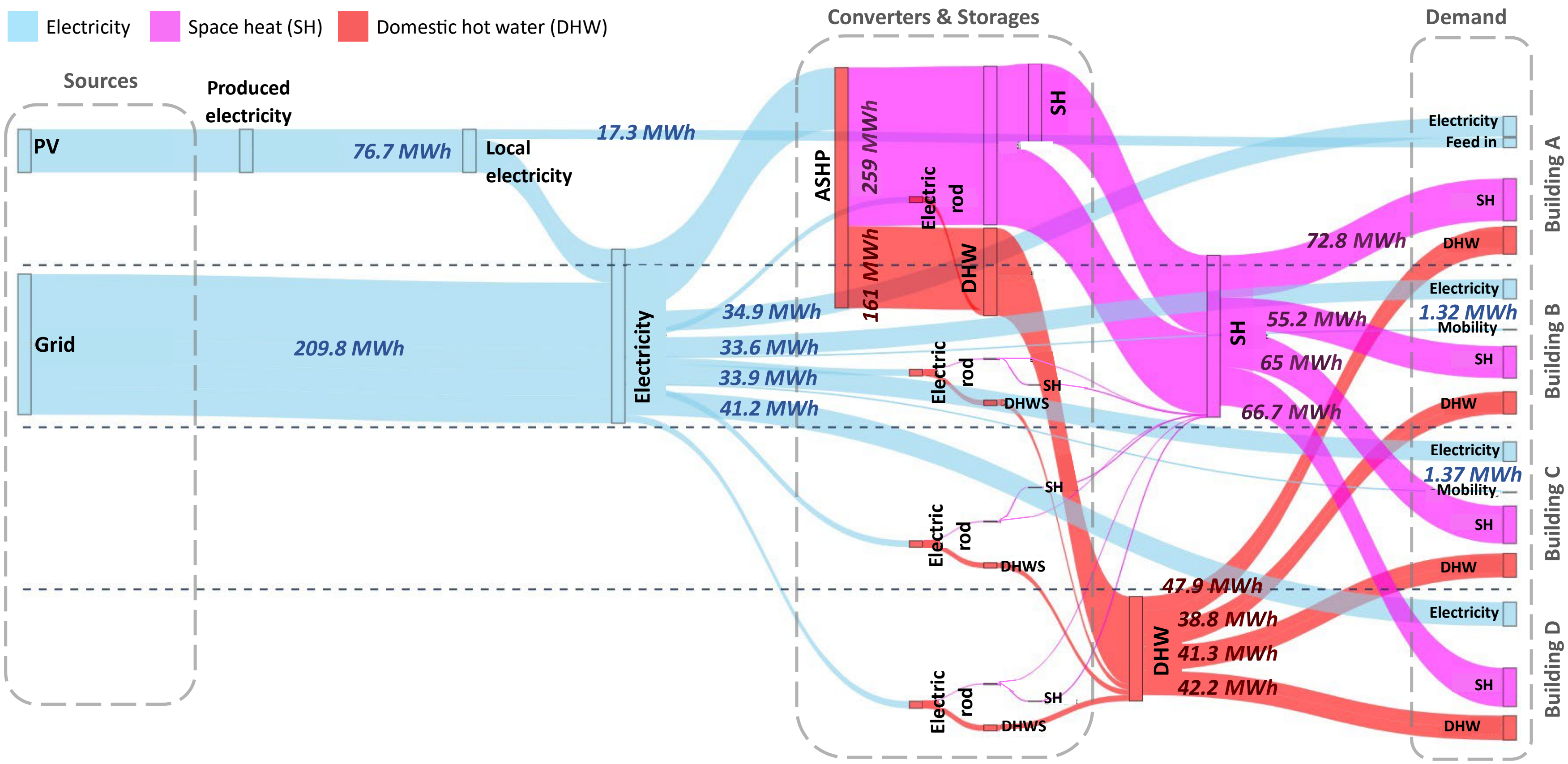

Figure 56: Result from grouped cost optimization of the Energie360 case study. The plot reads from left (energy sources) to right (energy demands).

If cost optimization is performed for individual buildings (without thermal/electric grids), then the installation of PV is not found to be economical. However, ASHP is still selected as the cost optimum technology for heating and domestic hot water. Therefore, each building has a decentralized ASHP, with DHW and SH thermal storages in the cost optimum. The incorporation of thermal and electrical links was found to reduce the total cost by 7 % and the environmental impact by 3 % compared to individual optimization. Since we neglect the cost of linking the buildings in this case study, grouping the buildings can be considered economical if the links do not cost more than 7 % of the total cost. It is worthwhile to note here that the introduction of thermal/electrical links would benefit from even higher reductions if lower grid purchase costs were assumed. For example, a large group of consumers could purchase on the spot market directly or might get lower energy prices due to group size in combination with low consumption on peaks periods due to load shifting.

The influence of the relative cost of the GSHP with respect to ASHP on the optimization results is highlighted in Figure 57. The optimal solutions at different ratios of cost of GSHP to cost of ASHP are shown. The red dashed line depicts the total cost of the optimal solution with an ASHP, while the green bars denote the cost of the optimal solution with GSHP. A GSHP was observed to become more economical compared to ASHP, if the cost of GSHP becomes less than 1.5 times higher than ASHP per kW of installed heating capacity including the borehole length.

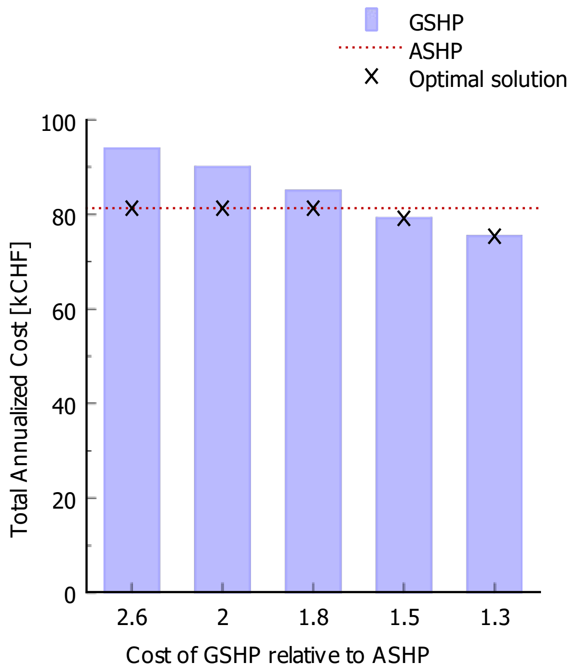

Figure 57: Sensitivity analysis on the cost of GSHP relative to ASHP for Energie360 case study.

Table 18 summarizes the capacities of the components along with the SPF (Seasonal Performance Factor) of the heat pumps, for the installed case and for the optimal solutions obtained using the optihood framework. The cost optimal PV capacity was found to be 60 % lower than the currently installed capacity. Moreover, the total installed heat pump capacity was reduced to less than half as a result of optimization, while a 37 % larger storage compared to the existing one was selected. The substantial reduction in the capacity of the heat pump, however, should be interpreted with caution, since the period used in the optimization was not a cold year, while the installed heating system is based on typical design values by the building codes.

Total installed capacities	ASHP (kW)	GSHP (kW)	SPF	PV (kWp)	DHW storage (m^3)	SH storage (m^3)
Actual	-	125, 129	-	205	4	3.8
Group with ASHP	107	-	3.7	76	3.7	6.9
Group with GSHP	-	103	4.1	74	4.2	15.0

Table 18: Comparison of the installed capacity for the actual neighborhood and the cost optimum for Energie360 case study.

Figure 58 shows the results of multi-objective analysis based on cost and emissions as the two target criteria by means of a Pareto front both for individual and grouped optimization. Here, the leftmost point on the top, with highest emissions, denotes the cost optimum (shown in for group optimization), while the rightmost point (with the highest cost) is the environmental optimum. The points in between these two extremes are obtained using the epsilon constraint method on the two objectives, i.e. limiting one while optimizing the other. As shown, optimization of technologies by grouping the buildings together leads to cost savings of 7-40 % when compared to buildings being optimized individually. The optimizer chooses an ASHP over a GSHP as the heating technology in all the optimization runs. In the environmental optimization (rightmost point on the Pareto), the size of installed PV and ASHP increases by more than 2 times compared to the cost optimum (leftmost point on the Pareto). The reason for the selection of an ASHP over GSHP in the environmental optimum could be associated with the COP of ASHP being higher than expected (see Table 18), while the environmental impact of GSHP (infrastructure) was assumed to be about 2.7 times higher than that of ASHP (after including the impact of the boreholes). However, if the environmental impact of the GSHP infrastructure is assumed to be the same as ASHP, then the optimizer chooses the GSHP in the environmental optimum (resulting from the higher COP). Moreover, batteries of about 40-50 kWh capacity are employed in each building to store the PV electricity for use during low sunshine hours in order to minimize the environmental impact from the use of grid electricity.

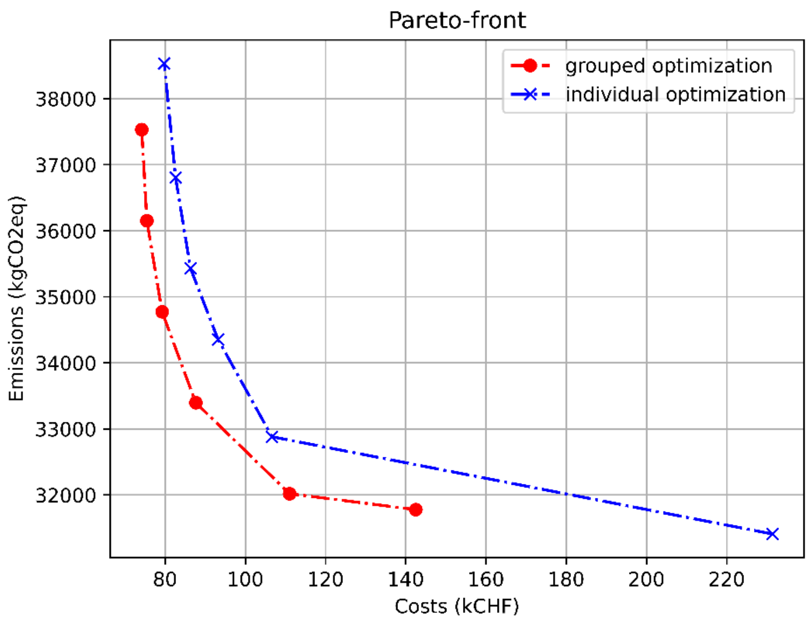

Figure 58: Multi-objective analysis of grouped optimization with both electrical and thermal links for Energie360 case study.

3.2.1 Comparison of five design configurations with PV and GSHP:

Here, we present a comparison of five system design configurations constituting of decentralized and centralized installations within the neighborhood of the Energie360 case study. A description of these five cases has been presented in section 2.5.2. Figure 59 illustrates the optimum capacities of the energy conversion and storage technologies in each case. The case acronyms ending with *i* denote individual optimization and therefore, the results comprise of decentralized installations. The case acronyms containing a *g,* represent grouped optimization where a centralized installation might appear. The results presented here discuss the cost optimum technology solutions in each case. Furthermore, the allowed energy conversion technologies are represented in the case acronyms. For example, the case GridGSHPi presents the cost optimum of decentralized GSHP installations to meet the heating demands of the case study, while the electricity demands (including e-mobility) are covered by the grid. In the GridGSHPi case, four decentralized GSHP installations of 28 kW, 24 kW, 25 kW and 27 kW (total of 104 kW), together with electrical heating rods of 6 kW, 5 kW, 6 kW and 6 kW capacities, are chosen in the cost optimal solution. When PV is introduced as the electricity production technology (case PVGSHPi), an overall PV capacity of 76.6 kWp, including the decentralized capacities of 20.7 kWp, 17.5 kWp, 18.9 kWp and 19.5 kWp for each building, was obtained. Note that in the absolute cost optimum, the optimizer would not select decentralized PV systems over simply using the grid in this case. This is because the total annualized cost of the PVGSHPi case is higher than that of the GridGSHPi case. Furthermore, centralized installations of PV, GSHP and storages for DHW and SH needs are selected in the PVGSHPg case (Group with GSHP case in Table 18). The DesignOptimalOperation case denotes the actual installation on site, based on the design values. Note that for this case, we fix the capacities of the system components (shown in Figure 59 and Table 18) and evaluate an operational optimization (or dispatch optimization), i.e. the cost optimal use of energy resources. The DesignOptimalOperation case has higher installed capacities of technologies, no electric heating rods and considerably smaller storage capacities. In the first three cases (GridGSHPi, PVGSHPi and PVGSHPg), the installed GSHP(s) is(are) capable of generating both domestic hot water and space heat. PVGSHPg_split case is similar to the DesignOptimalOperation case, where two separate GSHPs are used for the production of DHW and SH, with the added benefit of providing partial redundancy for the heating production. The total installed GSHP capacity in PVGSHPg_split case is 63 % lower than in the DesignOptimalOperation case. However, decentralized electric rods of a total of 25 kW capacity and 3 times higher total storage capacity are employed to support the reduction in GSHP capacity.

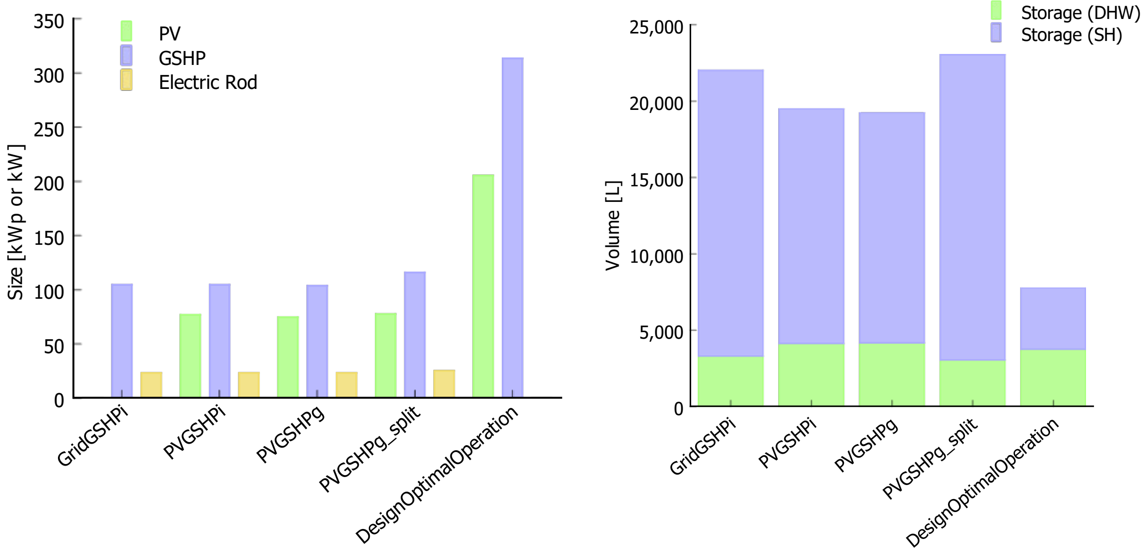

Figure 59: Installed capacities of energy conversion and storage technologies in five design cases for Energie360 case study.

Figure 60 shows the total annualized cost (operation and investment both) and the total annualized GHG emissions in each case. The grouping of buildings in the PVGSHPg case reduce the annualized costs and the annualized GHG emissions by 10% and 12%, respectively. As stated before, these reductions are without the consideration of costs and emissions from the installation of district heating links. Moreover, by developing central PV and GSHP installations with central DHW and SH storages (i.e. PVGSHPg case), the annualized costs are 14% lower at a negligible higher (<1%) environmental impact than corresponding decentral installations (PVGSHPi case). Moreover, not installing a PV in individual optimization (GridGSHPi case) is 5% cheaper than a decentralized installation (PVGSHPi case). The DesignOptimalOperation case (with two separate heat pumps) has 1.7 times higher costs and 1.2 times more GHG emissions compared to PVGSHPg case, where a single heat pump can deliver both SH and DHW. Here, it is worthwhile to note that we did not include any environmental benefits from feeding excess PV electricity into the grid. If such benefits are included, then the equivalent emissions in the DesignOptimalOperation case could be much lower. Furthermore, installing significantly lower energy conversion system capacities with higher storage capacities in PVGSHPg_split case accomplishes 36% lower costs and a reduction of 15% in the GHG emissions (compared to DesignOptimalOperation case).

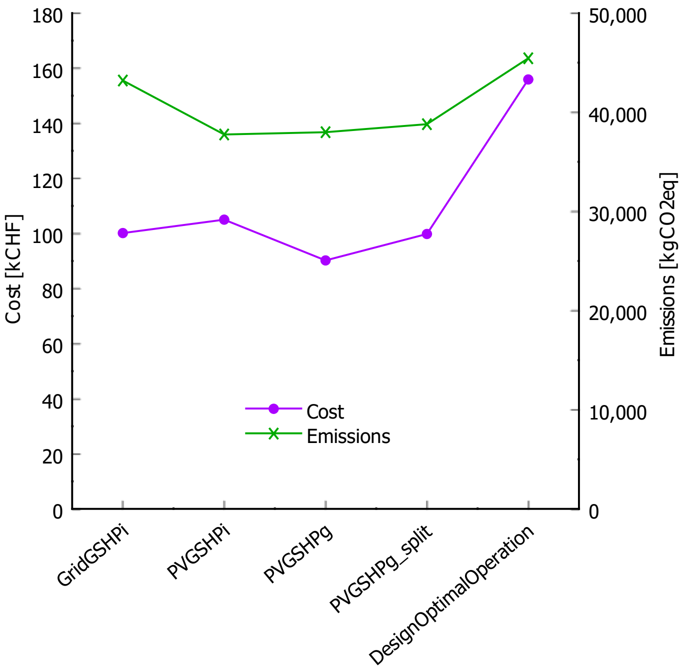

Figure 60: Total annualized cost and annualized GHG emissions for the five design cases in Energie360 case study.

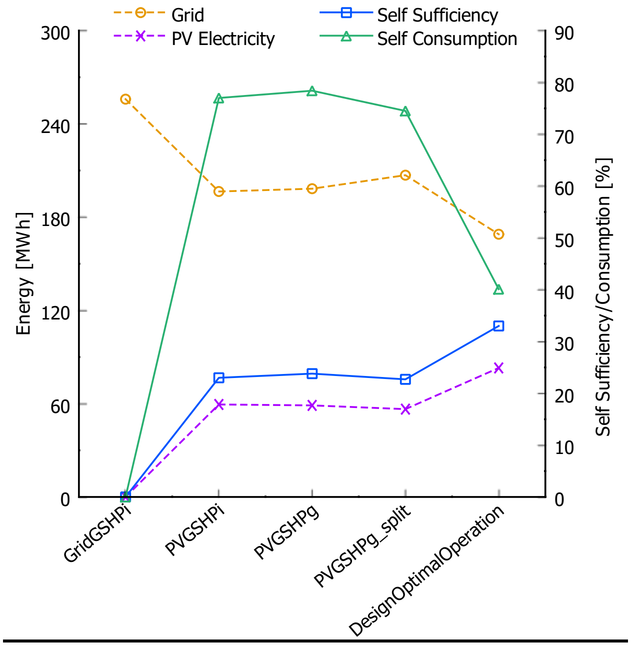

Figure 61: Grid electricity consumption, PV electricity generation, self-consumption and self-sufficiency factors for the five cases in Energie360 case study.

Figure 61 depicts the annual grid electricity consumption, the annual PV generation, the self-sufficiency and self-consumption factors for each case. The self-sufficiency factor increases with PV electricity, as expected. Moreover, centralized installations in the PVGSHPg case lead to higher self-consumption and self-sufficiency factors at a lower annualized cost compared to the GridGSHPi case (i.e. the cost optimum decentralized solution). A self-sufficiency of 24% and a self-consumption of 78% was obtained for the PVGSHPg case. The self-sufficiency factor of the DesignOptimalOperation case is 9% higher than the PVGSHPg case in the cost optimum operation. However, a major portion of the generated PV electricity is fed into the grid to generate revenues and therefore, the self-consumption factor is reduced to 40%. Furthermore, a total grid electricity consumption of about 256 kWh was observed in the GridGSHPi case, where PV is not installed. The use of central PV, central GSHP and central thermal storages reduces consumption of grid electricity by 22%, 19% and 34% in PVGSHPg, PVGSHPg_split and DesignOptimalOperation cases, respectively.

3.2.2 PV installation cost sensitivity

Based on the cost assumptions given in Table 11, the optimum decentralized installation with electricity grid alone (GridGSHPi) as the source of electricity was found more economic than having decentralized PV installations (PVGSHPi). If the PV installation costs are reduced by 5%, then the optimum PV, GSHP and storage capacities obtained when minimizing total annualized costs are shown in Figure 62. The total PV capacity in the PVGSHPi case increases to 340 kWp, while the total decentralized storages capacity reduces by about 12%. The resulting annualized cost and GHG emissions of the GridGSHPi and PVGSHPi case are shown in Figure 63 and Figure 64, respectively. The benefits earned from the PV electricity fed into the grid are illustrated by means of a separate bar column labelled as PVGSHPi with feed-in. The sub-bar area represented by feed-in electricity in the annualized costs (Figure 63) refers to the revenue earned from feeding PV electricity to the grid and therefore, is subtracted from the total cost. Similarly, the sub-bar area labelled as 'Feed-in' in Figure 64 represents the environmental benefits of the electricity fed into the grid and is subtracted from the annualized GHG emissions in the

PVGSHPi case. The environmental benefits from feed-in electricity at a given hour are assumed to be equal to the environmental impact from grid electricity in that given hour.

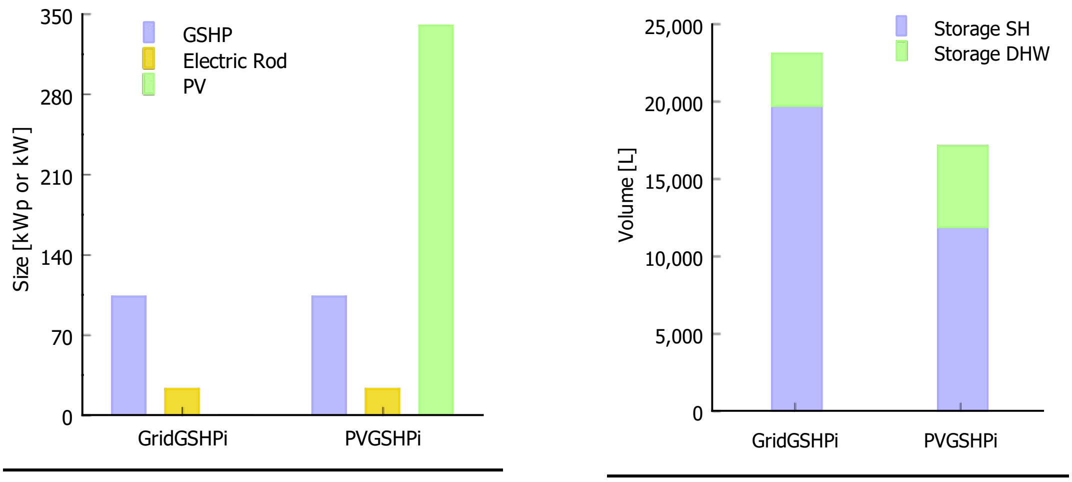

Figure 62: Installed PV and storage capacities for the individual optimization design cases in Energie360 case study (5% lower PV installation cost assumption).

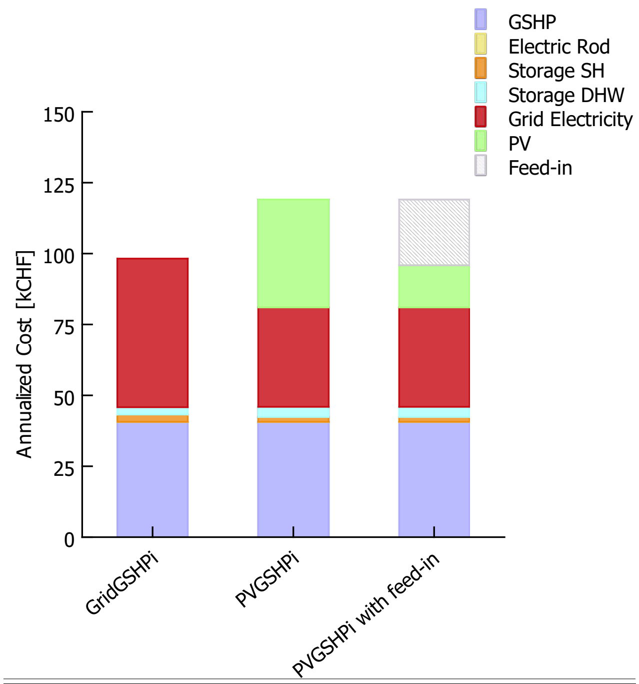

Figure 63: Total annualized cost for the individual optimization design cases in Energie360 case study (5% lower PV installation cost assumption).

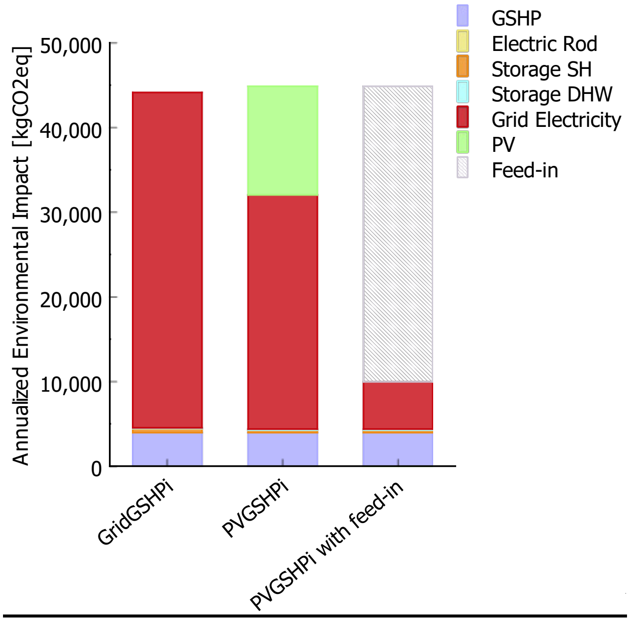

Figure 64: Annualized GHG emissions for the individual optimization design cases in Energie360 case study (5% lower PV installation cost assumption).

As shown, the installation cost of PV in the PVGSHPi case with 5% lower PV installation cost assumption is compensated to a great extent by the cost savings from the feed-in of PV electricity into the grid (Figure 63). And therefore, the installation of PV in the PVGSHPi case becomes more economical compared to the GridGSHPi case. Moreover, from Figure 64 we can see that the GHG emissions from PV installation are completely compensated by the environmental benefits earned from the feeding in the excess PV electricity in the PVGSHPi case.

3.2.3 Grid Purchase cost variation.

The impact of cost of electricity purchased from the grid on the optimization results of PVGSHPg case is depicted in Figure 65. The minimum (8.49 c/kWh), maximum (70.78 c/kWh) and median (27.2 c/kWh) tariffs for the year 2023 published by Eidgenössische Elektrizitätskommission were selected to prepare three scenarios with low, high and medium grid purchase costs, respectively. The reference case assumes the grid purchase cost of 20 c/kWh of electricity. The dashed lines denote the respective results for the reference case. The optimal PV capacity was found to increase with the grid purchase cost, as expected, with no PV installation in the optimal solution if the grid electricity tariff is low. Increasing the tariff from the reference value of 20 c/kWh to 70.78 c/kWh (the highest value announced by a Swiss provider for 2023) results in an almost 3.5 times larger PV array in the cost optimum. Further, when the tariff increases from medium to high the optimal PV capacity was found to be more than 2.5 times higher. The capacity of the GSHP remains nearly the same in all the three cases. Moreover, the total costs were observed to increase 2.8 times as the grid purchase cost increases from low to high (i.e. 8.3 times higher grid tariff).

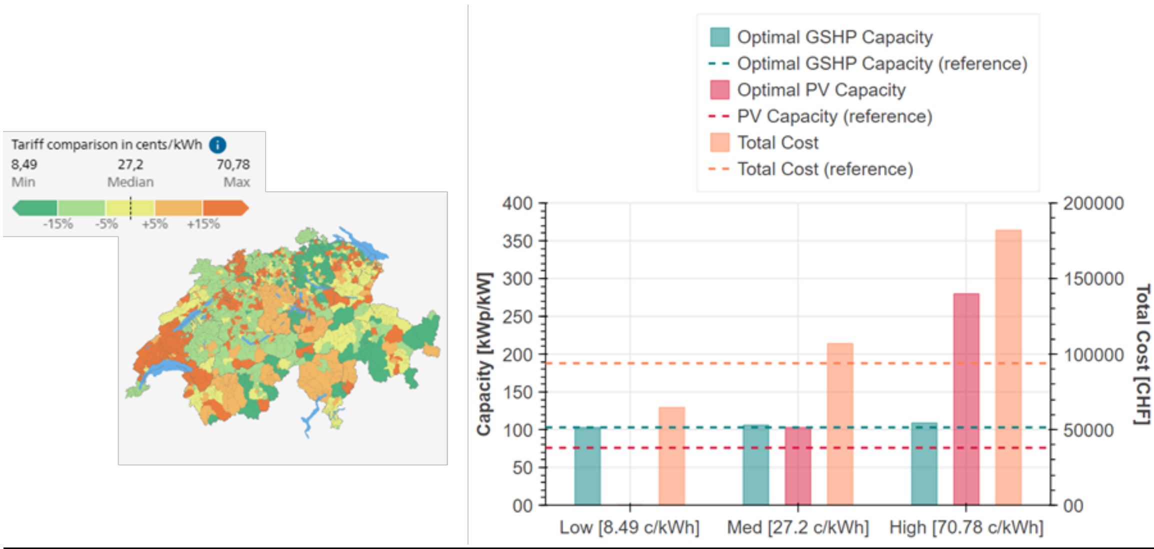

Figure 65: Sensitivity analysis on grid-purchase cost for the PVGSHPg case of Energie360 case study based on the data obtained from Eidgenössische Elektrizitätskommission ElCom[19] for 2023. Reference cost of grid electricity is assumed as 20 c/kWh (Table 11).

3.2.4 Feed in Tariff variation.

Similar to the grid purchase cost variation, here we study the sensitivity of the feed-in tariff assumptions on the grouped optimization results depicted under the PVGSHPg case. Three feed-in tariffs namely low (3.77 c/kWh), medium (12.76 c/kWh) and high (21.75 c/kWh) were assumed based on the minimum, average and the maximum tariffs, respectively, published by VESE pvtarif for the year 2023.

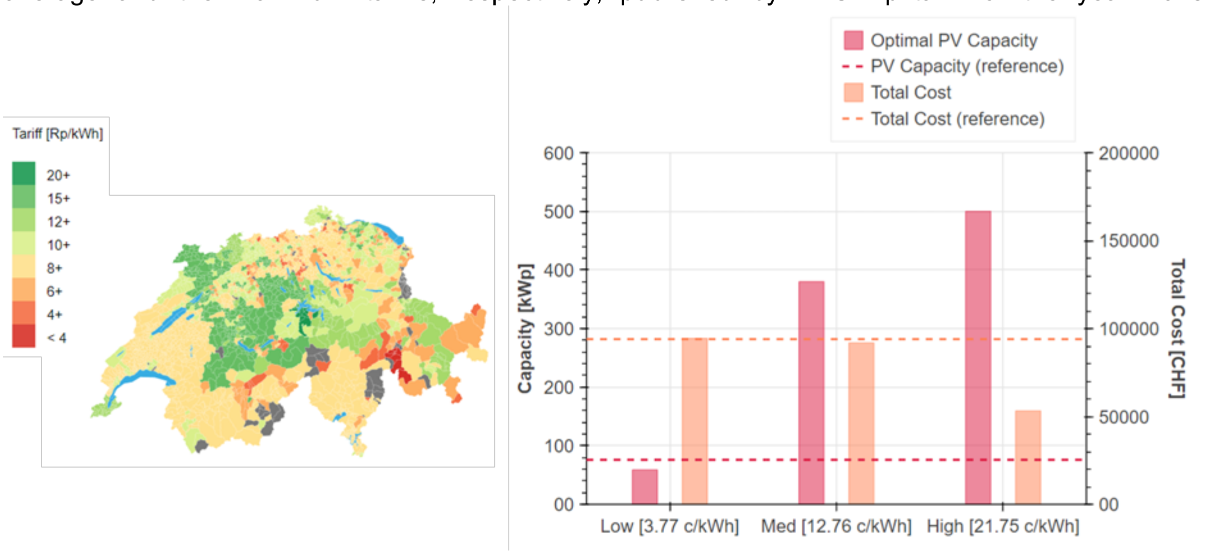

Figure 66 shows the influence of feed-in electricity tariffs on the optimal PV capacity and the total annualized cost for the PVGSHPg case. The dashed lines denote the respective results for the reference case (feed-in tariff assumption of 9 c/kWh). The optimal PV capacity is 8.6 times higher when the feed-in tariff varies from 3.77 c/kWh (low) to 21.75 c/kWh (high). The installed PV capacity in the reference case is about 29% higher than the case with low feed-in tariff. The installed PV capacity is 5 times and 6.6 times higher compared to the reference case when changing the feed-in tariffs to medium and high respectively. Moreover, the total annualized cost reduces with the increase in the PV feed-in tariff. While

19 https://www.strompreis.elcom.admin.ch/

the investment costs increase for higher installed PV capacities, the share of PV electricity fed into the grid as well as the revenue gained from higher feed-in tariffs increase. Therefore, the case with high feed-in tariff gains from higher rates of revenues earned by feeding the excess PV electricity into the grid.

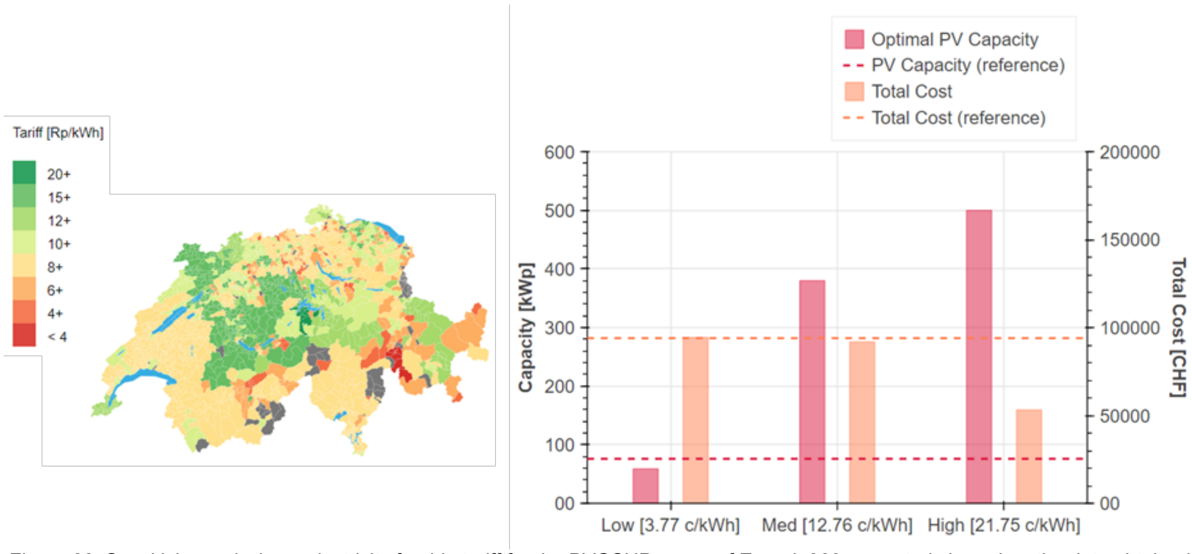

Figure 66: Sensitivity analysis on electricity feed-in tariff for the PVGSHPg case of Energie360 case study based on the data obtained from VESE pvtarif[20] for 2023. Reference feed-in tariff was assumed as 9 c/kWh (Table 11).

3.2.5 Summary of case study

This case study, composed of 4 residential buildings with 77 dwellings (10'300 m^2), involved an investigation of the benefits from grouping the buildings together as opposed to individual solutions. The buildings were thermally and electrically connected, and the same grid electricity pricing scheme was considered in both individual and grouped building optimizations. The investigation included the optimal sizing and choice between heat pumps (ASHP and GSHP), PV, thermal energy storages and electric rods for covering the heating peaks. Optimizing the buildings collectively reduced the costs by 7 % to 40 %, respectively, at the cost optimum and environmental optimum (without considering infrastructure cost of the grids). Therefore, the economic benefits of collective optimization (i.e. centralized solutions) would arise only if the network infrastructure does not cost more than the respective reductions gained. These reductions would be even higher if lower grid purchase costs were assumed in collective optimization. The cost optimum collective solution for buildings was to implement a central PV, central ASHP and central storages for DHW and space heating. While decentral installations of ASHP and thermal energy storages (without any PV installation) were selected when buildings were optimized individually. An intriguing observation was noted in the environmental optimum, where again an ASHP installation was selected over a GSHP when minimizing the emissions. This choice, though, could be associated with the higher LCA impact of GSHP (2.7 times more) and a higher-than-expected SPF of the ASHP (3.7 compared to 4.1 from GSHP, Table 18). Compared to the current installation, the PV capacity and heat pump capacity could be reduced by 60 % and to less than half, respectively, by incorporating 37 % higher thermal energy storage capacity as a result of collective cost optimization. The currently installed heating system was designed based on the typical design values by the building codes, and the PV capacity was selected to maximize the utilization of the available roof area. It should be noted that the measurement data used in the optimization was not from a typically cold period. Also, the lower capacities rely on the optimum control of the systems and optimum use of power-to-heat conversion synergies. This could be achievable, in practice, by using a smart controller to operate the real system. Therefore, these reductions in the installed capacities should be interpreted rather carefully.

20 https://www.vese.ch/pvtarif/

For places where ASHP cannot be installed, energy systems with GSHP were also investigated within this case study in decentral and central design configurations. Grouping buildings and using centralized PV and GSHP installations with central thermal energy storages achieved 10% lower (excluding grid infrastructure costs) total annualized cost when compared to the corresponding cost optimum decentral installation without any PV. The GHG emissions in the former case were found to be 12% lower than optimum decentral installations without PV. This is due to the use of emission-free PV electricity in the case of central PV and GSHP installation. If decentral PV installations are included as well along with decentral GSHP and decentral storages, the cost of the corresponding central installation was found to be 14% lower at a negligibly (< 1 %) higher environmental impact. Further, an operation optimization of the currently installed system design in this case study resulted in both higher costs and emissions (1.7 times and 1.2 times, respectively) than the cost optimized design of central PV, central GSHP and central thermal energy storages. The higher costs and emissions are predominantly due to the higher installed capacities in the current installation on-site, which is based on the design values from the planning process and not the actual measured data during system operation. Also, the actual on-site installation consists of two separate GSHPs for producing space heat and DHW (providing partial redundancy), instead of a single GSHP producing both in the cost optimized central design. Moreover, the self-sufficiency factor of the currently installed system with optimum operation was 9% higher than the cost optimum central design of PV, GSHP and thermal energy storages. However, the generated PV electricity was primarily fed into the grid in the former case and as a result, the self-consumption factor was about 38% lower.

Finally, we found that both the choice and the sizing of technologies in the optimum design solutions are rather sensitive to the cost/price assumptions. The results presented above are based on an assumption where a ground-source heat pump (GSHP) costs 2.6 times more than an ASHP per kW of installed heating capacity (including boreholes). A GSHP, however, would be more economical if it costs 1.5 times (or less) higher than an ASHP, which may not be unrealistic in reality. Moreover, based on the assumptions made, the cost optimum solution for buildings optimized individually was to implement decentral installations of ASHP and thermal energy storages (without any PV). If the installation cost of PV was reduced by 5%, then installing decentral PV resulted in lower total annualized cost compared to using just the grid. If we assume the environmental benefits from electricity fed into the grid to be equal to the environmental impact of grid electricity, then the annualized environmental impact as well is lower in the former case. Moreover, the optimal PV capacity increases with the grid purchase cost. This is because it becomes more cost-effective to generate electricity on-site using PV when the grid purchase cost is high. Increasing the grid electricity tariff from the reference value of 20 c/kWh to 70.78 c/kWh (the highest value announced by a Swiss provider for 2023) results in an almost 3.5 times larger PV array in the grouped cost optimization. Further, it was not found cost-effective to install any PV at all when the buildings were optimized collectively if the grid electricity tariff is low (8.49 c/kWh). This is because the cost of generating electricity on-site using PV will be higher than the cost of purchasing electricity from the grid. The cost optimum installed PV capacity increased from no PV installation in case of low grid-purchase cost (8.49 c/kWh) to central PV installations for both medium (27.2 c/kWh) and high (70.8 c/kWh) grid-purchase costs. The resulting central PV installation was observed to be approximately 2.5 times higher as the grid-purchase tariff increased from medium to high. Furthermore, the optimal size of the PV array was found proportional to the grid feed-in tariffs. The cost optimal capacity of central PV installation increased 8.6 times as the assumption in the electricity feed-in tariff was varied from low (3.77 c/kWh) to high (21.75 c/kWh). This is because the increased revenue from feeding in the excess PV electricity offsets the higher investment cost. As a result, the total annualized costs were also found to decrease with an increase in the feed-in tariff.

3.3 Case study – SGSW

In this section results from the use case described in section 2.5.3 are presented.

3.3.1 Scenario 1: 12 MFH buildings

Here we present an optimum choice of energy conversion and storage technologies for a group of 12 MFH buildings. These buildings are supplied by a 242 kW_{th} and 120 kW_{el} CHP plant installation on site, while the remaining heat demand is met by gas fired boilers (564 kW in total). A centralized CHP plant of 404 kW_{th} capacity along with hot water storages for domestic use of 1.3 m^3 capacity and space heating of 28 m^3 capacity, were selected in the cost optimum solution for these buildings. Therefore, the gas boilers can be completely replaced by increasing the capacity of the installed CHP plant. Moreover, renewable gas could be used as the primary source of such a CHP plant, instead of natural gas, in order to completely replace the use of non-renewable energy resources. Out of the available energy conversion technologies, CHP came out as the optimum technology in terms of cost when all the 12 buildings were considered.

An important question which arises from the above results is to determine the size of the group (i.e., how many buildings) for which installing a CHP plant would be the economic optimum. Figure 67 shows the optimum selection and capacities of technologies in the cost optimization of different cluster sizes of buildings (out of these 12 MFH buildings). When an individual building, i.e. cluster size of 1, is optimized with the goal of cost minimization, a 95 kWp PV installation is selected for the generation of electricity. However, about 70 % of the PV electricity is fed into the grid in order to generate revenues in the cost optimization. The peak power used for the building's own consumption, in this case, is merely 25 kW (26 % of the installed PV capacity). If the cost of PV installation is increased by just 7 %, then it no longer appears in the cost optimum result for an individual building. Since the uncertainty in the PV cost data is roughly ± 50 %, the sensitivity of the PV installation cost in this case is too high to derive a conclusion that installing PV for a single building would be economical. To supply the heating demands of the single building (cluster size 1), a 35 kW ASHP complemented by a 10 kW electric heating rod is selected. As explained previously, the electric rod is used only a few hours over the whole year to allow a perfect match between the production and demand within optimizations. As we move to a group of 2 buildings, PV is no longer the cost optimum solution, while a centralized 40 kW ASHP is used together with an 11 kW electric heating rod and thermal energy links (for domestic hot water and for space heating) to cover the heating demands. ASHP remains the optimal energy conversion technology, along with heating links and electric rod, up until the cluster size of 5 buildings. From the cluster size of 7 buildings, CHP plant comes up as the optimum energy conversion technology. The optimum CHP plant capacity for the cluster of 7 buildings is 224 kW_{th}, and when the remaining 5 buildings are included the optimum CHP plant capacity becomes 404 kW_{th}.

In addition to the selection of technologies, the sizing of storages is equally important since storages help in flattening out the peaks in energy demand and therefore, reduce the required capacity of the installed energy conversion technology. The storage capacities, both absolute in L and relative in L per kWp of energy demand, for each cluster size are also depicted in Figure 67. While the absolute storage capacities increase with the increase in cluster size, as expected, the relative storage capacity remains nearly the same from cluster sizes of 2 and beyond. The relative storage capacity decreases when centralized installations appear in the optimization results (i.e., from the cluster size of 2 onwards), as expected. Also, the sizes of thermal energy storages for DHW are much smaller than those selected for space heating (SH). This is because a DHW storage is two times more expensive than a SH storage per liter of installed capacity.

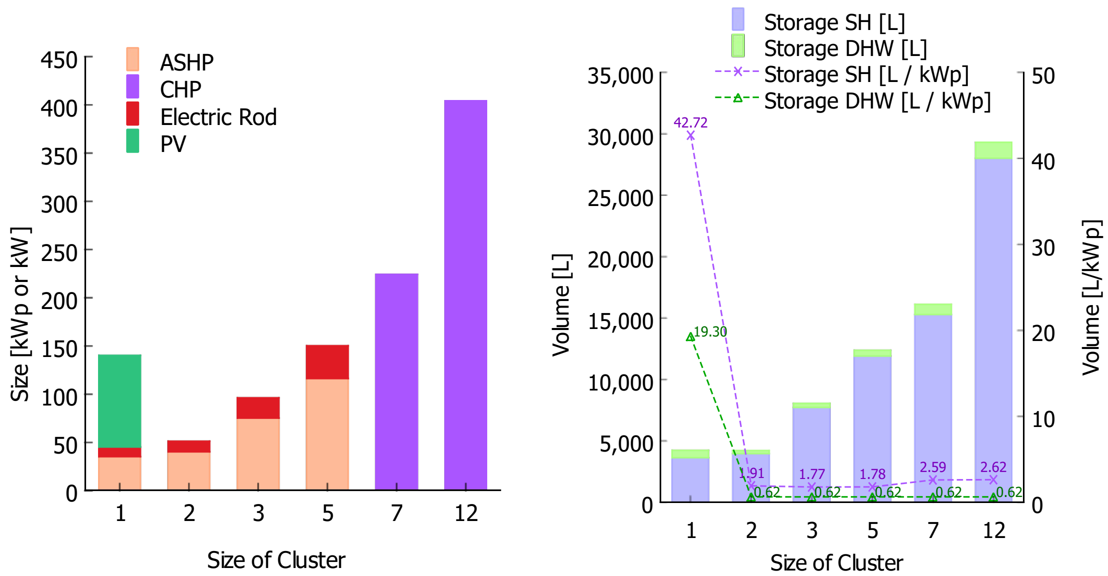

Figure 67: Capacities of technologies and storages selected in the cost optimum solution as a function of the cluster size for Scenario 1 of the SGSW case study.

Based on the cost assumptions made (shown in Table 11), installing an ASHP is 30 % cheaper than a CHP plant per kWth capacity. If we reduce the capital expenditure (CAPEX), i.e. the base investment and cost per unit capacity, of a CHP plant by 30 %, still it is more economical to install an ASHP for a single building. This is because, even though grid electricity is more expensive than natural gas, ASHPs are quite efficient (high COP) when compared to the energy conversion efficiency of a CHP plant. Furthermore, the cost assumption made within the optimizations for a CHP plant, i.e. 24879 CHF + 1153 CHF/kW_{th}, is 16 % lower (per kWth of capacity installed) than those assumed by the SGSW project planners. Our assumptions for the base investment cost of CHP plant are similar, however, the cost per kW_{th} of installed capacity from the SGSW project planners is 6 times higher. Therefore, a sensitivity analysis by further reduction of the installation cost of CHP plant might not be relevant to this study.

In the following, we investigate the influence of the reduction in gas price on the implementation of a CHP plant in the cost optimum solutions. Figure 68 shows the sizes of CHP plants selected in the cost optimal solutions for different cluster sizes of MFH buildings with a variation of gas price. In the reference case, we assume a gas price of 8.7 c/kW and as observed earlier in Figure 67, CHP is not selected as the cost optimum technology for cluster sizes of 1 through 5. Moreover, with this assumption of the gas price, the cost of electricity produced by a CHP plant is 34.8 c/kW, while the grid electricity is tariffed at 20.4 c/kW (41 % cheaper). Now, if the gas price is reduced by 20 % (or more up to 50 %) then a CHP plant of 180 kWth capacity is selected in the cost optimum solution for the cluster size of 5 MFH buildings (instead of an ASHP). However, it is still not economical to install a CHP plant for the smaller cluster sizes (1, 2 and 3 MFHs). If the gas price is reduced by 30 % a CHP plant of 117 kW_{th} capacity replaces the 75 kW ASHP as the cost optimum technology in the cluster of 3 MFH buildings. Therefore, depending on the gas price in the future (also resulting from the use of renewable gas) CHP plant might be an economical choice for a cluster size of 3 or 5 buildings. However, installing a CHP plant was not found economical for an individual MFH or 2 MFHs even at 50 % lower gas prices. Finally, if we compare the cost of electricity produced from CHP plant against the cost of grid electricity, it can be seen that the electricity produced by CHP will be cheaper than the grid if the cost of gas reduces by more than 40 %.

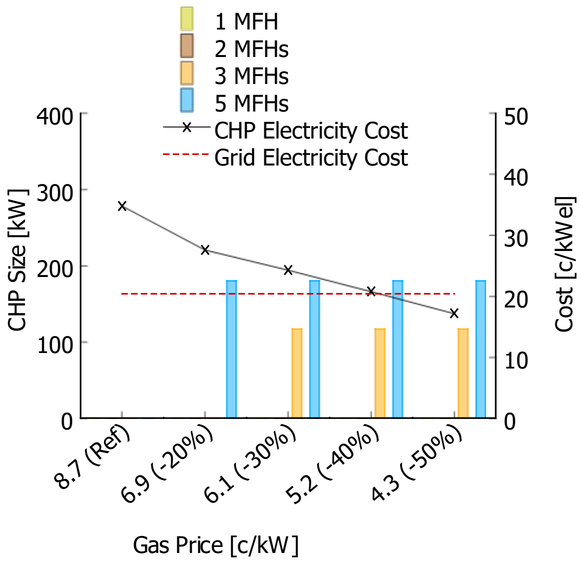

Figure 68: Variation of the CHP plant installations in the cost optimum and the cost of electricity produced by CHP with the gas price for different cluster sizes in Scenario 1 of the SGSW case study. Red dashed line shows the grid electricity tariff.

As observed in the previous case studies, the choice of technologies looks very different when the target of optimization is to minimize the GHG emissions (instead of cost). Table 19 shows the optimum capacities of the energy conversion and storage technologies based on the cost and environmental targets. In the environmental optimum, solar thermal collectors, ASHP (supported by electric heating rod) and PV replace the CHP plant (driven by natural gas). Moreover, batteries are employed in the environmental optimum to use the electricity generated by PV during off and low sunshine hours. As a result, the consumption of grid electricity is 54 % lower in the environmental optimum solution. For that, a very large electrical battery able to store 6.7 hours the peak PV power is chosen that reduces the LCA, but increases the cost massively as shown in Figure 69.

Total installed capacities	**ASHP (kW)**	**STC (m^2)**	**CHP (kW_{th})**	**PV (kWp)**	**El Rod (kW)**	**DHW storage (m^3)**	**SH storage (m^3)**	**Battery (kWh)**
Cost Optimum (Group)	**-**	**-**	**404**	**-**	**-**	**1.3**	**28**	**-**
Environmental Optimum (Group)	**351**	**1210**	**-**	**610**	**100**	**48.7**	**36.7**	**4124**

Table 19: Comparison of the installed capacities for the cost and environmental optimum solutions for Scenario 1 of SGSW case study.

The annualized cost and GHG emissions for the two results given in Table 19 are shown in Figure 69. The costs due to the use of grid and natural gas denote the operation cost, while the rest appear due to the installation of different system components. Similarly, the emissions during operation are represented by the stacked sub-bars for grid electricity and natural gas, and remaining emissions come from the installation of the selected technologies. The annualized cost of the environmental optimum is 3 times higher than that of the cost optimum. Moreover, about 70 % of the annualized cost comes from the operation of the system in the cost optimum solution. Whereas, in the case of environmental optimum, the share of operation cost within the total annualized cost reduces to 5 %, which is only due to the use of grid electricity. Furthermore, a major contribution of batteries (~58 %) in the total annualized cost of the environmental optimum can be clearly seen. A battery is often sized to store 1 to 2 hours of the PV peak power, but the environmental optimum chooses to store up to 6.7 times the PV peak power. The annualized GHG emissions of the cost optimum solution are 2.4 times higher than those of the environmental optimum. Around 95 % of the emissions arise due to the use of natural gas and grid electricity, i.e. from the operation of the system. However, in the environmental optimum, the emissions from the operation, which are only due to the use of grid electricity, are about 38 % of the total annualized emissions.

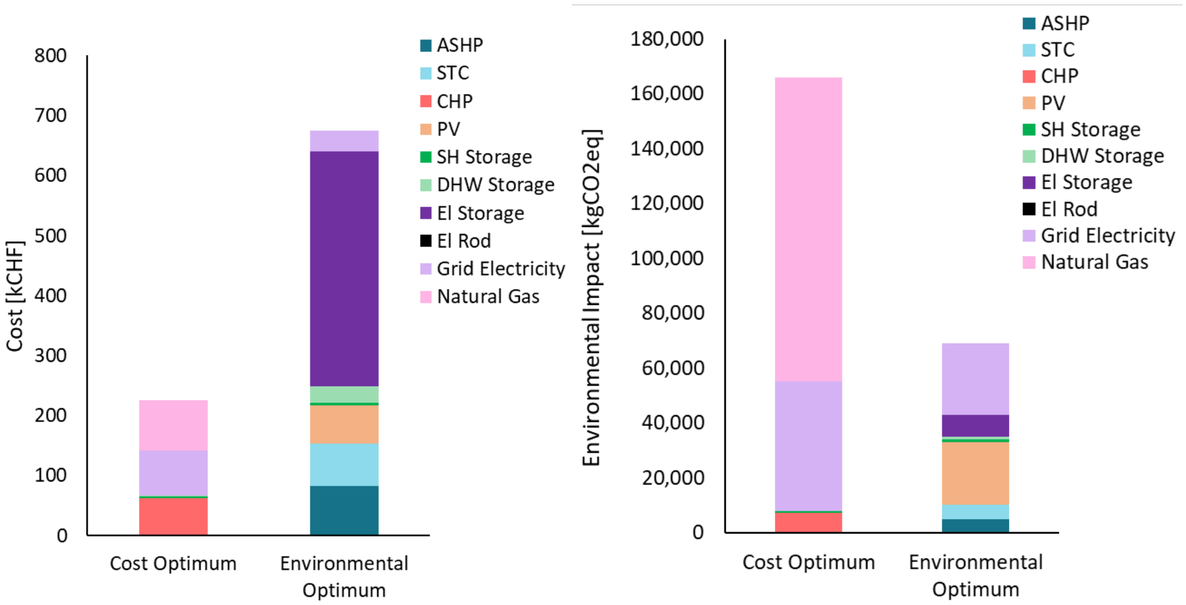

Figure 69: Comparison of the annualized cost and the annualized GHG emissions for the cost and environmental optimum solutions in the Scenario 1 of SGSW case study.

3.3.2 Scenario 2: All 56 buildings

In Scenario 2, we consider all the 56 buildings within this case study. As described earlier in section 2.5.3, the district in this case study comprises of heterogeneous use buildings belonging to 7 different sectors namely, residential, office, school, shop, sport, trade and hotel (Table 12). To analyze and compare the optimum selection of technologies in individual and grouped optimization in terms of both economic and environmental targets, multi-objective optimization was carried out based on the method described in section 2.2.7. The results are presented by means of a Pareto front in Figure 70, with a total of 6 points on each curve denoting 6 optimization runs. The leftmost points on both the curves, for individual and for grouped optimization, denote the cost optimum (referred to as optimization run 1 in Figure 71 and Figure 72). The rightmost points on the two curves in Figure 70 represent the environmental optimum (denoted as optimization run 6 in Figure 71 and Figure 72) for the individual and grouped optimization.

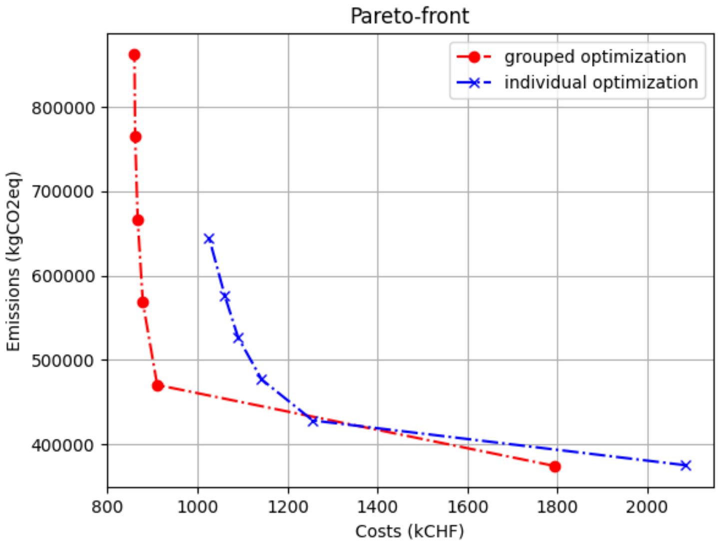

Figure 70: Multi-objective analysis of individual and grouped optimization with both electrical and thermal links for Scenario 2 of SGSW case study.

Figure 71 and Figure 72 show the optimum selection and capacities of the installed technologies in each optimization run for both individual and grouped optimizations. The cost optima and the environmental optima points in Figure 70 form the two extremes on the Pareto front, between which four more optimization runs were evaluated (represented from left to right by optimization runs 2 to 5 in Figure 71 and Figure 72). These four points were obtained by running cost optimizations in which the emissions were limited by a constraint (epsilon constraint method).

For both individual and grouped optimization, the selected energy conversion technologies are PV, ASHP and CHP plant for the cost optimum. The CHP plant comes up in individual optimization for only 5 buildings (2 hotel buildings and 3 shop buildings). PV is selected for 27 buildings in individual optimization, mostly for all the buildings except some multi-family houses, all single-family houses and trade. Furthermore, every building has an ASHP in the cost optimum solution of individual optimization.

In case of grouped optimization, centralized solutions are selected in the cost optimum, i.e., a centralized PV, a centralized CHP and a centralized ASHP. The capacity of the centralized CHP plant is 2.5 times higher, while the installed centralized ASHP capacity is almost half of that in individual optimization. As a result, the emissions from the operation of CHP plant using natural gas (instead of using the ASHP which is driven by grid electricity) are significantly higher in grouped optimization and therefore, the emissions of the cost optimum solution are 33 % higher than in individual optimization.

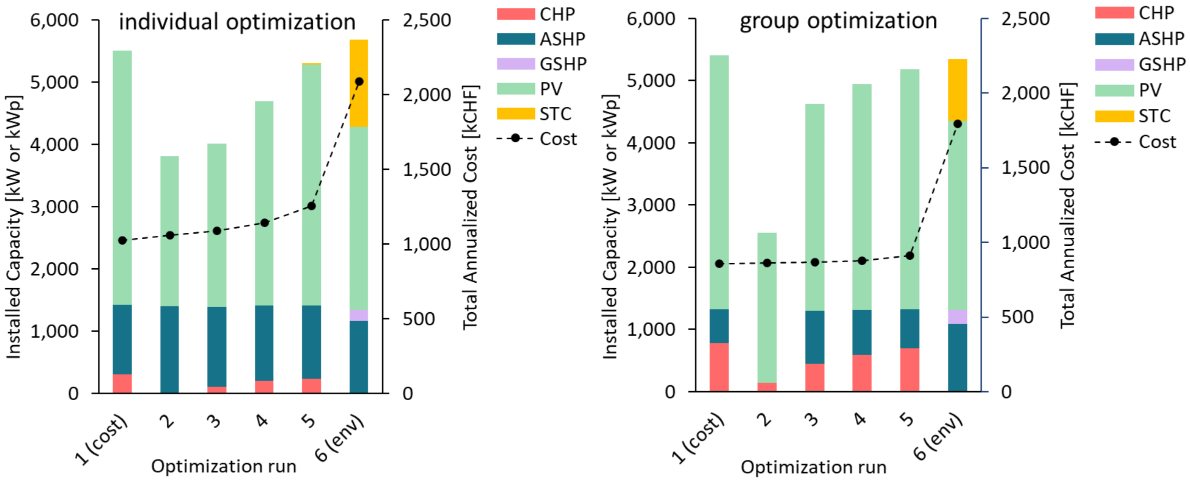

Figure 71: Comparison of installed capacities of energy conversion technologies in different runs of the multi-objective optimization for the Scenario 2 of SGSW case study. The chart on the left shows the results from individual optimization, while the results of group optimization are on the right.

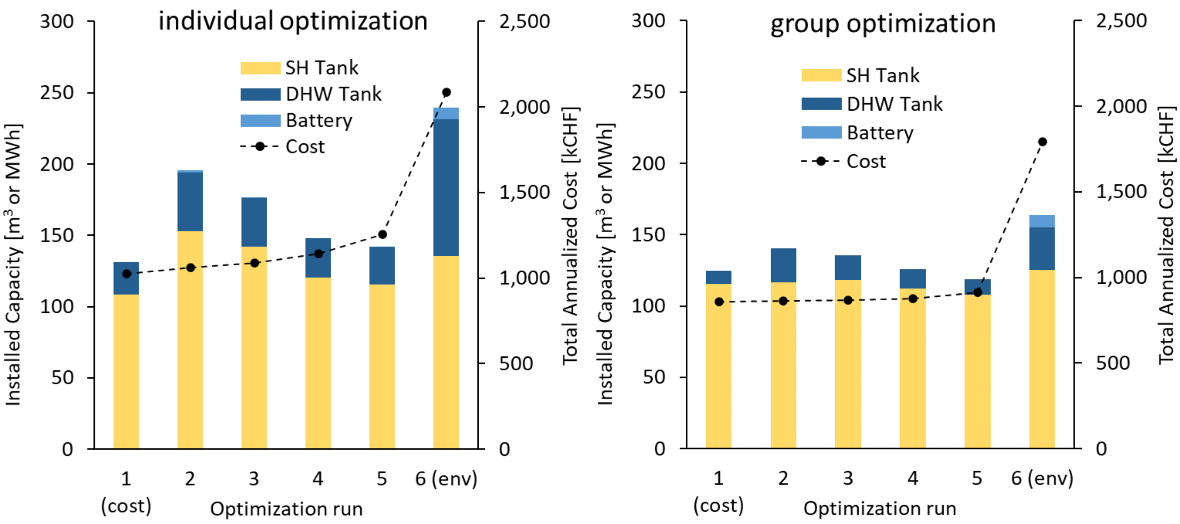

Figure 72: Comparison of installed storage capacities in different runs of the multi-objective optimization for the Scenario 2 of SGSW case study. The chart on the left shows the results from individual optimization, while the results of group optimization are on the right.

The cost optimum solution of individual optimization costs 19 % higher than that of grouped optimization. It is worthwhile to note here that the costs of district heating and microgrids are not included in these evaluations. Hence, the centralized setup in grouped optimization may be considered economical over the decentralized systems (individual optimization) if these costs do not exceed 19 % of the total annualized cost. Another observation which can be made here is about the installed capacities of storages in the cost optimum of individual and grouped optimizations (Figure 72). Batteries are not selected in neither the cases, while the total installed thermal energy storage capacity reduces by 5 % by allowing thermal flows among the buildings.

In environmental optimum, all the technologies except CHP plant (i.e. PV, STC, ASHP and GSHP) are selected in both individual and grouped optimization. The use of STC is clear in this context since cost makes no difference in the optimization results, but the installation of GSHP supplementary to the ASHP system might not be that obvious. GSHP have a large LCA impact from the installation of the boreholes.

However, they offer better efficiency compared to ASHP, especially when ambient air temperature is very low. For the environmental optimum the solution is composed of both solutions since GSHP will operate in the periods combining high CO_2 emissions and low ambient air temperatures.

The main difference between the grouped and individual optimization here arises due to the installed capacities of STC and storages. Around 39 % higher STC capacity and about 3 times bigger DHW storages are installed in individual optimization. It can be seen from the Pareto front in Figure 70, that the costs of both the environmental optima are significantly higher than those of the other optimization runs. This is because both the environmental optima result in including large electrical batteries to reduce electricity consumption in high CO_2 emissions periods, which increase the cost significantly. In the case of environmental optimization, the target is only to minimize the annualized GHG emissions. Although we consider emissions from the installation of technologies, they are much lower in magnitude relative to those from the use of energy resources (like grid or natural gas).

In each of the intermediate optimization runs (2 to 5), the group optimization leads to centralized installations and a reduction in the optimum SH and DHW storage capacities. Also, the optimum in individual optimization in the intermediate runs cost about 23-38 % higher than the optimum centralized installations with electricity, DHW and SH links. Therefore, the centralized installations could be considered economical if the DH links don't cost more than 23-38 % of the total annualized costs in these cases. In optimization run 2, decentralized ASHPs come up as the solutions for individual buildings, however, it is more economical to install a CHP plant instead when the buildings are optimized as a group. In the optimization runs 3 and 4, the total installed PV capacity in grouped optimization is higher than that of individual optimization by 27 % and 11 %, respectively. Also, installing a higher capacity of CHP plant is found to be more economical when buildings are optimized as a group. The shares of the different technologies in the electricity, domestic hot water and space heating consumption are discussed next. Figure 73 to Figure 75 highlight the contributions of each technology in the total annually consumed energy in case of buildings optimized individually and as a group from both cost and environmental perspectives. In each of these figures, the shares in individual optimization are depicted on the left and those in grouped optimization are on the right. From Figure 73, we can clearly see that the electricity production in the cost optimum from CHP plant and from PV is 11 % higher and 4 % higher, respectively, when the buildings are optimized as a group. This causes an equivalent reduction in the grid electricity consumption when centralized installations are employed i.e., in grouped optimization. The electricity fed into the grid is not considered here. The label 'electricity used to produce heat' denotes the total electricity used by conversion technologies, for example heat pumps to provide heat demands. The reduction in the electricity consumed by power-to-heat devices in grouped optimization by cost arises due to reduced use of ASHPs (Figure 74 and Figure 75) by the increase of CHP compared to individual optimization. Particularly, the portion of energy demand covered by the CHP plant in grouped optimization by cost is higher for DHW (relative to the demand covered by ASHP). This is because DHW is produced at a higher temperature (65 °C) compared to SH (35 °C), causing the ASHP to work at a lower COP and therefore, a higher electricity consumption from the grid. Based on the same reasoning, the production from ASHP in the cost optimum is higher for space heating production (lower operating temperature and thus, higher COP) compared to the share for DHW in both individual and group optimization.

Moreover, the electricity purchased from the grid and the PV production are quite identical in case of individual and grouped optimization for the environmental optimization (Figure 73). Moreover, the space heating productions from ASHP and GSHP are also rather similar. As explained earlier, environmental optimization results in decentralized installations both when the buildings are optimized individually and collectively as a group. Therefore, the usage of technologies is not too different in case of electricity and space heat consumption. Solar thermal collectors are only employed to cover DHW demands in the environmental optimum. Since the installed capacity of STC is higher in individual optimization than in grouped optimization, the resulting share of DHW consumption from STC is also greater. Furthermore, the purchased grid electricity in environmental optimizations is reduced to about 39 % for both individual and group optimization, while PV self-consumption is relatively higher compared to cost optimization (61 % instead of 39 %). Furthermore, the electricity under the 'electricity used to produce heat' label was also found to be higher for environmental optimization. This is due to the increased usage of heat pumps (and electric heating rods) to replace the CHP plant (natural gas driven).

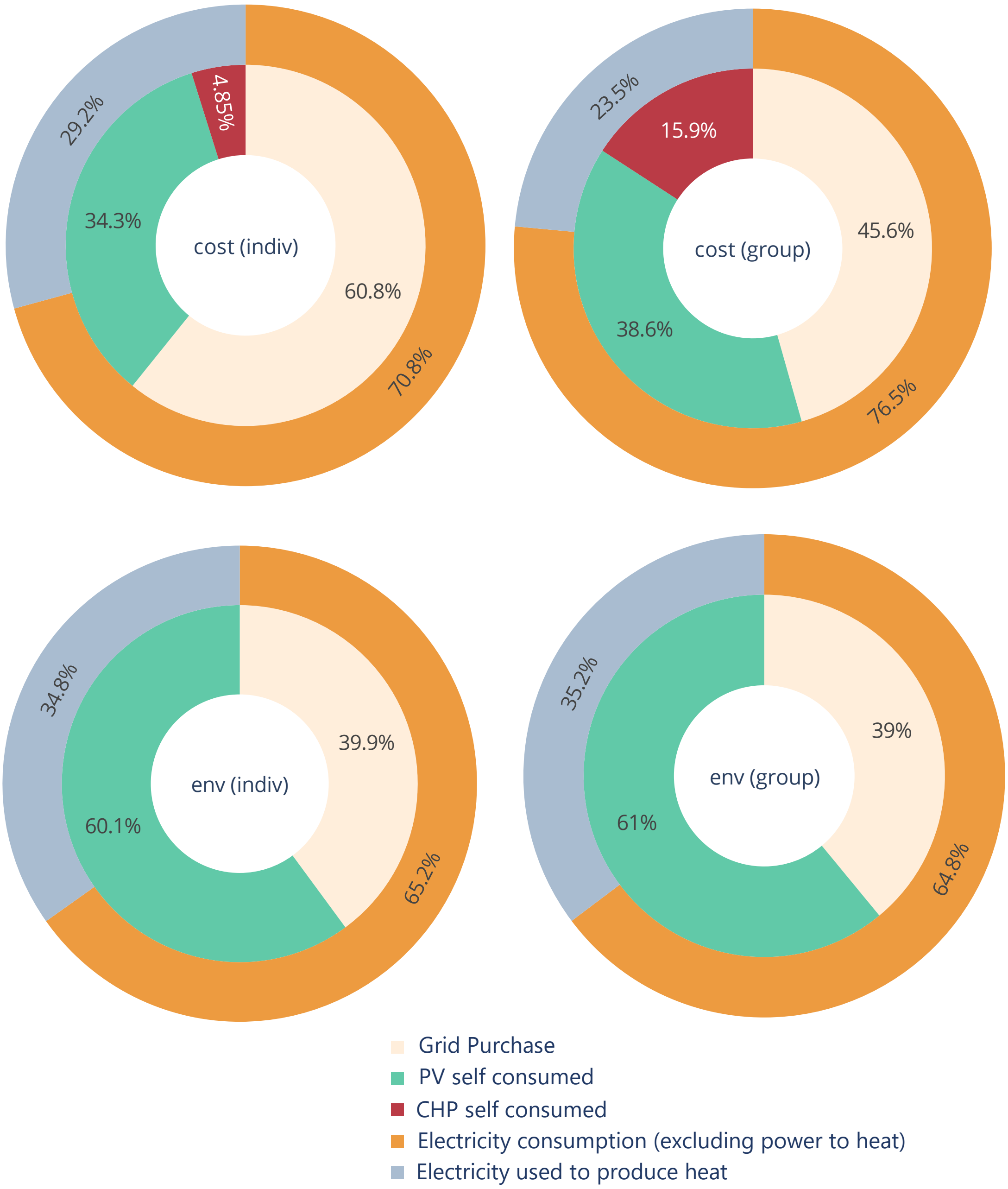

Figure 73 Share of different technologies in the total electricity consumption for the cost and environmental optima (runs 1 and 6 in Figure 71 and Figure 72) in Scenario 2 of SGSW case study. The charts on the left show the results from individual optimization, while the results of group optimization are on the right.

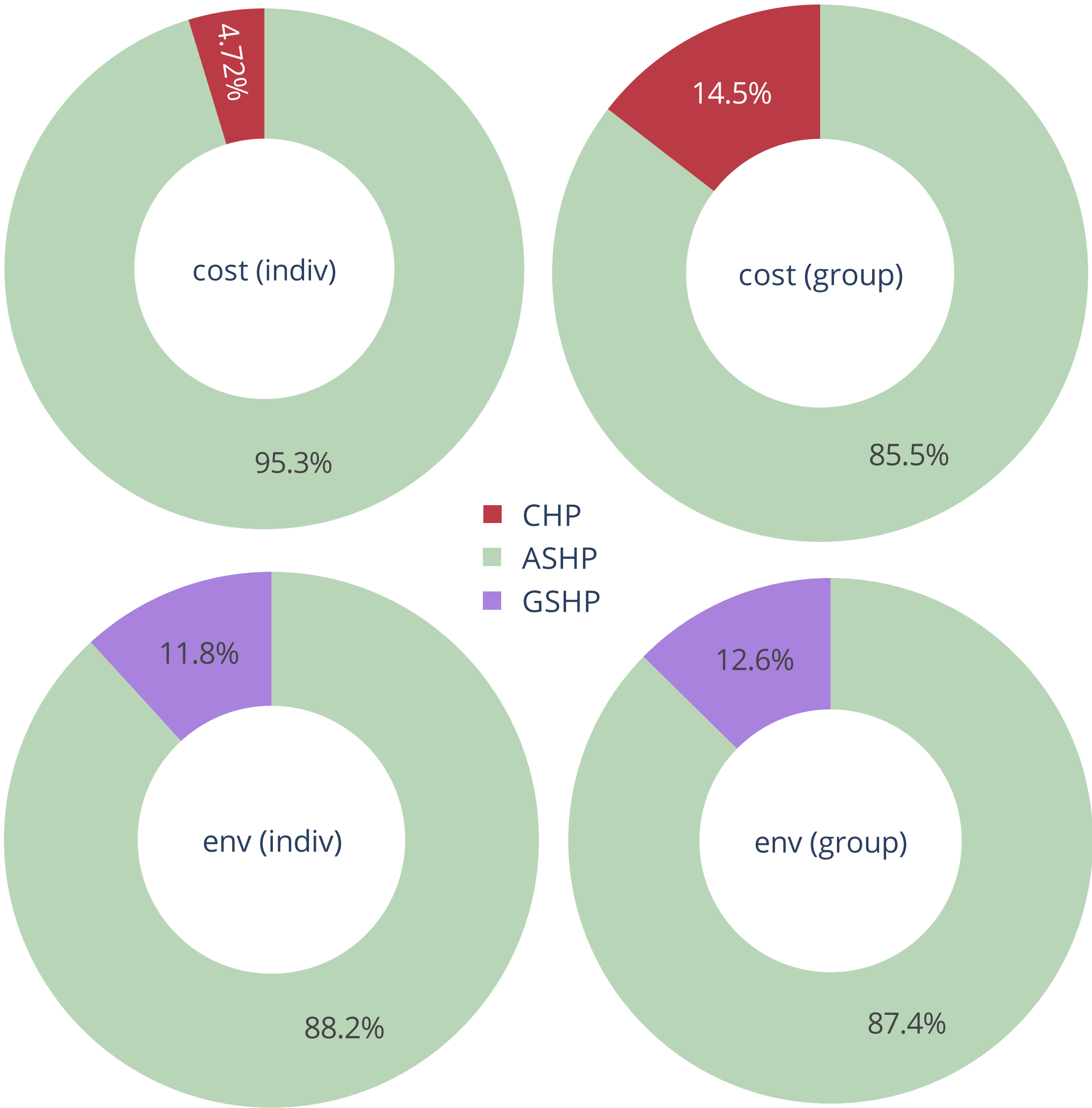

Figure 74: Share of different technologies in the total space heat consumption for the cost and environmental optima (runs 1 and 6 in Figure 71 and Figure 72) in Scenario 2 of SGSW case study. The charts on the left show the results from individual optimization, while the results of group optimization are on the right.

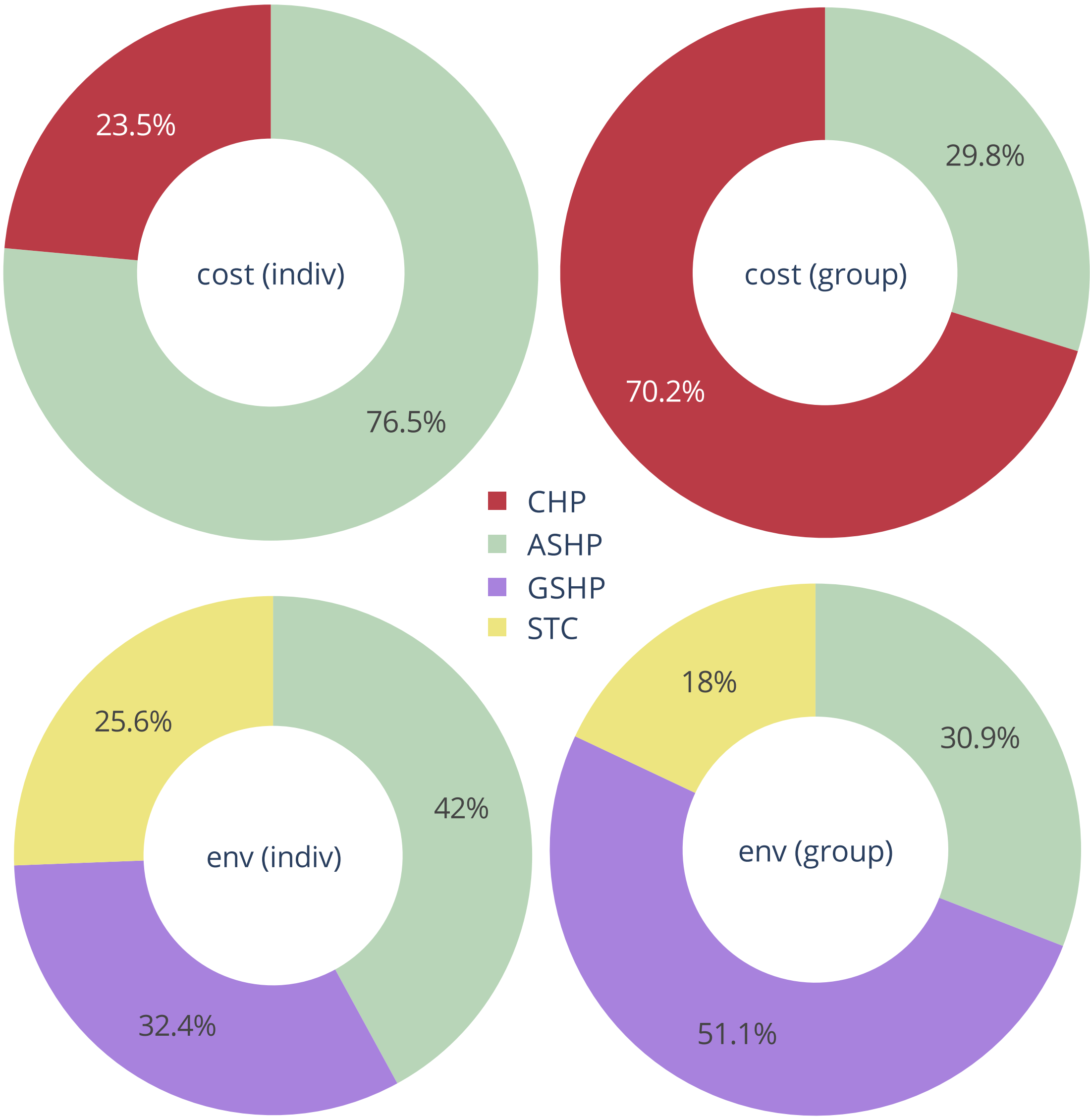

Figure 75: Share of different technologies in the total domestic hot water consumption for the cost and environmental optima (runs 1 and 6 in Figure 71 and Figure 72) in Scenario 2 of SGSW case study. The charts on the left show the results from individual optimization, while the results of group optimization are on the right.

3.3.3 Summary of the case study

This case study from SGSW examines the optimal energy system designs for a diverse-use district in St. Gallen. The district comprises 56 buildings with various usage types. Two scenarios are analyzed: the first focuses on 12 multi-family houses connected to a CHP plant (at the actual installation site), optimizing energy conversion and storage technologies individually and grouped for different cluster sizes; the second considers all 56 buildings, optimizing them individually and grouped while comparing the optimal system configuration to existing technologies and inspecting the share of energy demand supplied by renewable energy sources.

In the first scenario, installing a central CHP plant was chosen the cost optimum choice when a cluster (or group) of at least 7 MFH buildings were optimized collectively. A 224 kW_{th} CHP plant was selected as the most economical solution for the cluster of 7 MFH buildings, while a central CHP plant of 404 kWth capacity was chosen for the group of 12 MFH buildings. The current on-site installation for these 12 MFH buildings is as well a CHP plant of 242 kW_{th} capacity (40% lower than the cost optimum sizing) along with decentral gas boilers (overall 564 kW capacity) to supply the remaining heating demand. Therefore, by increasing the capacity of the CHP plant, it would be possible to completely replace the decentral gas boilers. The use of non-renewable fuels could be avoided if renewable gas is used as the primary energy source of the CHP plant, in future, instead of natural gas. For cluster sizes up to 5 MFH buildings, a central ASHP along with small electric heating rods to cover the peaks was concluded as the optimum heating technology. Based on the assumptions made (Table 11), an ASHP costs 30% lower per kW_{th} of installed capacity than a CHP plant. Moreover, ASHPs have a higher performance efficiency. So, despite the grid electricity being more expensive than natural gas, the operational cost of an ASHP could be relatively lower. Therefore, for the CHP to become more economical over an ASHP installation, the benefits from the combined production of heat and electricity would need to overcome these cost and performance gaps. A CHP plant is not economical for 1 or 2 MFHs even at 50% lower (4.3 c/kWh) gas prices. CHP plants become economical for cluster sizes of 3 buildings if the gas price is reduced by at least 30% (6.1 c /kWh): a CHP plant of 117 kW_{th} capacity replaces the 75 kW ASHP as the cost optimum technology in this case. Similarly, if the gas price is reduced by at least 20% (6.9 c/kWh), then a CHP plant of 180 kWth capacity is selected in the cost optimum solution for the cluster size of 5 MFH buildings. Finally, if we compare the cost of electricity produced from CHP plant against the cost of grid electricity, it can be seen that the electricity produced by CHP will be cheaper if the cost of gas reduces by more than 40% (5.2 c/kWh). Solar thermal collectors (STC), ASHP (supported by electric rods) and PV replace CHP plant in the environmental optimum. Electrical batteries were employed to store PV electricity during low sunshine hours, which led to a 54% decrease in grid electricity consumption compared to the cost optima. To achieve this, a very high capacity was chosen for the electrical batteries (capable of storing 6.7 h of peak PV power), which reduced the LCA but increased the cost significantly. Furthermore, in case of cost optimization about 70 % of the annualized cost resulted from system operation, i.e. the use of grid electricity and natural gas. While the operation of the systems contributed towards a mere 5 % of the total annualized cost in the environmental optimum resulting only from the use of grid electricity. Nonetheless, the annualized cost of the environmental optimum design was found to be nearly 3 times higher than that of the cost optimum design. A major contribution (about 58 %) here comes from the large batteries installed in the environmental optimum. Moreover, about 95 % of the GHG emissions in the cost optimum design arise from the system operation. Therefore, optimization of system operation would be quite relevant for obtaining the highest benefits from the cost optimum design. This could be achieved, in reality, by implementing a smart control to optimize the use of grid electricity and natural gas during the operation of the system. The contribution of GHG emissions resulting from the system operation in the environmental optimum design were found to be around 38 %.

In scenario 2, cost optimization selects PV, ASHP, and CHP technologies both when the buildings are considered individually and as a group. Central solutions appeared when the buildings were optimized together, while decentral installations of the said technologies were chosen for individual building optimization. From the environmental perspective, PV, STC, ASHP and GSHP technologies were chosen for both individual and grouped optimizations. The selection of STC in the environmental optimum is expected, however, the selection of both GSHP and ASHP technologies might not be that apparent. GSHPs suffer from a large LCA impact from the installation of boreholes (by a factor of 2.7 times), but they have better efficiency especially at lower ambient air temperatures. Therefore, in the environmental optimum GSHPs operate during the periods with high GHG emissions and low ambient air temperatures. Grouped solutions were proven to be more cost efficient. The cost optimum solution of individual optimization has 19% higher costs than that of grouped optimization (without considering cost the district heating and microgrid). Still for grouped optimization, the emissions of the cost optimum solution were 33% higher than in individual optimization, due to higher consumption of natural gas. By allowing thermal flows among the buildings, the installed capacity of the central CHP plant was 2.5 times higher, while that of the central ASHP was reduced to half compared to optimal individual solutions. Furthermore, the total installed thermal energy storage capacity in the cost optimum design was reduced by 5% by incorporating district heating. In terms of the share of technologies in the total electricity production, we observed that the contribution from PV and CHP increased by 11 % and 4 %, respectively, when the buildings were optimized collectively (leading to centralized system installations). Therefore, the grid electricity consumption was found to be lower in collective building optimization. Additionally, in collective building optimization the share of DHW demand covered by the CHP plant is higher when compared to the share covered by an ASHP. This is due to higher operation temperature and consequently, a lower COP of ASHP for DHW than for space heat production. The production from ASHP in the cost optimum is higher in case of space heat than for DHW both when buildings are optimized individually and as a group. The environmental optimum on the pareto front (Figure 70) for collective solutions has lower GHG emissions and cost than the one on the Pareto for individual solutions. In both the environmental optimum configurations, decarbonization of the system is achieved by substituting the natural gas use with electricity through ASHP/GSHP and further by the reduction in grid electricity consumption (allowed by the installation of electric batteries). The overall installed capacities of STCs and DHW storages in the environmental optimum were 39 % higher and 3 times higher, respectively, if the buildings are optimized individually. Moreover, the cost of the environmental optima was significantly higher than the cost optimization (and the intermediate optimization runs) due to the inclusion of large electrical batteries to reduce grid electricity consumption during high GHG emission periods. The grid electricity consumption is reduced from 61 % in individual cost optimization and 46 % in grouped cost optimization to about 39 % in the environmental optimum solutions. Furthermore, in the intermediate optimization runs, the optimum decentralized system designs for individual buildings were found to be 23-38 % more expensive than the optimum system designs in group optimization (cost of district heating and microgrids excluded). Thus, the central installation setups suggested by optimizing the buildings together could be considered economical if the network costs do not exceed 23-38 % of the total annualized cost.

3.4 Case studies – Renewable gas assessment

Disclaimer: As an additional research question, the FOGA (Research, Development and Promotion Fund of the Swiss Gas Industry) analysed the impact of using renewable gas. According to the SFOE's heating strategy, the use of renewable gas for heating purposes should be avoided.

Only an independent study of each building (MFH13, MFH54 and MFH100) is realized, with a gradually growing percentage of renewable gas in the gas mix consumed. A Pareto front is drawn for 0% renewable gas, 10%, 30%, 50% and 100%, for each building. Here is the structure and variable input data of the optimizations done for this part:

biomethane %	0%	10%	30%	50%	100%
Emissions (g C02 eq. /kWh HHV)	230	219	198	177	124
Price (ct/kWh HHV)	9.87	10.47	11.67	12.87	15.87

Table 20 GHG emissions and price by percentage of biomethane in the gas mix

3.4.1 New building - MFH13

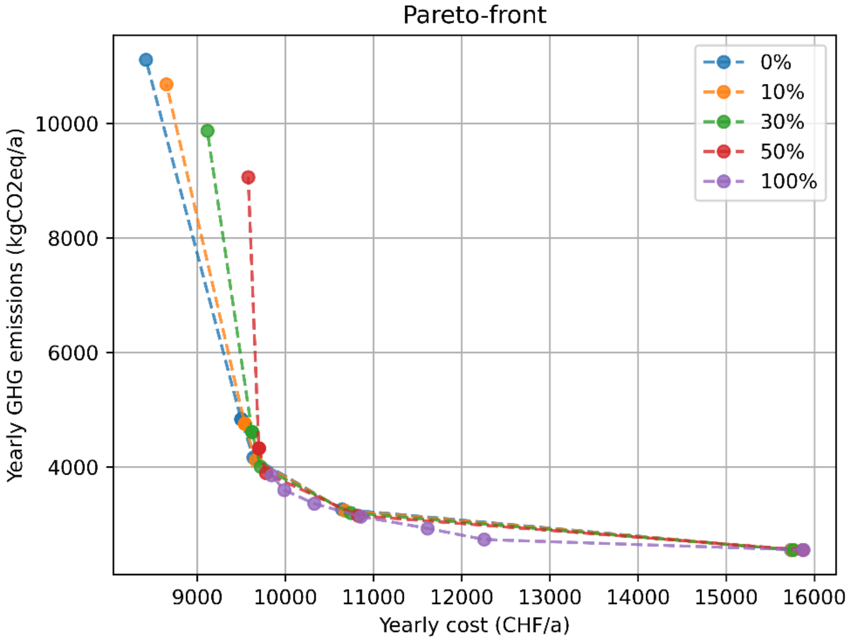

Figure 76: Pareto front representation of the optimal solutions for the MFH13 building and five different biomethane share with reference GHG emissions factors of 230 gCO_2eq/kWh for natural gas (0%) and 124 gCO2eq/kWh for biomethane (100%).

Figure 76 displays five distinct Pareto fronts, each representing varying biomethane proportions within the gas mix. Initially, it is evident that there exists a substantial gap in emissions between the first and second points. Additionally, if for instance we look at Figure 77, which describes the Pareto front for the 0% biomethane proportion, the solution stagnates after the gap as points 2,3,4 blend into one another. The cost optimum (1) solely uses a gas boiler to answer the heating demand. For points 2,3,4 the GHG emissions limit detailed in Table 21 forces to introduce a heat pump, but its capacity cannot be lower than 5 kW (to ensure realistic solutions). Therefore, a 5 kW heat pump is immediately introduced for solution 2. Combined with the low heating demand of MFH13, this explains the large GHG emissions interval between solutions 1 and 2. Moreover, we also understand why solution 2 has such low emissions compared to the GHG constraint, and thus why solutions 3 and 4 remain the same. The 0% front is taken as an example, but the same trend repeats itself for 10%,30% and 50% fronts. In the context of optimizations adopting 100% biomethane, the very high gas price renders the reliance on a sole gas boiler for heat production non-optimal, even for solutions without emission constraint. Thus, as presented on Figure 78 (top right heating capacities), the switch is made to a bivalent system. On a side note, MFH13 has a notably low energy consumption, which explains why a transformer of 5 kW has such a big impact, but the other buildings of the study present a different behavior that will be presented later.

Solution n°	1	2	3	4
mean annual cost [CHF]	8418	9496	9496	9496
GHG emissions [kgCo2eq]	11112	4836	4836	4836
GHG emissions limit [kgCo2eq]	no limit	8696	6805	5325

Table 21 Evolution of GHG emissions constraint for the 0% biomethane Pareto front

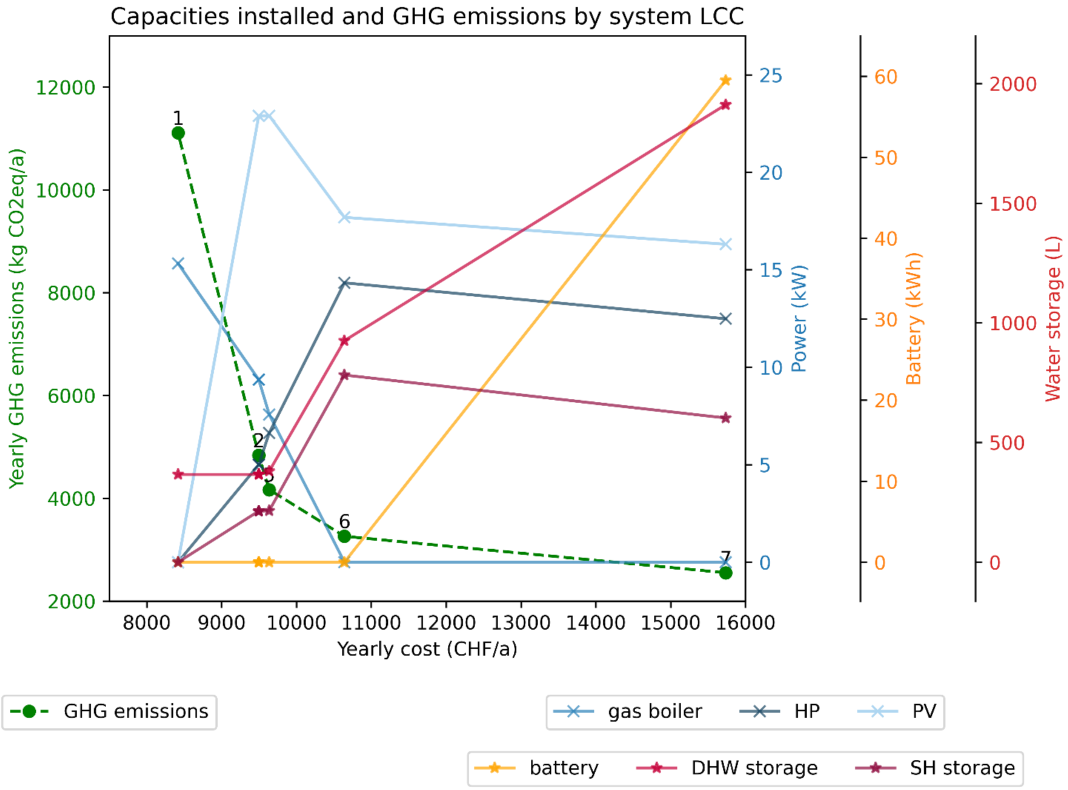

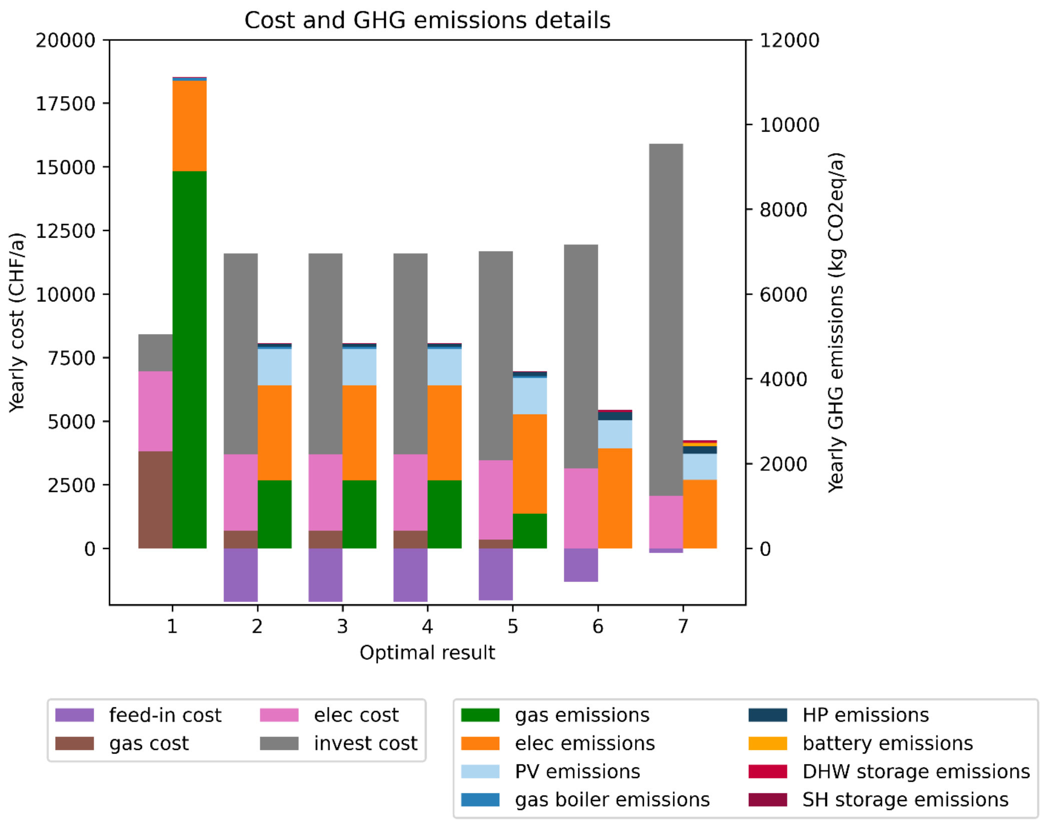

Figure 77 Complete results for the multi-objective optimization for MFH13and 0% of biomethane share.

Furthermore, upon examining the economical optimum of each front, it appears as evidence that the more biomethane there is in the gas mix, the more the emissions are reduced. However, the emission reductions come at the expense of an escalation of the cost. In terms of the technologies used, for a biomethane share between 0 and 50%, the results are exactly the same: the production of heat is solely done through a gas boiler, the electricity used comes from the grid and no electrical or space heating storage is installed. In regard to the 100% biomethane solution, noticeable differences appear: the heating demand is answered almost equally through a gas boiler and a heat pump, the maximum capacity of PV modules is installed and a small storage for water used for space heating is added. Nevertheless, as elaborated in the last paragraph and visually illustrated in Figure 78, these different choices for the most economical point of the purple front can mostly be explained by the elevated cost of gas. Therefore, it can be concluded that for economical optima of MFH13, the rising proportion of biomethane in the gas mix induces two impacts: a decrease of the emissions (between 0 and 50%, -18% CO_2eq or 2 tCO_2eq) and an increase of the cost (between 0 and 50%, +14% or +1160 CHF). Importantly, these shifts in biomethane proportion do not have an influence on the selection of technology pathways.

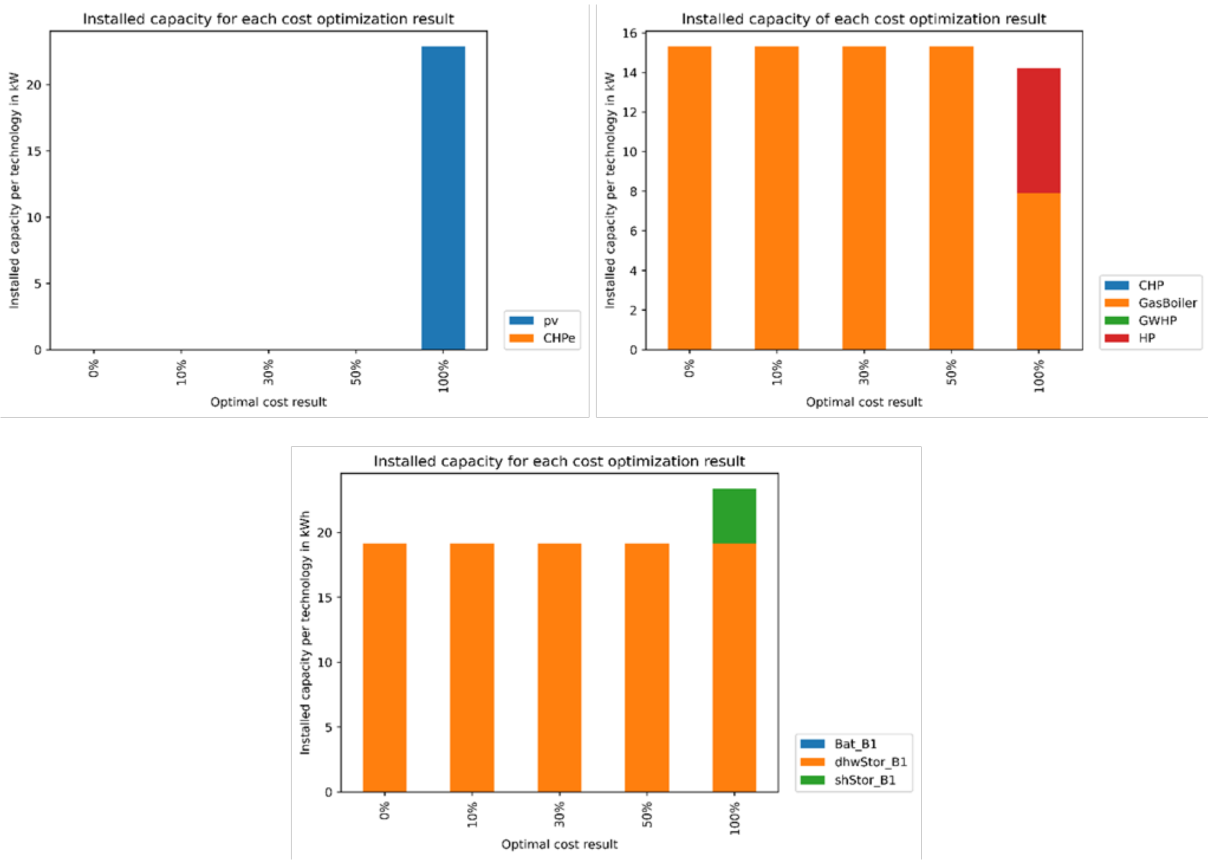

Figure 78 MFH13 Installed capacities for the cost optima of each Pareto front.

If we shift our focus on the other extremity of Figure 76, the environmental optima i.e. without cost limits, it appears that there is no correlation between the proportion of renewable gas and the emissions of the system. This independence can be explained by the choice of transformers: they remain consistent for every front and above all no transformer that uses gas is chosen. The general solution is composed of a heat pump, PV modules and storage. The use of battery is characteristic of the environmental optima, as their cost is high, and they allow to decrease the use of grid electricity that is more carbon-emitting than PV-produced electricity. For the cost, the same observation can be made: the cost exhibits minimal variance across the various fronts. The explanation is clear: the only parameter that differs between the

5 fronts is the price and environmental impact of gas, and it is not used in these solutions. We can thus infer that the use of biomethane with a pure environmental objective for MFH13 is essentially nonexistent.

3.4.2 Renovated building - MFH54

The overall trend depicted in Figure 79 underlines the similar trajectory of each front. Regardless of the renewable gas proportion, the solutions of each front do not get clearly dominated by the ones from another front, i.e. surpassed in terms of both cost and GHG emissions. If we look at the low-cost solutions on the left of the graph, we see contrary to MFH13 a gradual diminution of the emissions without any significant gap. An explanation for this could be the larger capacities of the machines composing MFH54's system, caused by the greater energetic consumption. Indeed, a gas boiler is present, like in the MFH13 cost optimum, but in conjunction with a heat pump as illustrated in Figure 80. This allows us to make the most out of the emission constraint on each optimization and thus find intermediate solutions.

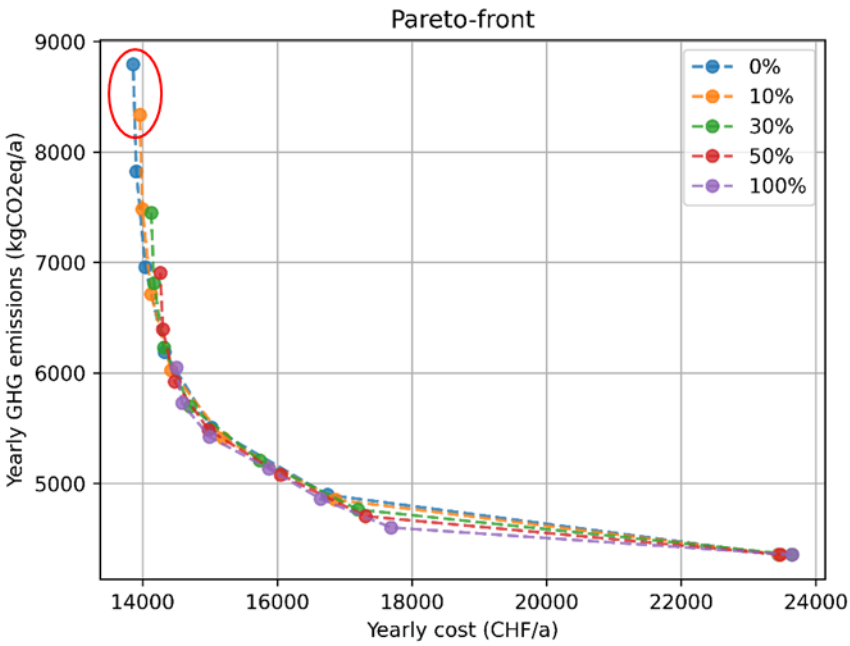

Figure 79 : Pareto front representation of the optimal solutions for the MFH54 building and five different biomethane share with reference GHG emissions factors of 230 gCO_2eq/kWh for natural gas (0%) and 124 gCO2eq/kWh for biomethane (100%).

More precisely, the economic optima, i.e. the first point of each front, shows that an increase of the biomethane share allows to improve the emissions in return of cost augmentation. Also, we see on Figure 80 that the maximum capacity of PV modules is installed for all cost optima, contrary to MFH13's solutions where this choice was only made for the 100% biomethane. This discrepancy can also be explained by the presence of heat pumps in every MFH54's cost optimum, which makes the electricity consumption rise in comparison with MFH13, and thus makes the investment in a large PV installation justifiable. It is worth noting that in terms of PV power installed, no middle-ground is never chosen, when it is although allowed by our constraints. The choices are binary: either 0 kW of PV capacity, or 22 kW. This behavior is most probably the result of an optimization found by the solver. Consequently, a tipping point in electricity demand is passed with MFH54, which will be confirmed in MFH100.

Focusing solely on the cost optima, it seems that increasing the share of biomethane can be beneficial as it lowers the GHG emissions in exchange for a slightly greater cost. However, if for instance we compare the cost optimum of the 10% front with the second less costly solution of the 0% front (red circle on Figure 79), it appears that the former is dominated by the latter. The cost optimum solution for the 10% front is valued at 14 kCHF and 8.3 4tCO_2eq, whereas its competitor in the 0% front is valued at13.9 kCHF 7.82 tCO_2eq. In fact, the 0% biomethane solutions are always better or equal to the ones including a share of biomethane. Therefore, the use of renewable gas in MFH54 to reduce the cost or even have less emissions for low-cost solutions is not recommended.

MFH54's environmental optima are exactly the same. The same phenomenon as in MFH13 occurs gas is completely absent of these solutions, thus the change in the proportion of biomethane in the gas mix has no effect on the solutions. The technologies used remain the same, with the same strategy for electricity storage. Globally, the outcomes from MFH54 align with those of MFH13, but the greater energetic consumption allows to underline some trends, such as the use of PV modules or bivalent systems.

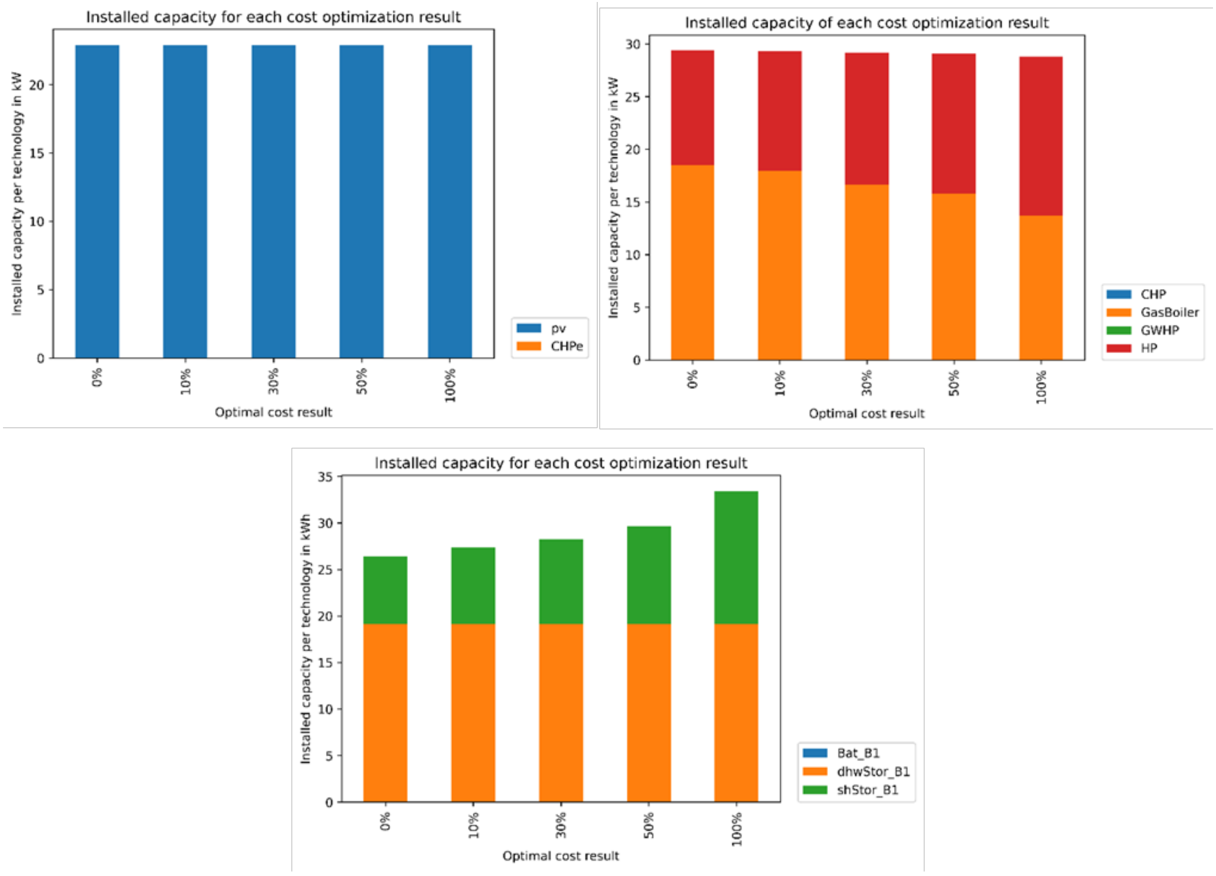

Figure 80 MFH54 installed capacities for the cost optimum of each Pareto front.

3.4.3 Old Building - MFH100

On Figure 81, the superiority of the 100% natural gas is even more conspicuous. Similar to our observations for MFH54, the cost-optimal solutions alone seem to indicate that adding renewable gas into the mix allows for a GHG emissions reduction. Nevertheless, the clear shift of the curves containing biogas towards a higher cost (red circle) shows that, considering all the solutions on each front, using biomethane in MFH100 is either unfavorable or at best insignificant.

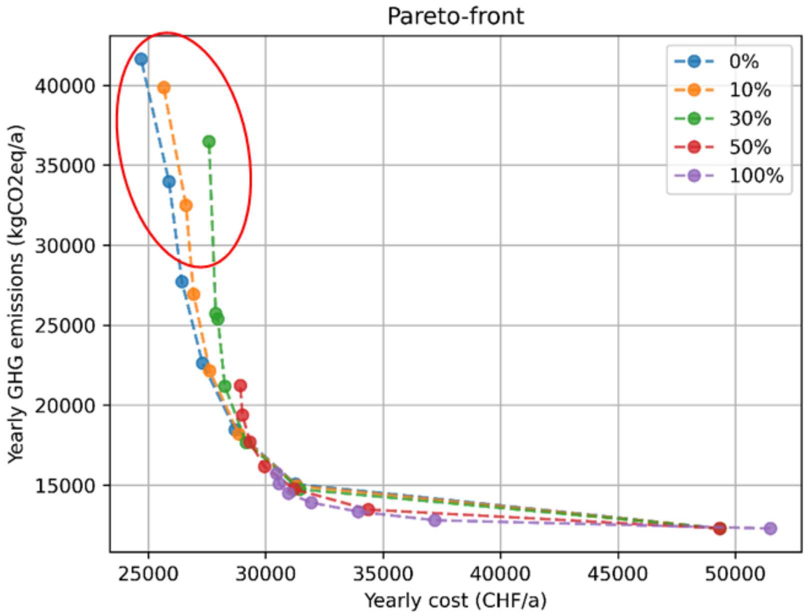

Figure 81 Pareto front representation of the optimal solutions for the MFH100 building and five different biomethane share with reference GHG emissions factors of 230 gCO_2eq/kWh for natural gas (0%) and 124 gCO2eq/kWh for biomethane (100%).

On technologies used for cost optima, we see on Figure 82 that the PV is maximized, which corroborates the idea developed for MFH54. On the heat generation front, we see the return of monovalent systems with only a gas boiler for low shares of biomethane, as it was the case for MFH13. However, MFH100's bivalent systems for high shares of biomethane are different in the fact that the total power installed for heat production grows and do not remain constant. Moreover, we observe as in MFH13 a GHG emission gap between the cost optimum of the 30% front and the 50% front, corresponding to the switch from a monovalent gas boiler system to a bivalent gas boiler/HP system.

Shifting attention to environmental optima, the situation described for the other buildings repeats itself, apart from the technologies used. As described in Figure 83, ground-water HP is used in conjunction with an air HP. Notably, a 10 kW CHP is installed for the 100% biomethane solution. It is the only occurrence of a transformer which uses gas in all the environmental optimizations done, which is significant. Nevertheless, the GHG emissions reduction achieved thanks to the CHP is only of 8 $kgCO_2eq$, in comparison with the other solutions with less biomethane. These 8 $kgCO_2eq$ have a cost of 2155 CHF, i.e. 269 000 CHF/tCO_2, which is exorbitant. This stands in stark contrast to the emission tax of 120CHF/tCO_2eq. In consequence, although significant by its existence, the use of a CHP is extremely unprofitable. Additionally, in real case situations, the environmental optima would never be chosen as the cost of the emissions reduction between the 6th point and 7th point of each front is far too important, as depicted in Table 22. It is even more true for MFH54 and MFH100: to reduce the emissions by less than 10% the cost rises by 40%. Thus, only the first 6 points would be considered.

MFH100, as the other buildings studied, underlines the lack of substantial advantage that renewable gas brings to a one-building energetic system. Heat pumps are far superior as their cost / emissions ratio is much better than the one for biomethane.

	MFH13 50 %		MFH54 50%		MFH100 50 %	
	cost	emissions	cost	emissions	cost	emissions
7th point	15868	2552	23469	4355	49334	12303
6th point	10822	3153	17308	4704	34365	13476
Difference	47%	-19%	36%	-7%	44%	-9%

Table 22 Cost optima comparison with other solutions.

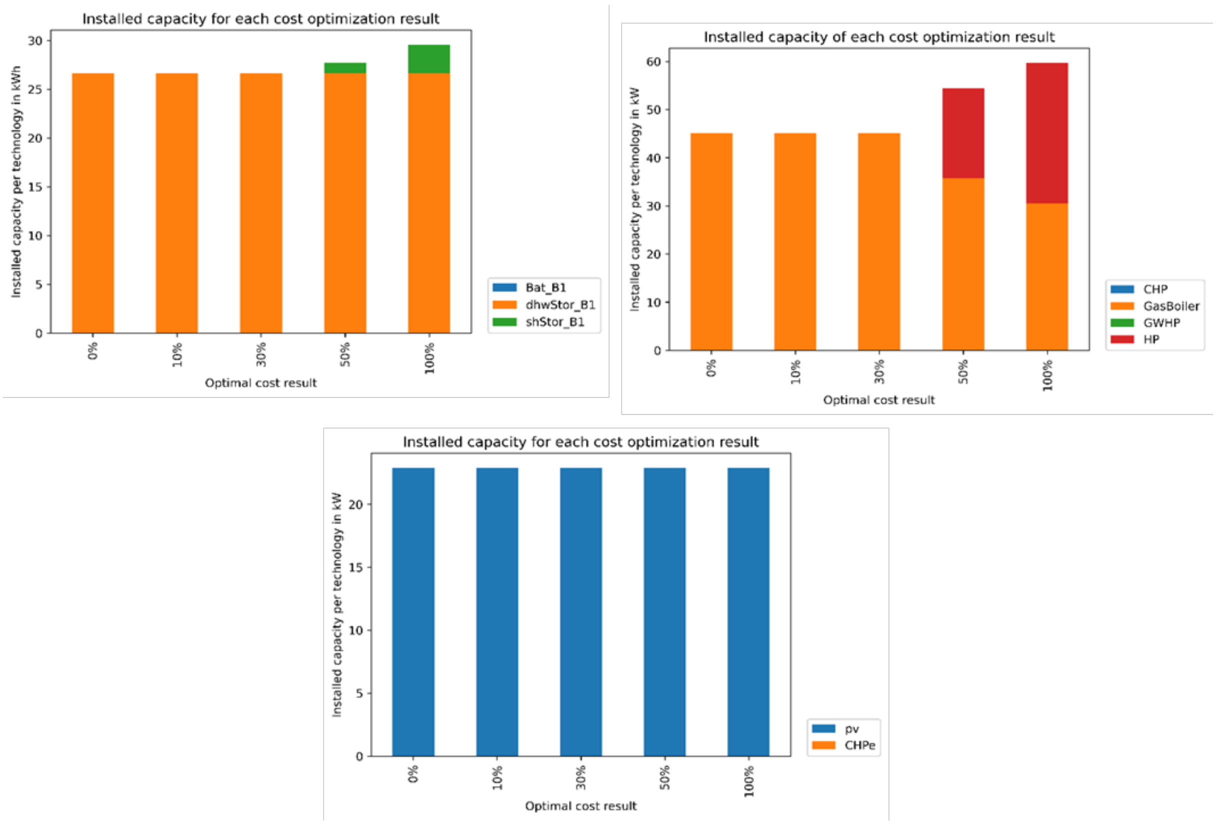

Figure 82: MFH100 capacities installed for the cost optimum of each Pareto front

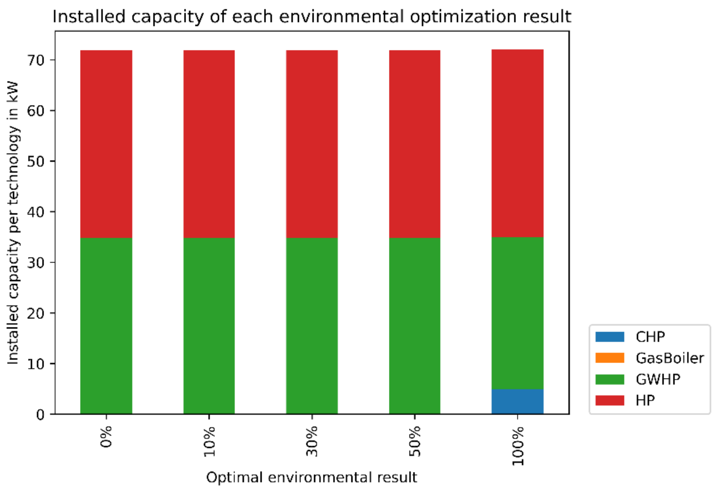

Figure 83 MFH100 capacities installed for the environmental optimum of each Pareto front.

3.4.4 Impact of lower biomethane GHG emissions

The analysis conducted in the preceding paragraphs for MFH13, MFH54 and MFH100 were realized with optimizations using the fixed KBOB value of 124 gCO_2eq/kWh HHV for the biomethane emission. The general conclusion which emerged from these results is that the implementation of biomethane is not advisable. Nevertheless, it is crucial to acknowledge that this conclusion is significantly contingent upon the cost-to-emissions ratio of biomethane. Notably, emissions exhibit a high degree of volatility, as outlined in section 2.5.4. To study this matter, similar optimizations were realized with MFH54 and MFH100, but with an emission value of 44 gCO_2/kWh HHV, justified in 2.5.4. This value corresponds to the biomethane produced in the Werdhölzli plant, calculated with and economic allocation (Table 16). The following parameters outline the specifics of these new optimizations:

biomethane %	0%	10%	30%	50%	100%
Emissions (g CO2 eq. /kWh HHV)	230	211	174	137	44
Price (ct/kWh HHV)	9.87	10.47	11.67	12.87	15.87

Table 23 GHG emissions and price of biomethane share in the mix.

In a second time, the influence of grouping buildings together is investigated for a 100% share of biomethane. The group of buildings comprises of 4 MFH54 connected through a thermal and electrical local grid.

1. Single Building investigation

The comparison of the Pareto fronts for the high emission value (Figure 84, a and b) with those for the low emission value (Figure 84, c and d) yields insightful conclusions. Within the biomethane proportion range of 0% to 50%, no discernible difference emerges. However, the Pareto front for 100% renewable gas shows a remarkable improvement. First it can be noted that this change underlines the existence of a threshold of the emissions-to-price ratio lying between (137 gCO_2eq/kWh HHV ; 12.87 ct/kWh HHV) and (44 gCO_2eq/kWh HHV ; 15.87 ct/kWh HHV). Crossing this threshold triggers the use of biomethane for emission reduction purposes. For both buildings, the 100% biomethane share induces the discovery of new dominant solutions. For the same cost, the emissions are globally reduced. For MFH100, the environmental optimum is largely improved compared to the 50% front with -3% (1577 CHF) for the cost and -38% (4667 kg CO_2eq) for the emissions. For MFH54, the comparison of the 6th point of the 100% biomethane front and the 7th point of the 50% biomethane front shows a remarkable improvement: -9% (2158 CHF) of the cost and -16% (712 $kgCO_2eq$) of the emissions. Consequently, in this first approach we understand that a mix of gas priced at 15.87 ct/kWh HHV and with emissions of 44 gCO_2eq allow for a substantial reduction of the GHG emissions, along with a smaller cost reduction. Although the cost reduction is small, the fact that it is a reduction is very significant and underscores the viability of biomethane.

To dive deeper into the changes brought by the reduction of the biomethane emissions, Figure 85 and Figure 86 depicts the Pareto fronts for a 100% biomethane mix for MFH54 and MFH100. If we first focus our attention on the evolution of the capacities installed, we can distinguish some tendencies. For both buildings, the heat generation goes through gas boilers and heat pumps for more economical solutions. Nevertheless, the progression from solution 1 to 4 for MFH54 involves decreasing the gas boiler capacity while increasing the HP capacity. In contrast, MFH100's progression follows the opposite pattern: HP capacity is reduced, and gas boiler's is increased. As the solutions progress towards the environmental optimum, we see the apparition of a CHP to partly replace the gas boiler. To finally reach the environmental optimum, the approach for the two buildings differs: CHP capacity remains stable for both, but MFH54 prefers to diminish the HP capacity in favor of the gas boiler, whereas the opposite is done for MFH100. Generally, we can see that in MFH54, the cumulated capacities of the gas boiler and CHP remain slightly inferior to the HP capacity for solutions 1 to 6, whereas in MFH100 they are approximately twice as large.

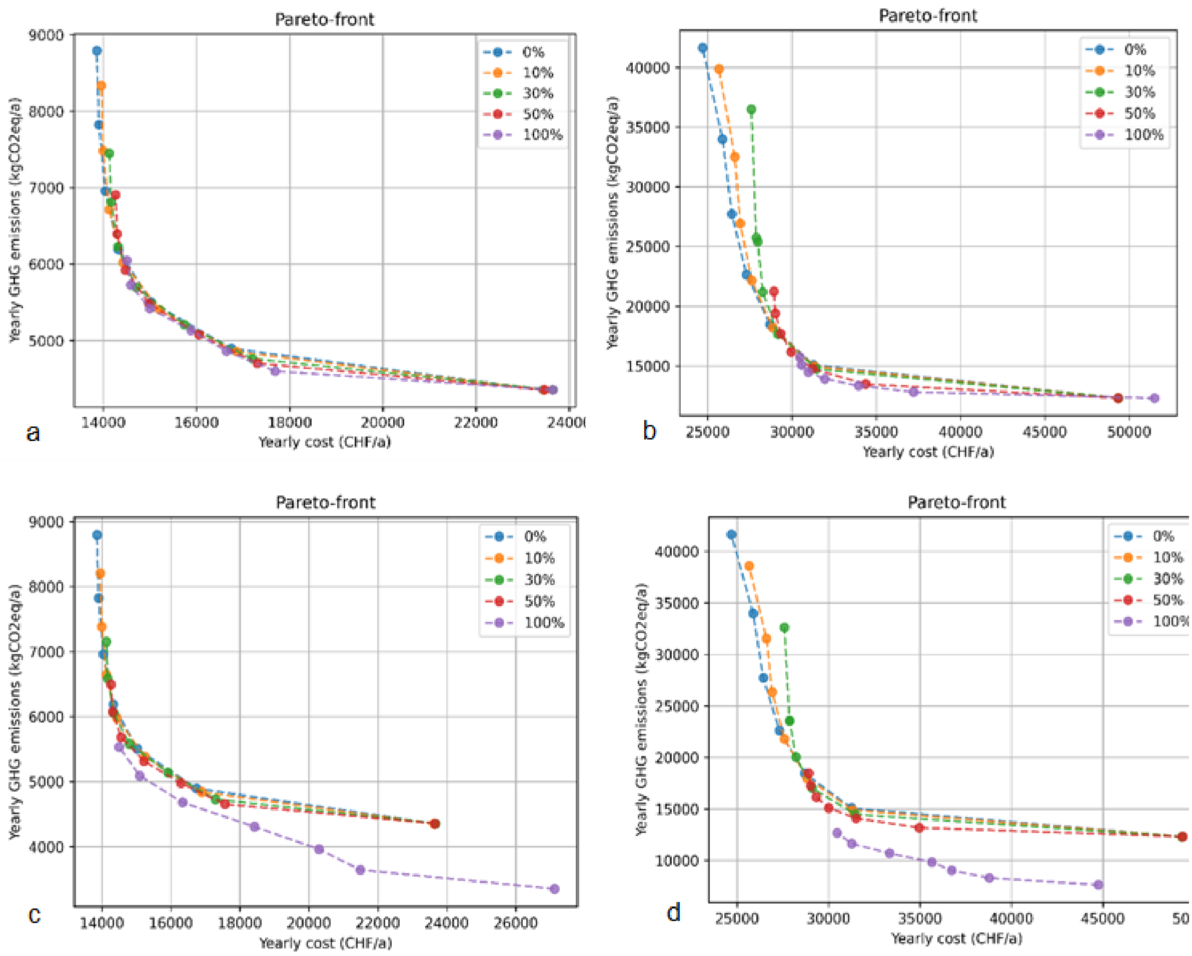

Figure 84: Pareto fronts for a: MFH54 Pareto fronts for 124 gCO_2eq/kWh HHV, b: MFH100 Pareto fronts for 124 gCO_2eq/kWh HHV, c: MFH54 Pareto fronts for 44 gCO_2eq/kWh HHV, and d: MFH100 Pareto fronts for 44 gCO_2eq/kWh HHV

Distinct results emerge for the storage of hot water between the two buildings. For MFH54, the SH storage rapidly grows from point 1 to 4 and then sharply decreases to end its course with a smaller capacity than the DHW storage for the environmental optimum. DHW storage remains smaller for almost all solutions but nevertheless steadily grows in capacity. For MFH100, SH storage is much less used all across the front and its capacity always remains low. DHW storage has a similar usage in both buildings.

Shifting our attention to the cost details described on the bar charts, we see that cost is composed of the investment to buy and install technologies, the cost of electricity and the cost of gas. From the cost optimum to the environmental optimum, we observe that the cost augmentation is mainly an augmentation of the investment to install more expensive equipment. Moreover, the money invested to buy energy is originally mainly used to buy electricity but this repartition shifts to a gas-predominant investment, as the emissions are reduced, and cogeneration is implemented. The emissions details corroborate the precedent observations, but also show the impact of batteries that allow to raise the auto consumption rate and thus rely less on the more polluting electricity from the grid.

To conclude, this analysis illustrates the great impact of the variability of the biomethane emissions evaluations. Reducing it to 44 g/kWh HHV allows for a major change in the solutions found. A gas mix with a price as high as 15.87 ct/kWh HHV but with low emissions is competitive with the heat pumps supplied by a mix of grid and PV electricity. The cost reduction brought by the use of such a gas mix is not game-changing, however the GHG emission reduction is significant.

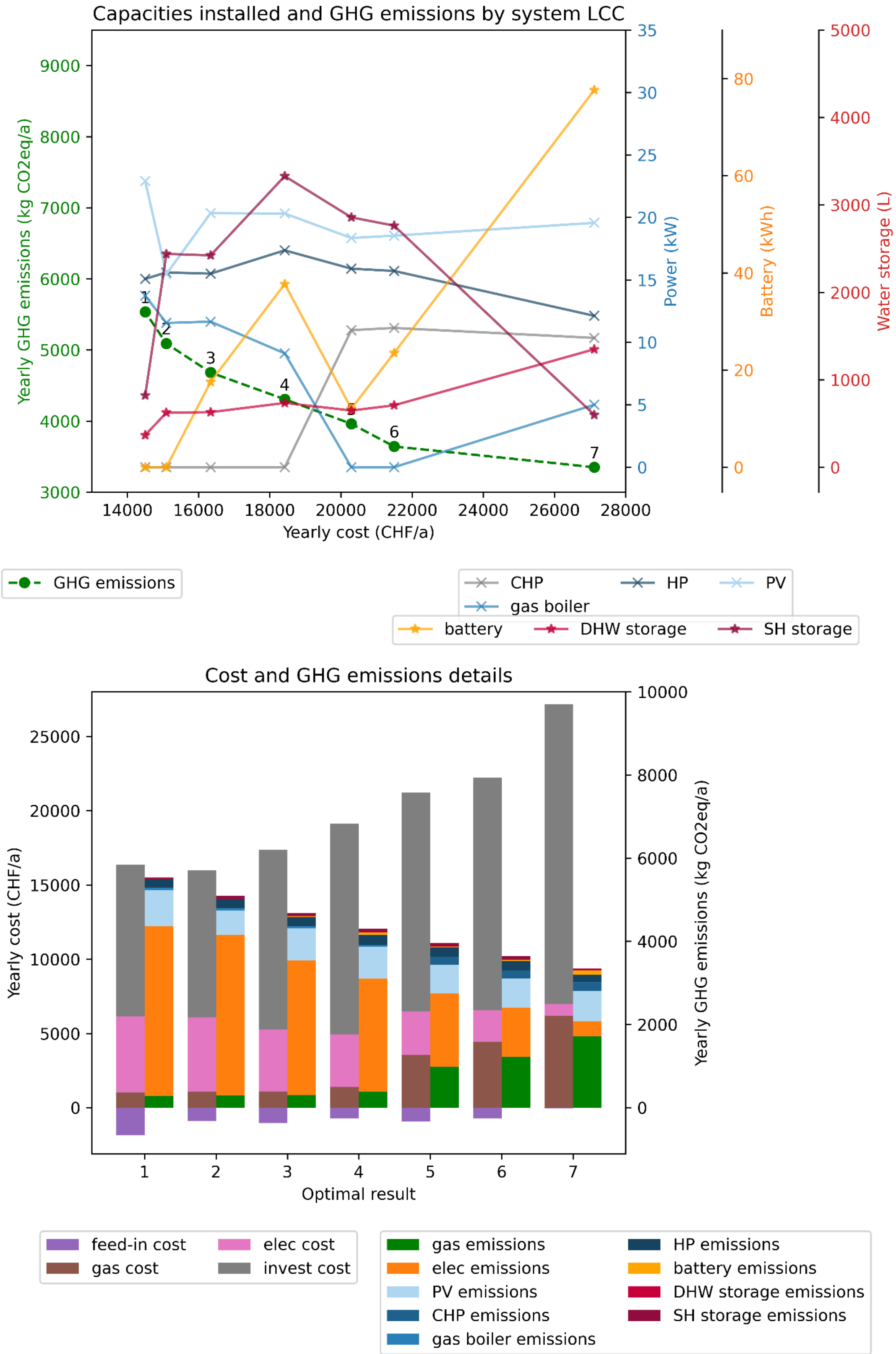

Figure 85 MFH54 100% biomethane Pareto front for 44 gCO_2eq/kWh HHV.

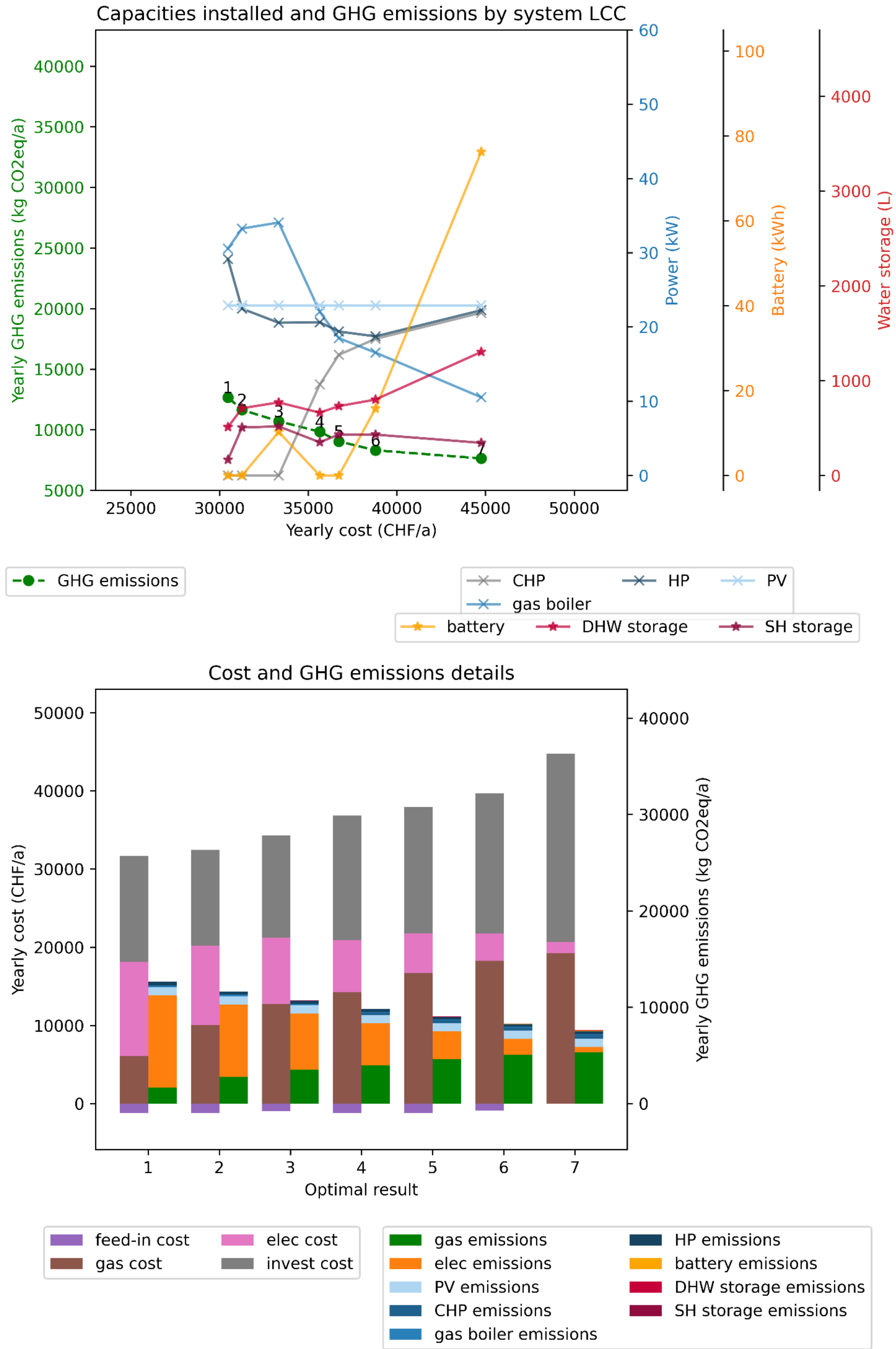

Figure 86 MFH100 100% biomethane Pareto front for 44 gCO_2eq/kWh HHV.

2. Group of buildings investigation - 4 MFH54

4 buildings were optimized within an energy community able to exchange energy through local electrical and thermal grid. Figure 87 and Figure 88 show the Sankey diagrams revealing the optimal energy concept for respectively the cost optimum and the environmental optimum. The cost optimum (Figure 87) relies on a centralized ASHP, a gas boiler and PV system on 2 buildings. Whereas at the environmental optimum (Figure 88) the energy system has decentralized CHP and ASHP and PV system in each building.

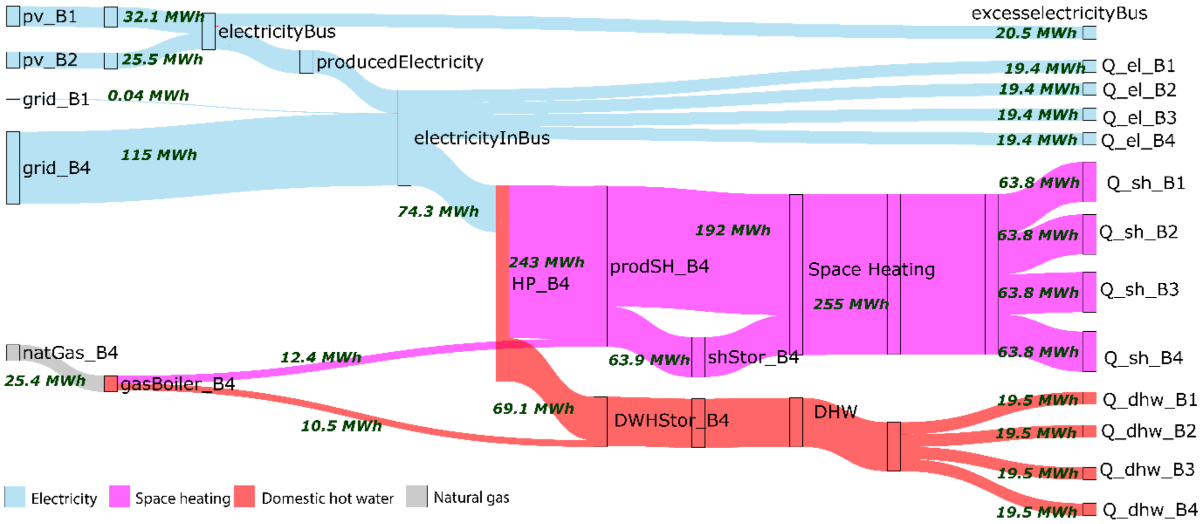

Figure 87 : Sankey diagram of 4 MFH54 at the cost optimum.

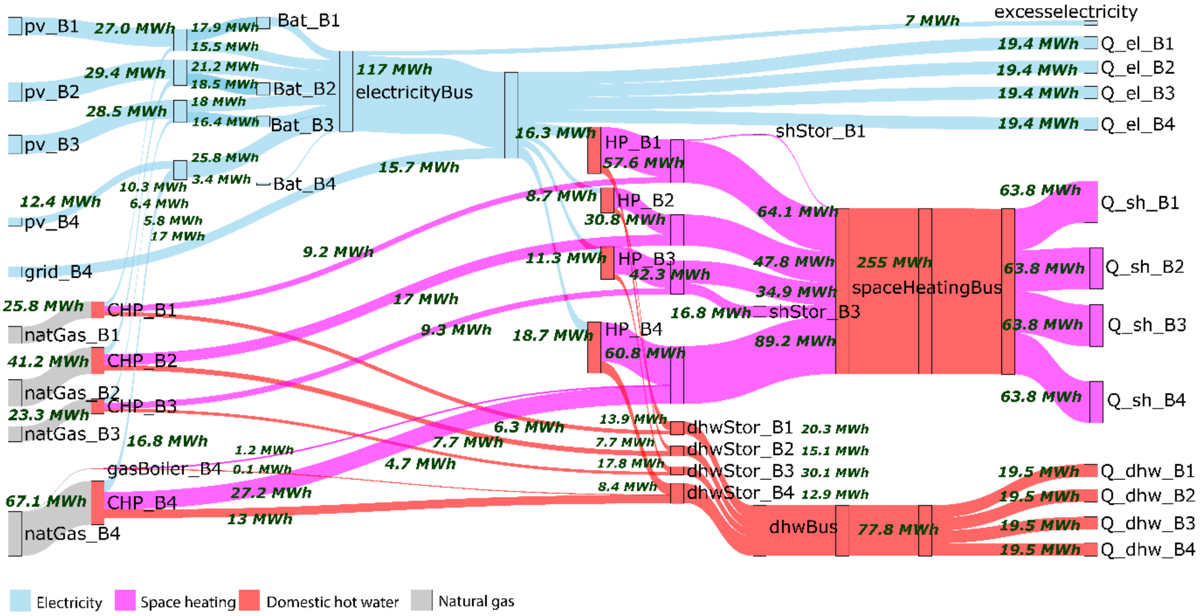

Figure 88 : Sankey diagram of 4 MFH54 at the environmental optimum.

The energy concept and total storage and converter capacities for grouped building are similar compared to individual buildings, as shown in Figure 89. One difference can be seen in the sizing of the PV system at the cost optimum. Moreover, storage capacities are higher in the group configuration to enable better use of the synergy between the building consumption. Under the same energy tariffication the group of buildings have 12% smaller cost compared to the individual solution, without taking the infrastructure for the local energy grids.

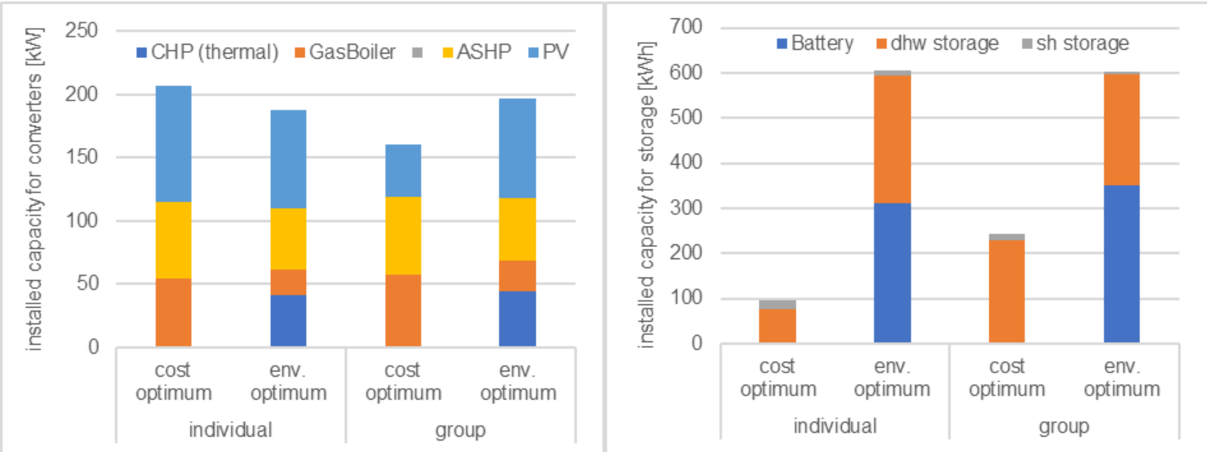

Figure 89 : Installed energy converters (left) and energy storage capacities (thermal and electrical) for individual buildings and for the group of building at the cost optimum and at the environmental optimum.

3.4.5 Conclusions

To conclude this study, the results found confirm our initial assumption that biomethane impact on the optimal energy systems heavily depends on the emission value and the cost associated. With mean values from the most trusted Swiss sources, its impact is either neutral or negative. Whether it is for a very modern building like MFH13, a renovated one like MFH54 or an old building like MFH100, natural gas emerges as the preferable option for cost reduction, while heat pumps prove effective in curbing pollution. However, the emission value of biomethane is markedly project specific. We observe that for a particular facility with emissions significantly lower than the mean value, biomethane becomes a competitive choice. For both price and environmental optimization, its use has clear benefits. Nevertheless, this holds true primarily for an input of pure biomethane, which considering the small production of this energy vector is only doable for very particular projects. To precise the results found in this study, the next objective could be to find the exact emission to price ratio which makes the biomethane viable as an energetic vector. When grouping four MFH54 within an energy community (thermal and electrical), the results obtained are similar compared to four individual buildings in terms of energy concept and installed capacities except for PV and energy storage technologies. Differences come from the optimal configuration whether the system is centralized (smaller PV system, and larger storage) or decentralized (only larger storages).

Moreover, it is worth noting that the Optihood framework used to realize the optimizations of this study is focused on the planning of DMES. This means that the optimization does not consider an existing situation to improve from. In the case of building renovation, we often find building equipped with gas boilers, which would represent an advantage for the use of renewable gas as its implementation would not require an investment, thus giving an advantage to boilers over heat pumps.

On the use of these conclusions beyond Switzerland, different comments can be made. Weather data used here is specific to the region but represents a climate common in the northern hemisphere. Prices are described in CHF and come from local studies, which makes the figures in the results difficult to exploit. However, the most important results are the choices of technologies, which makes the relative prices more important and thus make results generalizable. As for carbon footprints, the value used are not specific to Switzerland, except for the grid. Indeed, a particular advantage of this study is the inclusion of the dynamic emissions of the Swiss grid, which brings a greater precision, but the generalization of the results is affected. For instance, for a similar study realized in a country like France, where grid electricity carries much less emissions, it would be even harder for transformers using renewable gas to compete with heat pumps. In summary, while the exact conclusions are directly pertinent to Switzerland, they can be applied more broadly to all developed countries with similar weather conditions and grid characteristics.

3.4.6 Summary of the case study

This study explores the potential of renewable gas to power both single and grouped buildings while minimizing costs and environmental impacts. The research addresses 3 critical questions:

- Under what circumstances is biomethane utilization appropriate, considering building usage patterns, and building types?
- How does the proportion of renewable gas, carbon footprint, and specific cost influence the optimal energy system configuration?
- What are the most effective devices for utilizing renewable gas to meet energy requirements?

To address these questions, the study employs three hypothetical multi-family houses (MFH) of 3 stories with 2 to 3 appartement per floor that represent various space utilizations, energy standards (modern, renovated, and old) in the Swiss residential sector. Each type is designated based on its specific energy demand per square meter of the energy reference area (kWh/m2): MFH13, MFH54, and MFH100, under the climatic conditions of the Lausanne region.

	MFH13	MFH54	MFH100
Electricity (kWh/m^2/year)	13	17	32
DHW (kWh/m^2/year)	16	17	24
SH (kWh/m^2/year)	13	54	100
Total (kWh/m^2/year)	42	87	156
Energy reference area (m^2)	1 199	1 174	1 167

Table 24 Energy consumptions for MFH13, MFH54, and MFH100

In terms of energy inputs, the study uses mean energy prices, 19.5 c./kWh for electricity, 9 c./kWh for electricity feed-in, 9.9 c./kWh for natural gas and 15.87 c./kWh for pure biomethane. To assess the influence of the biomethane share on the optimal energy content, five different gas mixes are considered in the study. GHG emissions factors for natural gas (230 gCO_2eq/kWh) and biomethane (124 gCO_2eq/kWh) are based on the KBOB [27] (Table 25).

Biomethane share	0%	10%	30%	50%	100%
GHG emissions (g CO2 eq. /kWh)	230	219.4	198.2	177	124
Price (c./kWh)	9.87	10.47	11.67	12.87	15.87

Table 25 GHG emissions and price by percentage of biomethane in the gas mix

To assess the influence of the GHG emissions factor of biomethane, an additional case “100% low” is defined with a lower GHG emission factor at 44 gCO_2eq/kWh corresponding to a specific methanation plant in the Zurich region studied by EMPA [28]. In this study a 100% renewable electricity mix is used and treated biogas is considered with an economic allocation in the modelling perspective. This only constitutes a sensitivity analysis with a lower GHG emissions value that only represents the GHG emissions of the biogas produced by a specific methanation plant in Zürich with an economic allocation. No generalization of results can be done for other biogas power plants and thus these results cannot be directly compared with the ones using the KBOB value that is supposed to represent the supply of biogas in Switzerland without pointing to a specific biogas power plant.

The optimization results of the energy concept for single buildings with optihood represented for example in for MFH54 (left) show that the use of biomethane in single buildings generally yield either neutral (Pareto fronts are overlapped) or negative (higher share of biomethane induces higher cost) impacts on both cost and GHG emissions. The optimal concepts are mostly a gas boiler and ASHP combination, the optimal capacity and utilization share of each technology are dependent on the biomethane share. A higher biomethane share leads to a bigger heat pump. This finding highlights the importance of considering both emission and cost when evaluating the viability of biomethane. Whether it is for a very modern building like MFH13, a renovated one like MFH54 or an old building like MFH100, natural gas emerges as the preferable option for cost reduction, while heat pumps prove effective in curbing pollution. However, biomethane is more likely to be a competitive choice for buildings with high energy consumption buildings (MFH100). This is because the space heating distribution temperature is higher inducing lower COP for the HP, thus higher investment, and operation costs.

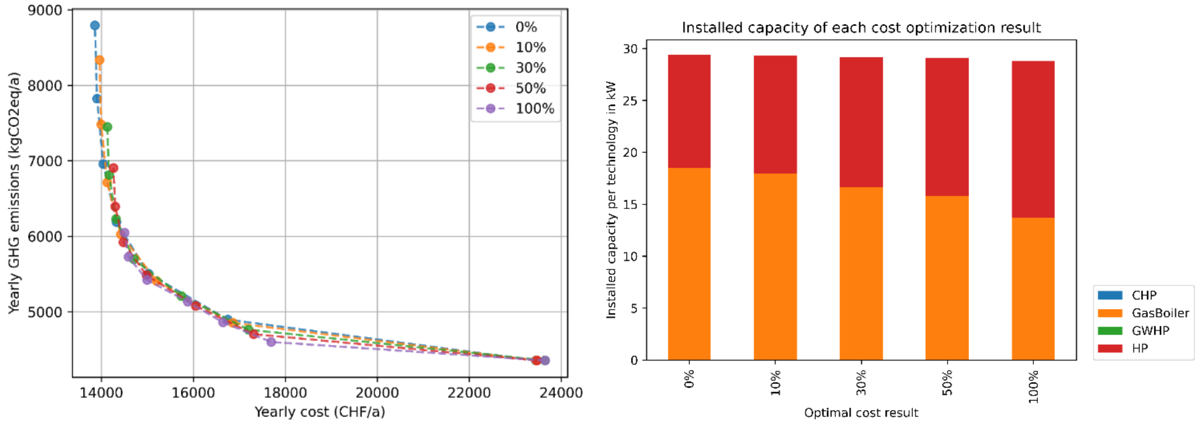

Figure 90: (left) Pareto front representation of the optimal solutions for the MFH54 building and five different biomethane share (KBOB value); (right) Installed converter capacities.

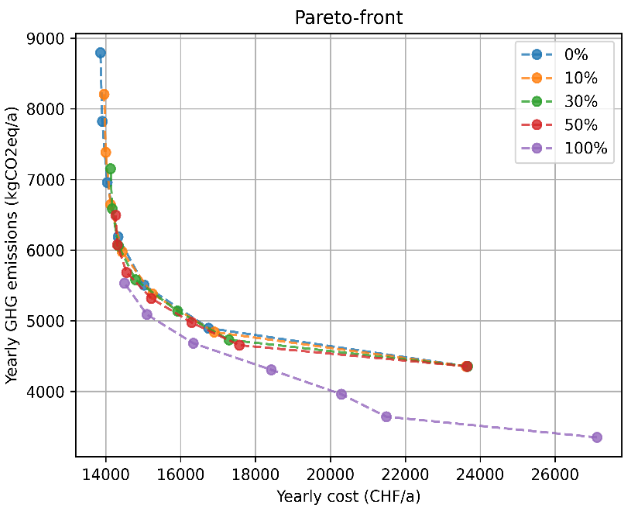

Figure 91: Pareto front representation of the optimal solutions for the MFH54 building and five different biomethane share with reference GHG emissions factors of 230 gCO_2eq/kWh for natural gas (0%) and 44 gCO_2eq/kWh for biomethane (100%).

We observe that for a GHG emission factor of 44 gCO_2eq/kWh, biomethane becomes a competitive choice. For both price and environmental optimization, its use has clear benefits. Nevertheless, this holds true primarily for an input of pure biomethane, which considering the small production of this energy vector is only doable for very particular projects. In this case, when GHG emission are optimized than the energy concept relies more and more on gas technology (gas boiler and CHP) which is a change in paradigm comparing to other case studies. When grouping four MFH54 within an energy community (thermal and electrical), the results obtained are similar compared to four individual buildings in terms of energy concept and installed capacities except for PV and energy storage technologies. Differences come from the optimal configuration whether the system is centralized (smaller PV system, and larger storage) or decentralized (only larger storages).

4 Conclusions

The project OPTIM-EASE allowed the development of the open-source python framework optihood for optimizing energy systems at the neighborhood scale. Built upon the oemof framework[21], it offers several enhanced features, including a simplified scenario/problem definition using config or excel files, multi-objective optimization based on cost and GHG emissions criteria, technology models for HP, individual or group building optimizations, and an option to improve computational speed through day clustering. optihood's versatility extends to optimizing a diverse range of energy systems, encompassing district heating, microgrids, and neighborhoods with a mix of residential, commercial, and industrial buildings. Optihood is an open-source framework readily available on GitHub[22] and accompanied by comprehensive online documentation[23].

From the case studies, grouping buildings within an energy community is seen to be beneficial in terms of cost as well as for mitigation of environmental impacts. If only electricity is shared within a microgrid, electricity price is seen as the main driver of the potential benefit allowing that more heat is delivered through heat pump. Then if heat flows are allowed to be shared between buildings, more gain can be expected if the infrastructure for the thermal grid was less than 7% to 40% of the equivalent annual cost. Specific conclusions for each case study can be found in section 3.

Based on the cost and greenhouse gases emissions assumption, photovoltaic is the preferred technology to be installed on roofs. However, for small buildings, installation of photovoltaic array is not suggested at the cost optimum. For larger buildings and for energy communities, photovoltaic panels are almost always installed.

The conclusions are drawn from specific case studies. Therefore, results from each case study are expected to be extrapolated to similar neighborhoods but not to cases with strong differences in energy demand and buildings with other shape factors or internal gains. The shape factor changes mostly the roof area available per square meter of heated floor area and thus the size of the potential PV system. It was also seen that neighborhoods with high heat and electricity demands including buildings like hotels or at least 7 MFH are more suited to be powered with CHP district heating systems. Heterogeneity in energy demands is also a key feature to benefit from grouping the buildings together.

5 Outlook and next steps

- Roof areas in some cases are totally covered with PV panels, additional space could be found on façade. While the efficiency is expected to be lower in the case of façade installations, the production in winters would be higher than in rooftop installations. Whether or not it would be optimal in terms of costs and/or environmental impacts as well as reducing CO_2 emissions of the winter electricity demand should be investigated further in future research.

[21] https://oemof.org/
[22] https://github.com/SPF-OST/optihood
[23] https://optihood.readthedocs.io/

- Sharing low temperature heat sources (geothermal, waste heat, …) through a low temperature grid was not investigated in this project. These concepts could further improve the benefit of grouping building and provide cooling to buildings. Adding a service to the energy concept would unlock more possibility to profit from the synergies between heat, cooling, and electricity demand in neighborhoods.
- The case studies in this work consider either buildings with a certain homogeneity in their energy demands (same type, similar geometry, …) or when some differences were present, their impact on the optimal energy concept were not thoroughly investigated. Thus, further research is needed to assess the influence of various energy demand profiles as well as considering cooling demand.
- Results are subject to the hypothesis in the cost and emissions parameters. Therefore, optimization studies should account for uncertainty in these assumptions. This has only been addressed through limited sensitivity studies. Therefore, it is difficult to conclude on which technology should be preferred over another because many factors can influence this decision. Future research should focus on the probability of a specific energy concept being optimal over the others.
- CO2 emissions of the borehole heat exchanger was updated in the KBOB in 2023 to half the previous value, this could change the competitiveness of GSHP in the investigated studies.

6 Publications

- The optihood framework and the Romande Energie case study were presented at the Brenet Status-Seminar in Aarau on the 9th of September 2022.
- The optihood framework was published as open-source on GitHub and an online technical documentation was prepared and made available on Read The Docs. The documentation is accessible at https://optihood.readthedocs.io/.
- Two peer-reviewed articles were presented at the scientific conference CISBAT, 13-15 September 2023, Lausanne:
    - Xavier Jobard, Massimiliano Capezzali, Neha Dimri, Alexis Duret, Marten Fesefeldt, Mija Frossard, Vincent Jacquot, Sebastien Lasvaux, *Economic and environmental benefits of decentralized multi-energy systems for energy communities,* Proceedings of CISBAT 2023, the built environment in transition, Hybrid International Scientific Conference, 13-15 September 2023, Lausanne, Switzerland
    - Neha Dimri, Daniel Zenhäusern, Daniel Carbonell, Xavier Jobard, Vincent Jacquot, Agnès François, Massimiliano Capezzali, Marten Fesefeld, *Optihood – a multi-objective analysis and optimization framework for building energy systems at neighborhood scale,* Proceedings of CISBAT 2023, the built environment in transition, Hybrid International Scientific Conference, 13-15 September 2023, Lausanne, Switzerland

References

[1] Lédée F, Padey P, Goulouti K, Lasvaux S, Beloin-Saint-Pierre D. Ecodynelec: Open Python Package to Create Historical Profiles of Environmental Impacts from Regional Electricity Mixes n.d. https://doi.org/10.2139/SSRN.4420940.

[2] Prognos AG. Die Energieperspektiven für die Schweiz bis 2050 - Energienachfrage und Elektrizitätsangebot in der Schweiz 2000 - 2050 - Ergebnisse der Modellrechnungen für das Energiesystem. SFOE; 2012.

[3] Bundesamt für Energie. Analyse des schweizerischen Energieverbrauchs 2000-2018 nach Verwendungszwecken. 2019.

[4] Office fédéral de la statistique. Bâtiments selon le type de chauffage, les agents énergétiques utilisés pour le chauffage et les cantons, 2009-20015. 2016.

[5] Kaufmann U. Schweizerische Statistik der erneuerbaren Energien - Ausgabe 2018. Bern: 2018.

[6] Barcellona S, Piegari L, Musolino V, Ballif C. Economic viability for residential battery storage systems in grid-connected PV plants. IET Renewable Power Generation 2018;12:135–42. https://doi.org/10.1049/IET-RPG.2017.0243.

[7] Karmellos M, Mavrotas G. Multi-objective optimization and comparison framework for the design of Distributed Energy Systems. Energy Convers Manag 2019;180:473–95. https://doi.org/10.1016/j.enconman.2018.10.083.

[8] Dong M, He F, Wei H. Energy supply network design optimization for distributed energy systems. Comput Ind Eng 2012;63:546–52. https://doi.org/10.1016/J.CIE.2012.01.006.

[9] Wu Q, Ren H, Gao W, Ren J. Multi-objective optimization of a distributed energy network integrated with heating interchange. Energy 2016;109:353–64. https://doi.org/10.1016/j.energy.2016.04.112.

[10] Orehounig K, Evins R, Dorer V. Integration of decentralized energy systems in neighbourhoods using the energy hub approach. Appl Energy 2015;154:277–89. https://doi.org/10.1016/j.apenergy.2015.04.114.

[11] Haller M, Amstad D, Carbonell D, Zenhäusern D. HybridStock - Hybrid Seasonal Storage of Renewable Heat and Electricity with an Aluminium Redox Cycle. Rapperswil: 2021.

[12] Battaglia M, Haberl R, Bamberger E, Haller M. Increased self-consumption and grid flexibility of PV and heat pump systems with thermal and electrical storage. Energy Procedia 2017;135:358–66. https://doi.org/10.1016/j.egypro.2017.09.527.

[13] Mavromatidis G, Orehounig K, Bollinger LA, Hohmann M, Marquant JF, Miglani S, et al. Ten questions concerning modeling of distributed multi-energy systems. Build Environ 2019;165:106372. https://doi.org/10.1016/j.buildenv.2019.106372.

[14] Cui Y, Geng Z, Zhu Q, Han Y. Review: Multi-objective optimization methods and application in energy saving. Energy 2017;125:681–704. https://doi.org/10.1016/J.ENERGY.2017.02.174.

[15] EMPA. Holistic Urban Energy Simulation (HUES) Platform, SCCER FEEB&D. Https://Hues-PlatformGithubIo/ n.d.

[16] Falke T, Krengel S, Meinerzhagen A, Schnettler A. Multi-objective optimization and simulation model for the design of distributed energy systems. Appl Energy 2016;184:1508–16. https://doi.org/10.1016/j.apenergy.2016.03.044.

[17] Padey P, Goulouti K, Capezzali M, Fesefeldt M, Lasvaux S, Beloin-Saint-Pierre D, et al. EcoDynBat – Final Report Dynamic Life Cycle Assessment of Buildings. 2020.

[18] Lédée F, Padey P, Goulouti K, Lasvaux S, Beloin-Saint-Pierre D. Ecodynelec: Open Python Package to Create Historical Profiles of Environmental Impacts from Regional Electricity Mixes n.d. https://doi.org/10.2139/SSRN.4420940.
[19] Geidl M, Andersson G. Optimal Power Flow of Multiple Energy Carriers. IEEE Transactions on Power Systems 2007;22:145–55. https://doi.org/10.1109/TPWRS.2006.888988.
[20] Afjei T, Wetter M. Yearly Utilization Model YUM WP, Holzbenutzerhandbuch mit Beispielen. 1995.
[21] Glize E. Méthodes exactes pour les problèmes combinatoires bi-objectif : Application sur les problèmes de tournées de véhicules 2019.
[22] Stocker TF, Qin D, Plattner G-K, Tignor M, Allen SK, Boschung J, et al. Climate Change 2013: The Physical Science Basis. Contribution of Working Group I to the Fifth Assessment Report of the Intergovernmental Panel on Climate Change 2013:1535.
[23] Jobard X, Demonchy G, Lasvaux S, Frossard M, Dimri N, Zenhäusern D, et al. OPTIM-EASE - Deliverable WP1: Buildings demand, technolgies, LCA and LCC data methodology. Yverdon-Les-Bains: 2022.
[24] Igor Bosshard-Mojic, Toni Calabrese, Sascha Crameri, Dani Sanchez Carbonell, Michel Haller. Reference Framework for Building and System Simulations: Multifamily house. 2023.
[25] Friedli R, Jauslin M, Meile O, Affentranger C, Steiner V, Faber C, et al. KBOB 2009/1: 2022. KBOB, Office Fédéral Des Constructions et de La Logistique, Fellerstrasse 2022;21.
[26] Beloin-Saint-Pierre D, Hischier R. Life cycle assessment of digestion and biogas treatment at Werdhölzli. 2021.
[27] KBOB, ecobau, IPB. KBOB-Empfehlung 2009/1:2022: Ökobilanzdaten im Baubereich, Stand Februar 2022. Koordinationskonferenz der Bau- und Liegenschaftsorgane der öffentlichen Bauherren c/o BBL Bundesamt für Bauten und Logistik 2022.
[28] Beloin-Saint-Pierre D, Hischier R. Life cycle assessment of digestion and biogas treatment at Werdhölzli. 2021.

8 Appendix

8.1 APPENDIX A: Linear heat pump model